

**Synthesis and Characterization of
Photocleavable Polymers and Block Copolymers**

Dissertation

Zur Erlangung des akademischen Grades
eines Doktors der Naturwissenschaften

-Dr. rer. nat-

des Fachbereichs Chemie der Universität Hamburg

von

HUI ZHAO

Hamburg

2013

Die vorliegende Arbeit wurde unter der Betreuung von Prof. Dr. Patrick Theato in der Zeit vom Mai 2010 bis April 2013 am Institut für Organische Chemie der Johannes Gutenberg-Universität Mainz, am Polymer Science and Engineering Department der University of Massachusetts, Amherst und am Institut für Technische und Makromolekulare Chemie der Universität Hamburg angefertigt.

Erster Gutachter: Prof. Dr. Patrick Theato
Zweiter Gutachter: Professor Dr. Malte Brasholz
Datum der Disputation: 07.06.2013

Contents

Abbreviations	2
1. Introduction	3
Polymers and block copolymers	5
RAFT polymerization	7
Polymeric activated ester	9
<i>o</i> -Nitrobenzyl alcohol derivatives in polymer and materials science	11
2. Scope and objectives	19
3. Results and discussion	20
3.1 Functionalized Nanoporous Thin Films and Fibers from Photocleavable Block Copolymers	
Featuring Activated Esters	21
3.2 Photocleavable Triblock Copolymers Featuring Activated Ester Middle Blocks:	
Synthesis and Application as Nanoporous Thin Film Templates	33
3.3 Photolabile Amine Semitelechelic Polymer for Light-induced Macromolecular Conjugation	43
4. Overview of Results	55
5. Summary	59
6. Experimental Part	61
7. References and notes	69
8. Appendix (published work)	76
8.1 Highly-ordered Nanoporous Thin Film from Photocleavable Block Copolymer	76
8.2 Copolymers Featuring Pentafluorophenyl Ester and Photolabile Amine Units: Synthesis and	
Application as Reactive Photopatterns	100
9. Lists of publications	115

10.Acknowledgements

116

**Additional information (Chemicals, Lebenslauf, Erklärung über frühere Promotionsversuche,
Eidesstattlicher Erklärung)**

117-125

Abbreviations

AIBN	azobisisobutyronitrile
ATR	attenuated total reflection
ATRP	atom transfer radical polymerization
CTA	chain transfer agent
DLS	dynamic light scattering
DMF	dimethylformamide
DMSO	dimethylsulfoxide
FT	fourier transform
GPC	gel permeation chromatography
IR	infrared radiation
LCST	lower critical solution temperature
M _n	molecular weight (number average)
M _w	molecular weight (weight average)
NMP	nitroxide mediated polymerization
NMR	nuclear magnetic resonance
ONB	<i>o</i> -nitrobenzyl
POEGMA	poly(oligo(ethylene glycol) methyl ether methacrylate)
PEG	poly(ethylene glycol)
PEO	poly(ethylene oxide)
PFP	pentafluorophenol
PNIPAM	poly(<i>N</i> -isopropyl acrylamide)
PPFPA	poly(pentafluorophenyl acrylate)
RAFT	reversible addition-fragmentation chain transfer
TEM	transmission electron microscopy
UV	ultra-violet (light)
Vis	visible (light)

1. Introduction

1.1 Polymers and block copolymers

Polymers have a very close relationship with our normal life, for example, the proteins and starch in food are polymers. They can be classified as natural and synthetic polymers based on their sources. A polymer has high relative molecular mass and polydispersity. From the view of chemistry, a polymer is a compound that contains repeating units created through polymerization. The repeating units in polymers are called monomers. Homopolymer is a polymer derived from one monomer while copolymer from two (or more) monomeric species. Copolymers are classified as alternating, period, statistical or block copolymers based on the manner in which the copolymers are connected together. Among the categories of copolymers, block copolymers consisting of chemically distinct polymers linked by a covalent bond have attracted increasing attention for their ability to self-assemble into a variety of ordered nanostructures.

1.2 Molecular structure of block copolymers

The molecular structures of a block copolymer (BCP) can be classified as linear AB, linear ABA, linear ABC and star ABC, depending upon the number and type of blocks and the manner in which the blocks are connected together (**Figure 1.1a**). The molecular structures of BCPs are not limited to the aforementioned 4 types. In a recent review by Bates and coworkers, linear multiblock and circle block copolymers were also reported.¹ The simplest type is the linear AB diblock copolymer shown in **Figure 1.1a**, in which a homopolymer A is covalently linked to a homopolymer chain B. A linear AB diblock copolymer is usually prepared by two routes: a) the repeated addition of monomers of B to the end of the previously synthesized chain of poly(A), b) conjugation or coupling reaction (eg. “click” reaction) between poly(A) and poly(B). Linear or star triblock can be prepared by similarly synthetic routes used for preparation of diblock copolymers.

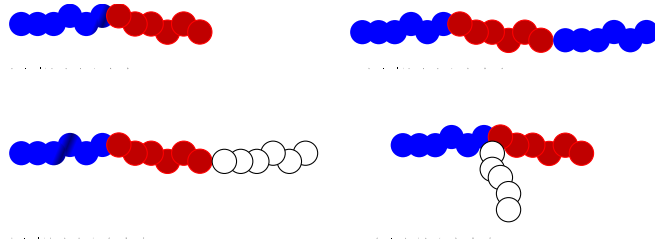


Figure 1.1 Block Copolymer Architectures. (a) Linear AB diblock copolymer. (b) Linear ABA triblock copolymer. (c) Linear ABC triblock copolymer. (d) Star ABC triblock copolymer

1.3 Diblock Copolymer Morphologies

As illustrated in **Figure 1.2**, linear AB diblock copolymers can form several different morphologies (spherical, cylinder, gyroid and lamellar) and many years of theoretical and experimental work were required to understand their phase behavior.¹ To a good approximation, AB diblock copolymers have a "universal" phase diagram in which the equilibrium structure is determined by the block volume fraction f_A and block-block interaction parameter $\chi_{AB}N$ while segment asymmetry ($P_A \neq P_B$), molecular weight and polydispersity shift the boundaries between phases.

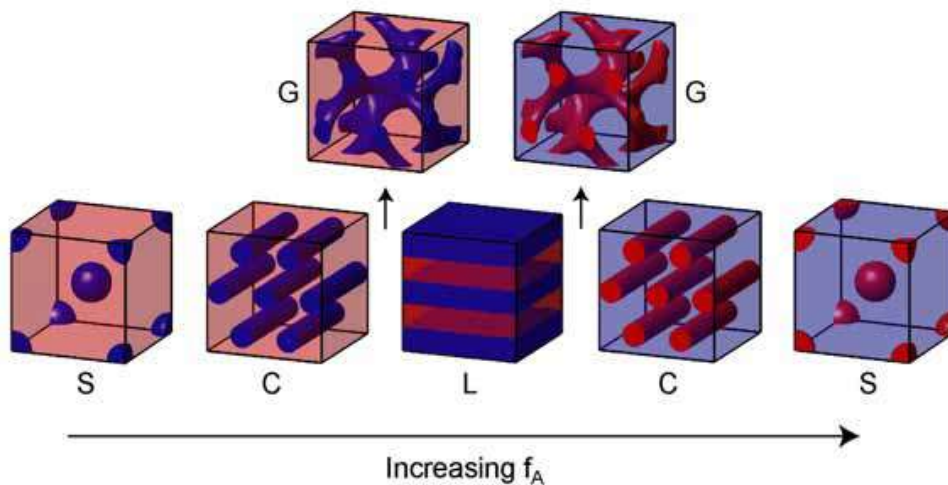


Figure 1.2 Diblock Copolymer Morphologies. Depending on the volume fraction of A (f_A) and interaction parameter ($\chi_{AB}N$), the A (blue) and B (red) blocks can form spherical (S), cylindrical (C) or lamellar (L) domains.

For volume fractions between those cylinder and lamellar structures, the double gyroid (G) network structure can form for some values of the block-block interaction parameter $\chi_{AB}N$.²

1.4 Nanoporous Thin Films from BCPs

Block copolymer lithography employing nanoporous thin films has received increasing attention as a road to enable the development of future technologies. Nanoporous thin films can be fabricated from a AB block copolymer thin films with aligned nanoscopic B cylinders in a matrix A. Figure 1.3 shows a visual schematic representation of this process. The blocks A and B should have enough contrast chemical or physical condition so that selective removal of B can be achieved. Further, the nonremovable block A should have a big modulus (it normally has high T_g , T_m or crosslinked structures), making the pores structure in the films stable after removing the block B. Diverse methods have been developed for the selective removal of one domain, such as chemical etching, ozonolysis, and UV degradation.^{2,3}

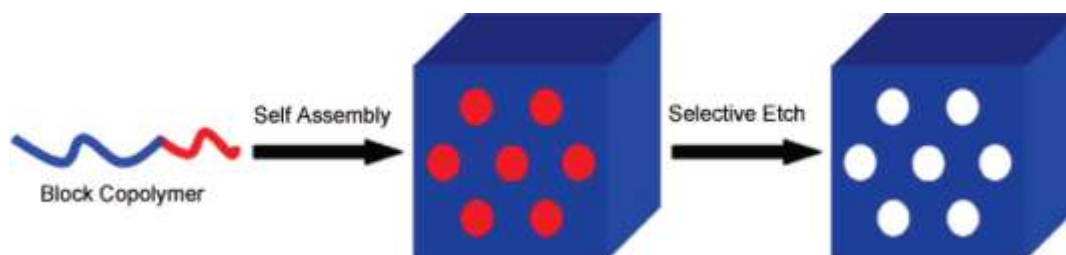


Figure 1.3 Schematic representation of the formation of nanoporous polymeric materials from ordered block copolymers.³

Here, Polystyrene-*block*-poly(methyl)methacrylate (PS-*b*-PMMA) was used as an example to illustrate how to prepare nanoporous thin films from degradable BCPs. As shown in Figure 1.4, once well-ordered films of PS-*b*-PMMA were obtained after substrate modification, spincoating, and thermal annealing, the nanoporous templates can be prepared by removing the PMMA block by deep UV irradiation ($\lambda = 254$ nm) under vacuum. The resulting pore size of the nanoporous templates can be simply tuned by varying the molecular weight of PS-*b*-PMMA BCPs. For cylindrical PS-*b*-PMMA, Xu

et al. demonstrated that the pore size can be tuned from 14 to 50 nm by changing molecular weight of PS-*b*-PMMA.⁴

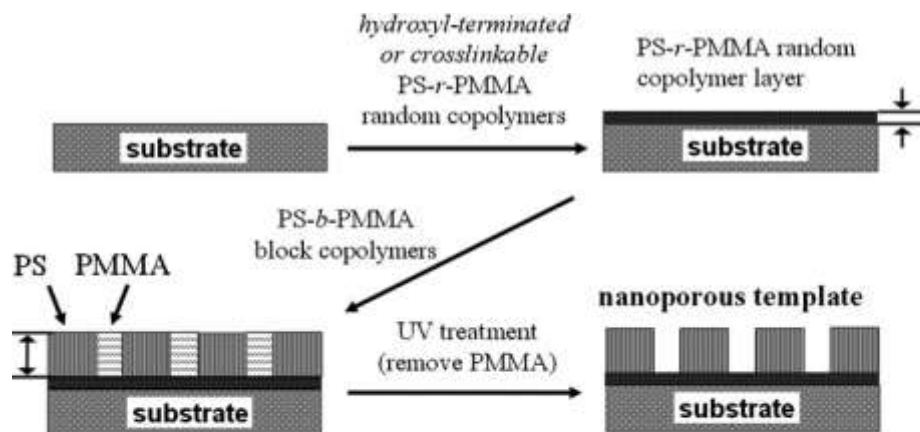


Figure 1.4 a) Schematics to prepare the nanoporous template from PS-*b*-PMMA thin film. The surface is first treated with PS-*r*-PMMA random copolymers, either having hydroxyl-terminated or crosslinkable group, and then PS-*b*-PMMA thin film is spin casted, and thermally annealed. Finally, the PMMA block is removed by UV irradiation to generate the nanoporous PS template.⁵

Table 1. General degradation methods to fabricate nanoporous thin films.

Degradable polymers in BCPs	methods	references
PB or PI	O ₃ , UV, RIE	6
PCL or PLA	basic or acidic solution	7
PDMS	anhydrous HF	8
PMMA	UV or thermal decomposition	4, 9
PPO	decomposition	10
PS	Fuming nitric acid	11
PαMS	UV	12
PtBA or PtBMA	acid condition	13

1.5 RAFT polymerization

The recent emergence of techniques for implementing controlled free radical polymerization (CRP) has provided a new set of tools that allow very precise control over the polymerization process. The living radical polymerization also provides the chance to make precise and complicated polymer structures for potential applications in many fields, such as self-assembly,¹⁴ crystallization,¹⁵ and biomaterials.¹⁶

Controlled or living free radical polymerization techniques normally include nitroxide mediated polymerization (NMP), atom transfer radical polymerization (ATRP) and the reversible addition-fragmentation chain transfer (RAFT) polymerization. The NMP technique was devised in the early 1980s. This polymerization method has been exploited extensively for the synthesis of homopolymers (especially for polystyrene) and block copolymers with a narrow molecular weight distribution. ATRP was discovered by Matyjaszewski^{17a} and Sawamoto^{17b} independently in 1995. ATRP is a versatile polymerization technique. However, it requires unconventional initiating systems, such as copper salts, which demonstrate poor compatibility to the polymerization media. Further, the use of transition metals in ATRP poses a potential problem toward biological uses of the resulting polymers. Substantial advances have been made to address this and other issues. RAFT, discovered at the Commonwealth Scientific and Industrial Research Organisation (CSIRO) in 1998, is probably the most widely used process for the commercial production of high-molecular weight polymers.¹⁸ RAFT polymerization uses thiocarbonylthio compounds, such as dithioesters, thiocarbamates, and xanthates, to mediate the polymerization via a reversible chain-transfer process. As with other controlled radical polymerization techniques, RAFT polymerizations can be performed with conditions to favor low polydispersity indices and a pre-chosen molecular weight. RAFT polymerization can be used to design polymers of complex architectures, such as linear block copolymers, comb-like, star, brush polymers and dendrimers.

The RAFT polymerization mechanism is illustrated in **Figure 1.5**. There are a number of steps in a RAFT polymerization: initiation, reversible chain transfer, re-initiation, chain equilibrium, and termination.¹⁹ In the initiation step, the reaction is started by a free-radical source, which may be a decomposing radical initiator such as AIBN. In the example in **Figure 1.5**, the initiator decomposes to

form two fragments ($I\cdot$) which react with monomer molecules to yield a propagating (i.e. growing) polymeric radical, denoted $P_n\cdot$. In the next step, reversible chain transfer, a polymeric radical with n monomer units (P_n) reacts with the RAFT agent ($S=C(Z)S-R$) to form a RAFT adduct radical. This adduct may undergo a fragmentation reaction in either direction to yield either the starting species or a radical ($R\cdot$) and a polymeric RAFT agent ($S=C(Z)S-P_n$). This is a reversible step in which the intermediate RAFT adduct radical is capable of losing either the R group ($R\cdot$) or the polymeric species ($P_n\cdot$). The losing group ($R\cdot$) from “reversible chain transfer” step will initiate the monomers and yield a polymeric radical $P_m\cdot$, this step is called “reinitiation”. “Chain equilibration” is the most important part in the RAFT process, in which, by a process of rapid interchange, the present radicals (and hence opportunities for polymer chain growth) are "shared" among all species that have not yet undergone termination ($P_n\cdot$ and $S=C(Z)S-P_n$). Ideally the radicals are shared equally, causing chains to have equal opportunities for growth and a narrow PDI. The last step, is “termination”. Chains in their active form react via a process known as bi-radical termination to form chains that cannot react further, known as dead polymer. In ideal conditions, the RAFT adduct radical does not undergo termination reactions.

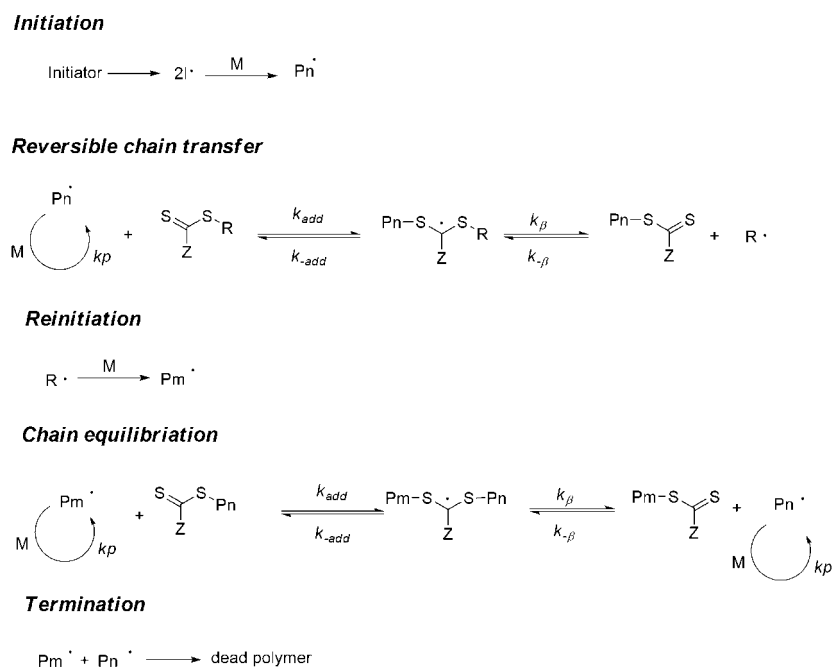


Figure 1. 5 Simplified mechanism of the RAFT process.

1.6 Polymeric Activated Ester

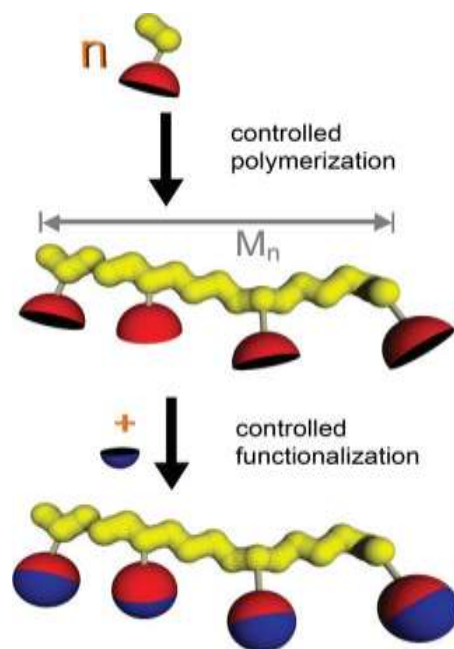


Figure 1.6 Schematic principle of a controlled polymerization of activated ester monomers followed by a controlled functionalization via a polymer analogous reaction.

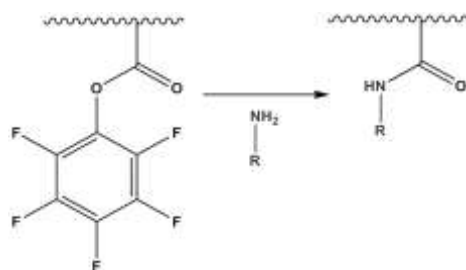


Figure 1.7 Polymeric activated ester-amine chemistry.

The synthesis of functional and well-defined polymers is still a challenge in polymer science. Functional polymers can be obtained from polymerization of functional monomers. In some case, protection of functional groups has to be carried out because the monomers cannot be polymerized directly. However, the subsequent deprotection step may not necessarily proceed to completion. The direct polymerization of monomers bearing functional groups is clearly a more favored strategy. Traditional living techniques, such as anionic polymerization only offer very limited possibilities for the direct polymerization of functional monomers. Nowadays, a system for controlled radical

polymerization can tolerate many functional groups. However, there is still a broad range of functionalities that cannot be introduced into a polymer by direct polymerization. Postpolymerization modification (also called polymer analogous reaction) has drawn increasing attention for its powerful behavior in the synthesis of functional polymers. The synthesis of functional polymers through a polymer analogous reaction is divided into two steps: a) polymerization of monomers with functional groups b) quantitative conversion of the functional group in the synthesized polymers into a broad range of other functional groups (see **Figure 1.6**). Consequently, polymer analogous reaction allows access to functional polymers that cannot be prepared by direct polymerization of the corresponding functional monomer.

The chemistry of activated esters and amines has found a broad application in peptide chemistry over many years. The synthesis and post-polymerization modification of active ester polymers was pioneered by Ferruti and Ringsdorf in the 1970s.²⁰ The reaction of active ester polymers with amines is probably the most frequently used post-polymerization modification strategy. Amines (**Figure 1.7**) are most often used for the post-polymerization modification of active ester polymers since they can react selectively even in the presence of weaker nucleophiles, such as alcohols. In recent years, activated esters polymers have found broad applications in polymer chemistry as well as in material- and life science.

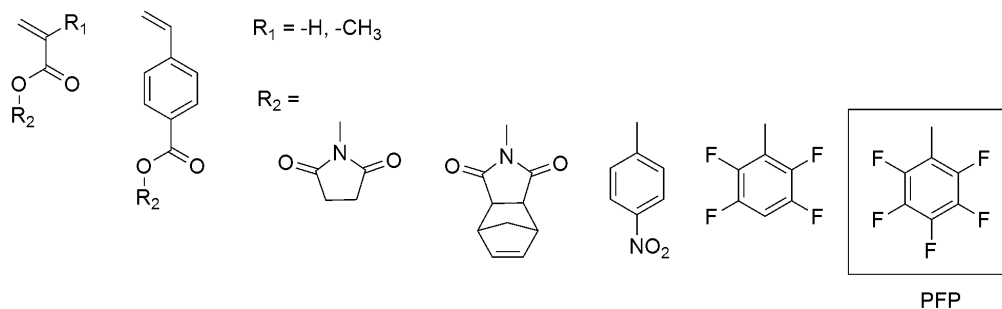


Figure 1.8 Monomers featuring activated esters for controlled radical polymerization.

Monomers featuring activated esters for controlled radical polymerization can be summarized in **Figure 1.8**. The vinyl monomers for CRP include acrylate, methyl acrylate and vinyl benzene. The leaving groups for activated ester-amine chemistry are strong withdrawing electron groups such as 1-hydroxypyrrolidone-2,5-dione, 4-nitrophenol, tetra and pentafluorophenylphenol.²¹ Among these

Polymers featuring photolabile groups are the subject of intense research because they allow the alteration of polymer properties simply by irradiation. The recent years have seen an explosive utilization of this chemistry and the following section tries to summarize the recent advances in this area in polymer chemistry. It covers the use of (i) ONB based crosslinkers for photodegradable hydrogels, (ii) ONB side chain functionalization in (block) copolymers, (iii) ONB side chain functionalization for thin film patterning, (iv) ONB for self-assembled monolayers, (v) photocleavable block copolymers, and (vi) photocleavable bioconjugates.

1.7.1 ONB based crosslinkers for photodegradable hydrogels

The first example of model cross-linked networks based on ONB linkers was reported in 2007 by Torro and co-workers.²⁵ Similarly, Kasko and co-workers combined the efficient light degradable property of ONB esters with the biocompatibility of PEO, resulting in a photocleavable hydrogel (Figure **1.10**).²⁶ This laid the foundation to trap living cells in the hydrogels, which may be released upon irradiation with light in a highly controlled manner (Figure 1a). Using two-photon photolithography, 3D channels for the migration of cells can successfully be obtained (Figure **1.10b**). This “smart hydrogel” takes advantage of ONB-based cross-links and thus opens an exciting application area for hydrogels.²⁷

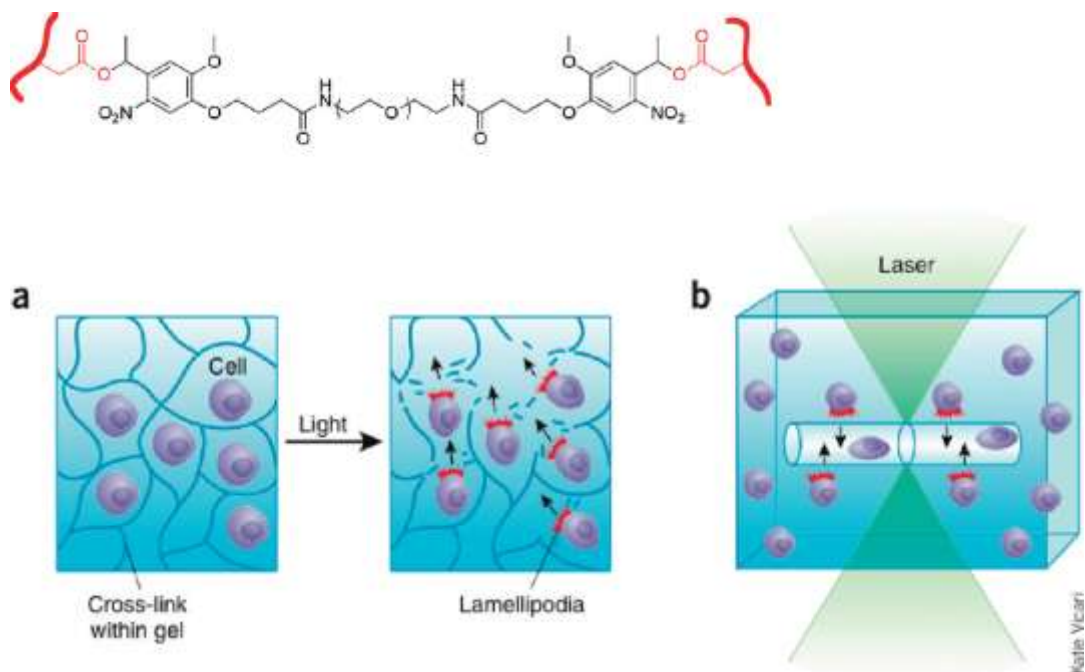


Figure 1.10 Chemical structure of a photodegradable hydrogel based on an ONB linker (upper) (redrawn after ref 17) and light-induced migration of entrapped cells (lower)

1.7.2 ONB side chain functionalization (block) copolymers

Light is an intriguing external stimulus; it is efficient and convenient and can be applied in a targeted and specific manner via a variety of focusing or lithographic techniques. Consequently, light responsive block copolymer micelles have been explored for entrapping dyes and drugs with the intention of releasing them at a defined time and location. ONB esters are a good candidate for constructing light responsive materials since they are efficiently cleavable upon UV exposure. Zhao and co-workers first reported that ONB functionalization in side chain of amphiphilic BCPs could be used to produce light responsive micelles (**Figure 1.11**).²⁸

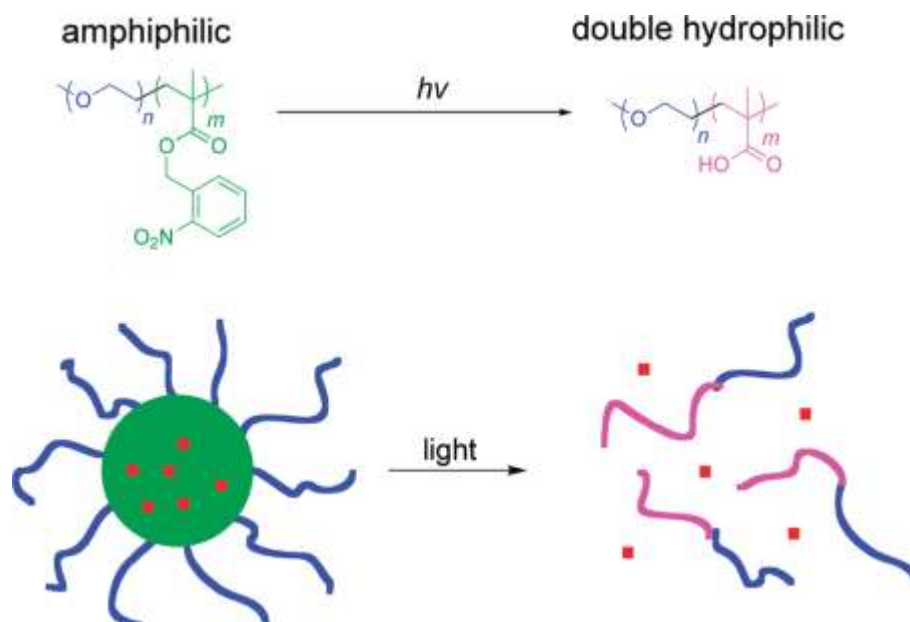


Figure 1.11 Chemical structure and photolysis of ONB-containing amphiphilic block copolymers and their use for photocontrolled drug release.

1.7.3 ONB side chain functionalization thin films patterning

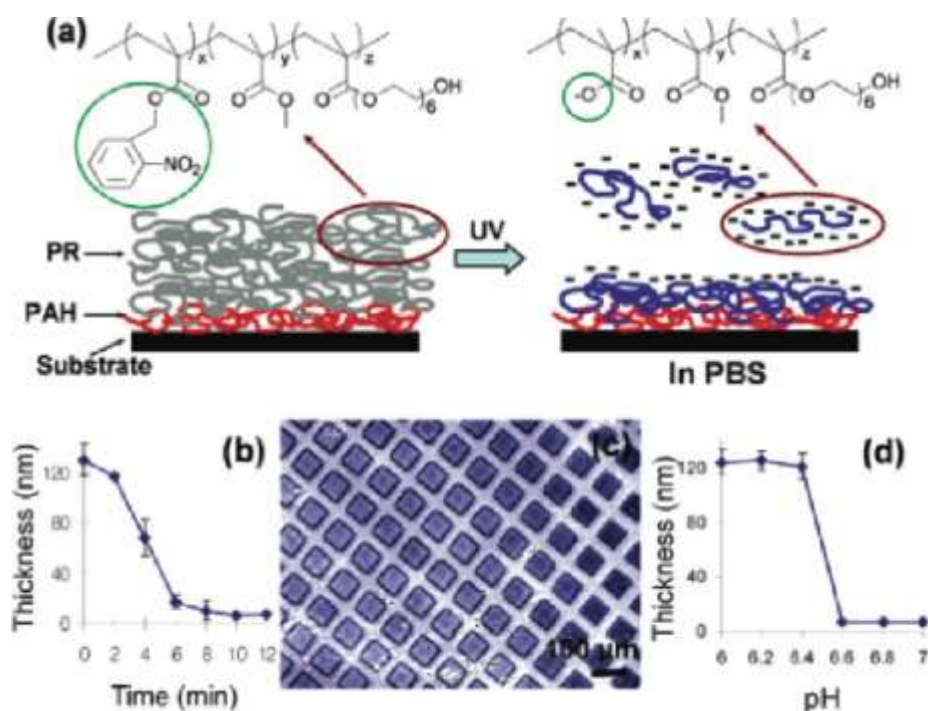


Figure 1.12 Chemical structure of a photosensitive terpolymer and its mechanism for patterning. (Reprinted with permission from ref 29. Copyright 2004 American Chemical Society.)

It has been reported that polymers prepared by polycondensation of 2-nitro-1,3-xylylenedibromide with 4,4'-isopropylidenediphenol, decomposed upon UV irradiation, suggesting that these materials can be used for positive-type photoresists.²⁹ Similarly, Lee and co-workers synthesized a polyimide precursor with ONB ester functionalities in the side chains.³⁰ They showed that this polyimide became soluble in basic solution after UV irradiation and thus can be used as positive photoresist. Doh and Irvine designed a terpolymer poly(onitrobenzyl methacrylate-co-methyl methacrylate-co-(ethylene glycol) methacrylate) (P(ONBMA-co-MMA-co-EGMA)) to prepare thin film patterns on the micrometer scale. They demonstrated that for a terpolymer composition of 43 wt % ONBMA, 38 wt % MMA, and 19 wt % EGMA the exposed areas of a thin film could be dissolved by phosphate-buffered saline after UV irradiation (see **Figure 1.12**).³¹

1.7.4 ONB for Self-assembled Monolayers to Control Surface Properties

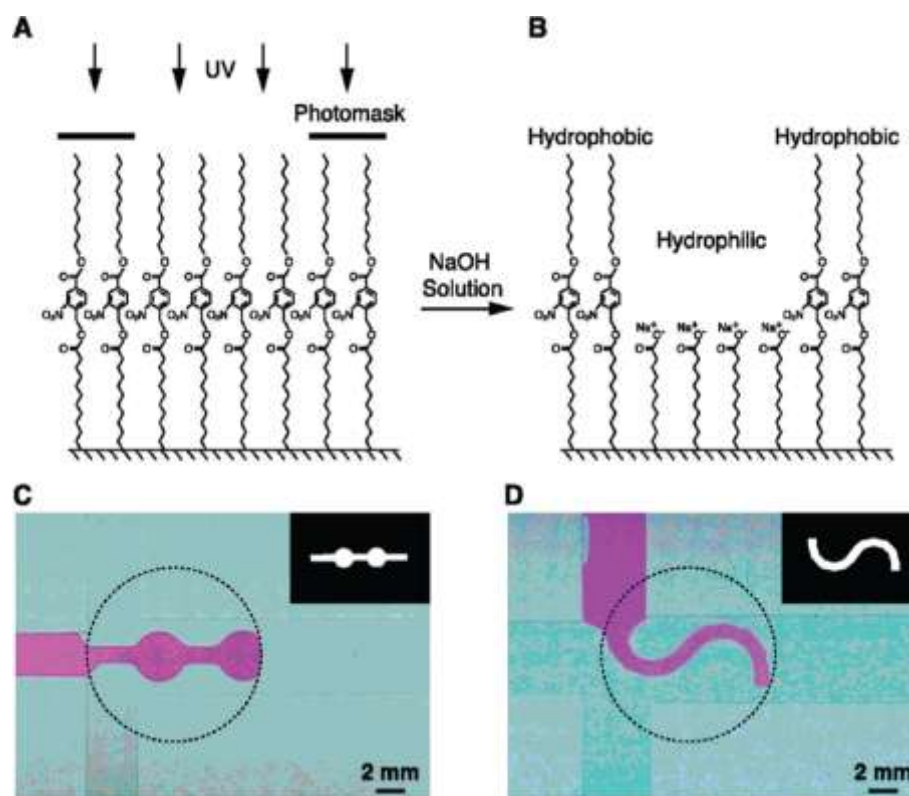


Figure 1.13 (A, B) Photopatterning by UV light to induce hydrophilic and hydrophobic surface patterns inside microchannels. (C, D) Flow profiles of dilute Rhodamine B aqueous solution inside the surface patterned microchannels.³²

Self-assembled monolayers (SAMs) have proven powerful tools to control surface energy and influence a variety of properties, e.g., adhesion, wetting and flow profiles, or etch resistance. It was reported by Moore and co-workers that photopatternable SAMs based on ONB chemistry could nicely direct liquid flow inside microchannels (**Figure 1.13**).³² Essentially, the ONB-based SAM was employed in a photolithographic and thereby contact free method resulting in patterns of differing surface free energies inside microchannels.

1.7.5 ONB junctions to cleave Block Copolymers

Block copolymers (BCPs) have been studied extensively due to their ability to self-assemble into a range of well-defined, well ordered structures. In recent years, the interest in block copolymers serving as nanotechnological templates has resulted in a multitude of research efforts. Block copolymer thin films with a morphology oriented perpendicular to the substrate are the current focus of many research groups, with a particular aim of preparing well-ordered, nanoporous thin polymer films.³³ Currently, several challenges have to be addressed to overcome the limitations still present in thin block copolymer films. The first is achieving high lateral order in the morphology, and the second is facile, selective removal of one phase. Several methods that allow for selective removal of one domain have been presented in the literature, such as chemical etching, ozonolysis, pH induced hydrolysis, and UV degradation. In particular, block copolymers with a cleavable junction are interesting since they can be used as precursors for generating hollow structures after cleavage and selective removal of one of the blocks. This can have an impact on the formation of hollow micelles and nanoporous polymeric materials.³⁴ As ONB is a well-known photocleavable junction, photocleavable block copolymers can be prepared based on this structure. Kang and Moon are the first to prepare and characterize photocleavable block copolymer thin films based on ONB (**Figure 1.15**).³⁵ They prepared the photocleavable diblock copolymer polystyrene-block-poly-(ethylene oxide) (PS-hv-PEO) by ATRP using an ONB

functionalized PEO macroinitiator (Figure 10). Recently, Fustin and co-workers developed a more versatile synthetic route toward photocleavable block copolymers on the basis of an ONB junction.³⁶ As copper(I) is known to be a catalyst for both ATRP and azide–alkyne cycloaddition (CuAAC) click reaction, they performed ATRP and click chemistry in a one-pot synthetic strategy using an ONB ester featuring dual functionality to synthesize several photocleavable block copolymers including PS-hv-PEO, which was used in the work of Kang and Moon (**Figure 1.14**). Theato, Coughlin, and co-workers extended this approach by combining RAFT polymerization and a subsequent intermacromolecular azide–alkyne click reaction, providing more flexibility in the synthesis of photocleavable block copolymers.³⁷ Highly ordered thin films were prepared, and after photoetching the resulting nanoporous films were used to prepare the first examples of nanostructures from a photocleavable polymer template.

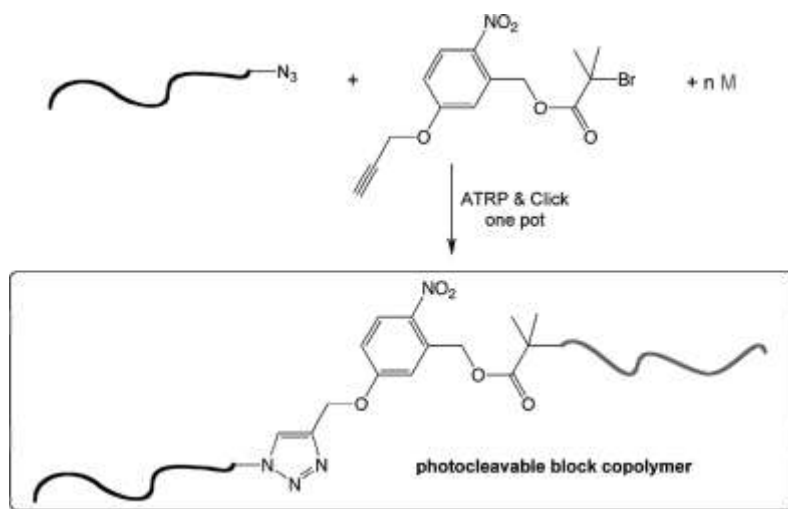


Figure 1.14 Synthesis of PEO-hv-PS by ATRP–CuAAC click reaction.³⁶

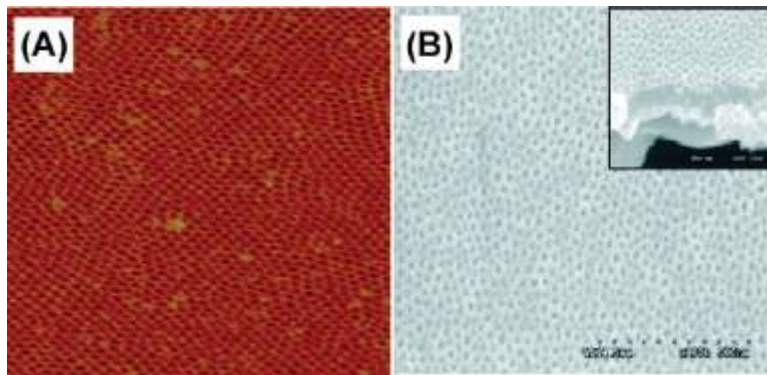


Figure 1.15 (A) AFM image ($1 \times 1 \mu\text{m}^2$) of PS-hv-PEO (23.7-b-5.0 K) films (thickness = 43 nm) spin-coated onto silicon wafers and solvent annealed for 2 h (benzene/water). (B) SEM image of the nanoporous PS thin film resulting from photocleavage and selective solvent removal (methanol/water) of PEO phase.³⁵

2 Scope and objectives

The general target of this thesis is to establish a synthetic method to produce block copolymers featuring photocleavable junctions. Further, to produce highly ordered nanoporous thin films based on photocleavable BCPs, the best process conditions will be explored. Finally, the possibility that the resulting nanoporous thin films are used for highly ordered templates will be studied. The key idea for nanoporous thin films from photocleavable BCPs is shown in **Figure 2.1**.

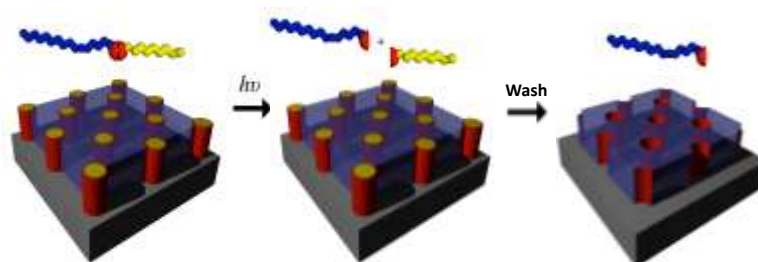


Figure 2.1 Schematic representation of the self-assembly of photocleavable block copolymers and the subsequent removal of one domain after UV irradiation.

The synthesis of well-defined polymers with ONB photocleavable groups will be developed utilizing modern polymerization methods, such as the reversible addition fragmentation chain transfer (RAFT) polymerization, combination with copper catalyzed azide-alkyne cycloaddition “click” chemistry and activated ester-amine chemistry.

Besides incorporating the ONB at the junctions between BCPs, ONB can also be as side chains or end groups in a polymer. Based on activated ester-amine chemistry, well-defined polymers with ONB as side chains and end groups will be introduced in this thesis.

3 Results and Discussion

3.1 Functionalized Nanoporous Thin Films and Fibers from Photocleavable Block Copolymers Featuring Activated Esters

Introduction

Nanoporous materials have received continuous attention since they find numerous applications, including as gas storage materials,³⁸ separation materials,³⁹ agents for controlled release of drugs,⁴⁰ supports for catalysts,⁴¹ cell scaffolds,⁴² photonic band gap materials,⁴³ filtration-separation membranes,⁴⁴ and templates for structure replication.⁴⁵ Among the strategies to produce nanoporous materials, self-assembly of block copolymers (BCPs) has received considerable attention as a promising platform for "bottom-up" fabrication of nanostructured materials and devices.⁴⁶ Generally, to fabricate nanoporous thin films, minor domains within the BCP films need to be removed or reconstructed.⁴⁷ Diverse methods have been developed for the selective removal of one domain in BCP thin films, including chemical etching,⁴⁸ ozonolysis,⁴⁹ and UV degradation.⁵⁰ However, most of these methods require harsh treatment conditions. Recently, the groups of Moon, Fustin, Coughlin and Theato developed block copolymers with photocleavable junctions based upon the *o*-nitrobenzyl ester (ONB). These investigations have established ONB-based BCPs as a promising platform for the synthesis of highly ordered nanoporous thin films.³⁵⁻³⁷

Nanoporous materials featuring reactive or functionalized nanoporous materials have attracted increasing interest as they can be tuned easily by incorporating a variety of functional groups into the nanoporous matrix. Hillmyer and coworkers developed an ABC (polystyrene-*block*-poly(dimethylacrylamide)-*block*-polylactide) triblock system to fabricate reactive nanoporous thin

films.^{52, 53} More recently, amine and carboxylic acid functionalized nanoporous thin films based on photocleavable diblock copolymers were reported by Fustin.^{51, 54} Most functionalization methods reported to date focus only on the surface modification of pore walls in porous thin films. The functional groups present on the porous thin films were found to be only partially active and react under limited conditions. There is a strong need for versatile synthetic routes toward nanoporous materials that provide possibilities for post-functionalization after removal of one component of the BCP. Herein, we report the synthesis of photocleavable block copolymers with reactive poly(pentafluorophenyl-(methyl)-acrylate)s (PPFP(M)A) as the major block and PEO as the minor block. The pentafluorophenyl ester, is known to react with amines under very mild conditions (room temperature and catalyst free) based on activated ester-amine chemistry, yielding the respective functional poly((meth)acrylamide).⁵⁵ This novel matrix functionality of pentafluorophenyl esters offers a more efficient way to tune the properties of nanoporous structures compared to surface functionalization of pore walls.

Results and Discussion

Synthesis and characterization. In previous reports, we presented polymers featuring pentafluorophenyl (PFP) esters as promising reactive polymeric precursors for the synthesis of multifunctional polymers.⁵⁵ In this paper, we chose perfluorophenyl acrylate (PFPA) and pentafluorophenyl methacrylate (PFPMMA) as monomers to serve as a hydrophobic block in the photocleavable block copolymers. The strong hydrophobicity of PPFP or PPFPMA blocks leads to a significant incompatibility with the hydrophilic PEO block and, as a result, large non-favorable Flory-Huggins interactions between the PPFP/PPFPMA and PEO blocks. We first attempted a RAFT-click route to synthesize the block copolymer (supporting information, Scheme S1): poly(pentafluorophenyl (methyl) acrylate) with an alkyne end group was obtained by RAFT polymerization and the PEO block was then conjugated with the PFP(M)A block using copper-catalyzed [2+3] Huisgen alkyne-azide cycloaddition (CuAAC) “click” chemistry. However, the click chemistry does not proceed efficiently,

which we attribute to the copper (I) catalyst interfering with the pentafluorophenyl (methyl) acrylate, leading to hydrolysis of the ester, followed by protonation and coordination of the ligands and copper, respectively.

Accordingly, we synthesized a macromolecular chain transfer agent (Macro-CTA) for subsequent RAFT polymerization of PFPA or PFPMA. As shown in **Scheme 3.1.1**, the Macro-CTA containing an ONB junction was prepared by a click reaction between and azide-functionalized PEO and alkyne-functionalized CTA (**Scheme 3.1.1**, see experimental section for details for Macro-CTA synthesis). The yield of the Macro-CTA is high (pink powder, yield up to 90%) and CTA end group functionality is over 85% (calculated by ^1H NMR, **Figure 3.1.1A**). This Macro-CTA can be efficiently controlled RAFT polymerization of PFPA and PFPMA monomers. All polymers were fully characterized by FTIR, ^1H and ^{19}F NMR. Take PEO-*h_v*-PPFPMA (**P4**) as an example: as can be seen from **Figure 3.1.1**, the proton resonance 1.0 to 2.8 *ppm* are assigned to the PFPMA block while the resonances between 3.3 and 4.5 *ppm* are assigned to the PEO block. Typical proton resonances (e, f in **Figure 3.1.1B**) from the ONB junction are also observed. As can be seen from **Figure 3.1.1**, the proton ratio between the labeled aromatic protons *c:b:d* is 1.00:1.98:1.96, which indicates the benzoic dithioester and *o*-nitrobenzyl ester groups in the Macro-CTA remained intact after the CuAAC “click” reaction. ^{19}F NMR results also support that we obtained block copolymers containing pentafluorophenyl esters (see **Figure 3.1.1C**). Control of the block copolymer dispersity (*D*) was not perfect as we expected for a RAFT polymerization, and the *D* values smaller than 1.5 were achieved, which is most likely due to the nitro-group of ONB functionality. (Figure 1 and Table 1, M_n : 10~32.4k g/mol, M_w/M_n :1.29~1.46). (For further details, see experimental section.)

Scheme 3.1.1 Synthetic routes to photocleavable BCP featuring activated esters

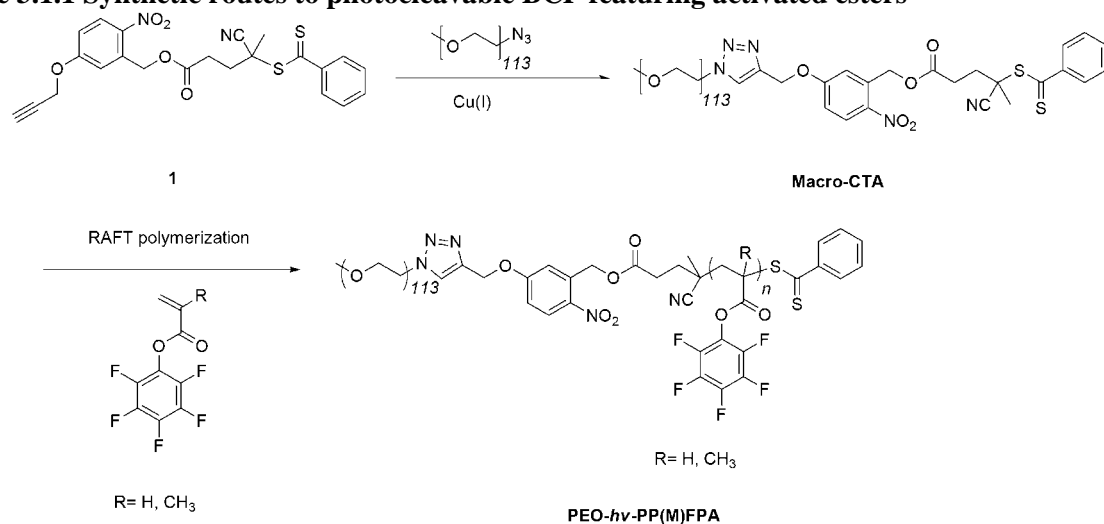


Table 3.1.1 Synthesis of Photocleavable BCP Featuring Activated Esters via RAFT polymerization using a PEO-based Macro-CTA ($M_{n,GPC} = 7000$, $\bar{D} = 1.10$, PS standard).

Polymer	Monomer	M_n (g/mol) ^a	\bar{D} ^a	f_{PEO} ^b
P1	PFPA	10 000	1.29	0.33
P2	PFPA	18 800	1.47	0.21
P3	PFPA	23 000	1.41	0.19
P4	PFPMA	25 300	1.31	0.17
P5	PFPMA	28 500	1.40	0.15
P6	PFPMA	32 400	1.46	0.14

^a GPC in THF using linear PS standards. ^b $M_{n,NMR}$ (g/mol) = 5000, ($M_n = 7000$ g/mol for GPC in THF).

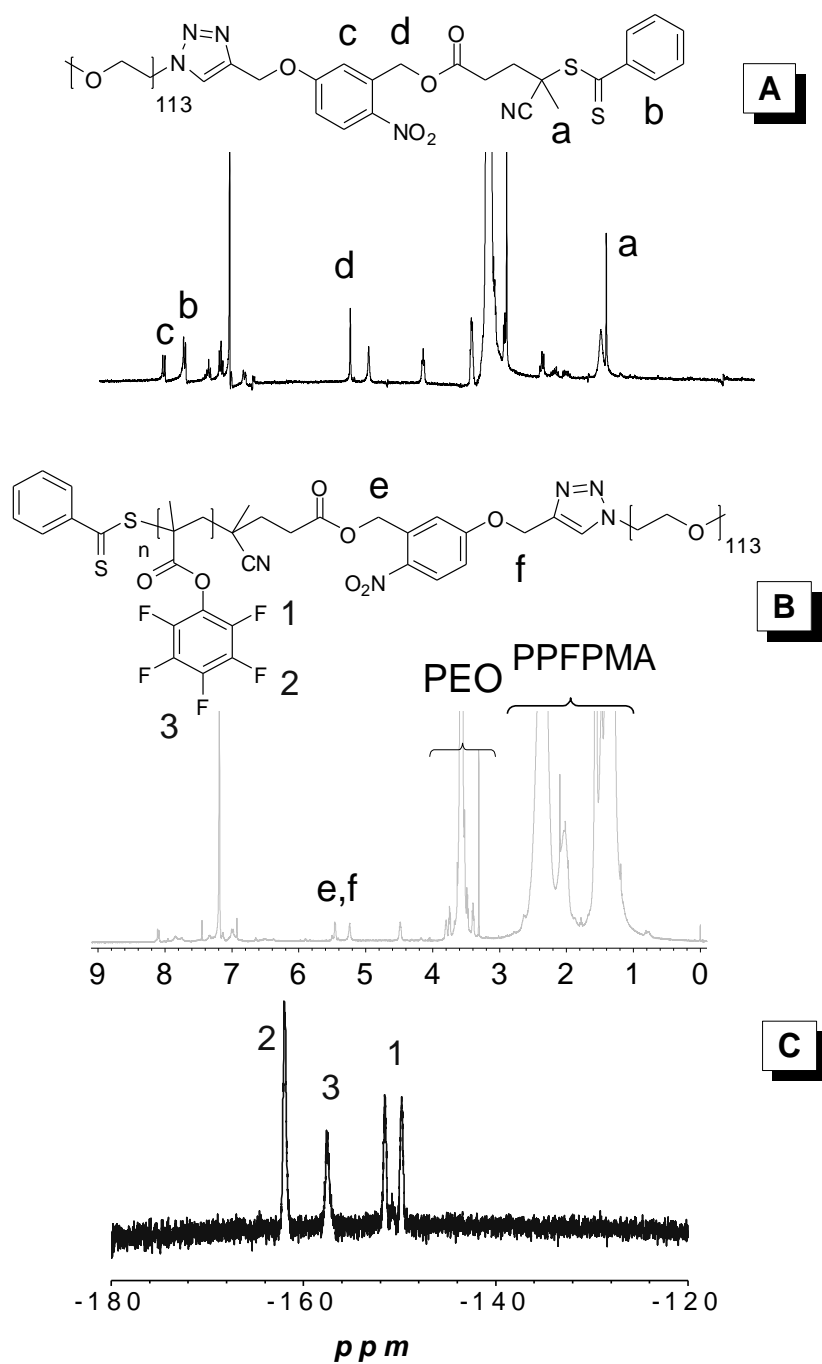


Figure 3.1.1 ^1H NMR for Macro-CTA (A) and PEO-*h\nu*-PPFPMA (B) in CDCl_3 . ^{19}F NMR for PEO-*h\nu*-PPFPMA (C) in CDCl_3 .

The photolysis of the photocleavable block copolymers was investigated by exposing solutions of this copolymer in THF to UV irradiation ($\lambda = 365$ nm, 500 W UV lamp). As shown in Figure 3.1.2 A, the

UV-visible absorption spectrum of **P4** changed significantly over the course of irradiation time. The absorption intensity at 310 nm (associated with the *ortho*-nitrobenzyl moiety) decreased with increasing irradiation time, while additional bands appear between 350 and 450 nm due to the formation of the *ortho*-nitrosobenzyl functionality.⁵⁶ The photocleavage of ONB proceeded rapidly under a high intensity 500W UV source, with complete photolysis reached within 15 min. Photocleavage was also confirmed by GPC, **Figure 3.1.2** analysis shows the complete photocleavage of PEO-*hν*-PPFPMA. After UV irradiation (1 h), the peak at the elution time associated with the block copolymer becomes two lower molecular weight peaks, which were assigned to PEO and PPFPMA respectively.

Preparation and functionalization nanoporous thin films.

The strong hydrophobicity of the PPFP or PPFPMA block results in a large Flory-Huggins parameter (χ) between PPFP/PPFPMA and PEO, which should result in strong phase-separation. The diblock copolymers **P3** and **P4** were annealed at 160 °C for 24 hours, followed by small angle X-ray scattering analysis (SAXS) to investigate the phase separated morphologies.

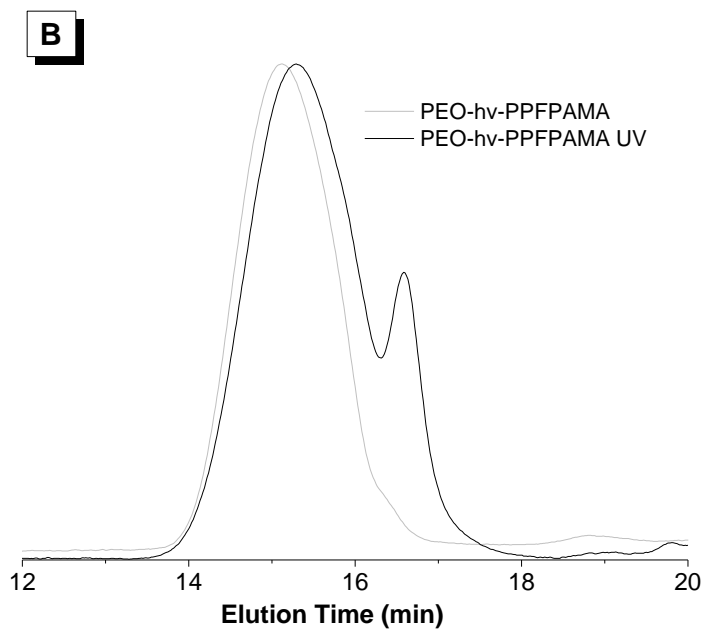
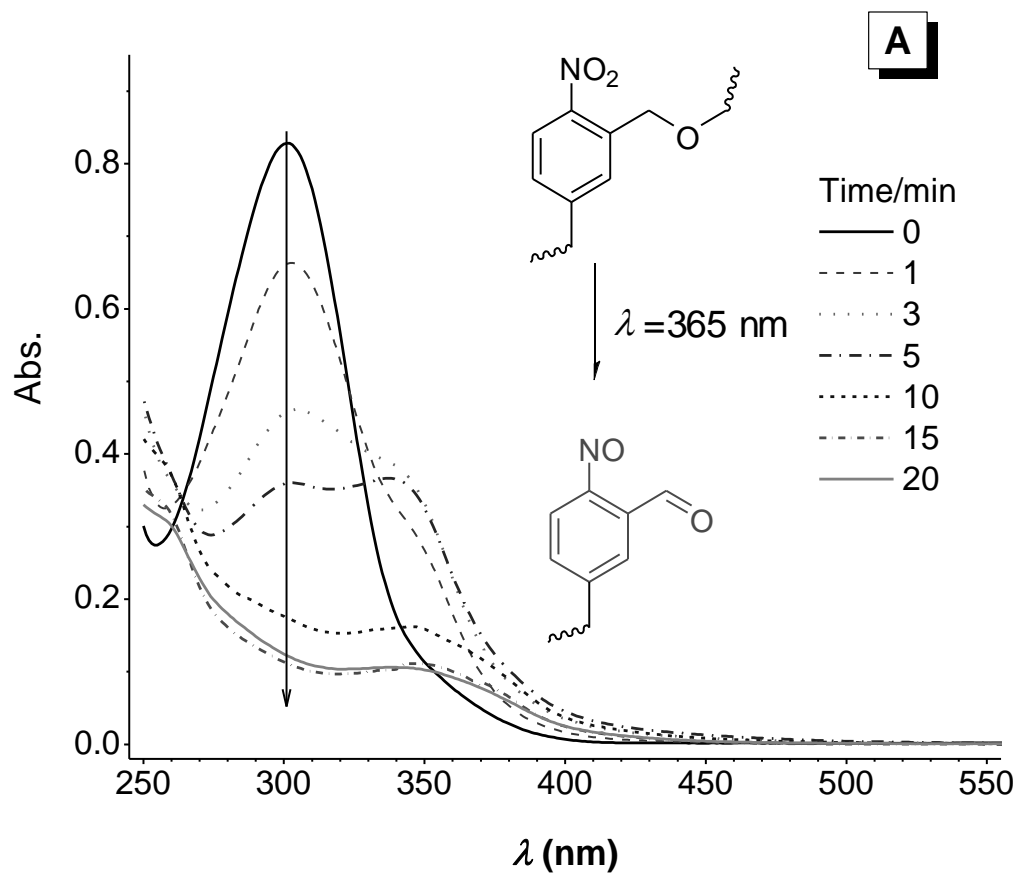


Figure 3.1.2 UV spectra (A) (Concentration: 0.02 mg/mL, THF) and GPC trace (B) for PEO-*hv*-PPFPMA before and after UV in THF.

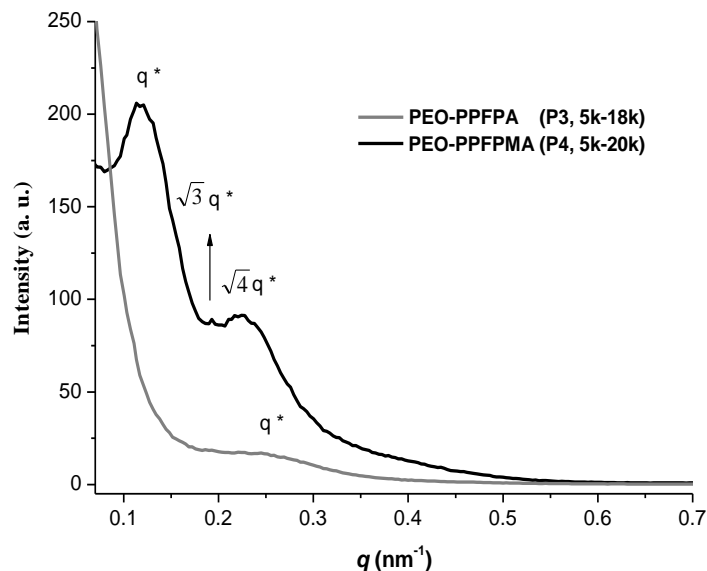


Figure 3.1.3 SAXS for PEO-*hν*-PPFPA (P3, 5k-18k) and PEO-*hν*-PPFPMA (P4, 5k-20k) after thermal annealing at 160 °C 24h. Gray, P3; black, P4.

As shown in **Figure 3.1.3**, SAXS results show that both samples display phase separation. However, PEO-*hν*-PPFPMA featured a better phase separation behavior than PEO-*hν*-PPFPA: a first order reflection at $q^* = 0.117 \text{ nm}^{-1}$ and two higher order reflections at $q_2 = 0.187 \text{ nm}^{-1}$ ($\sqrt{3} q^*$) and $q_3 = 0.229 \text{ nm}^{-1}$ ($\sqrt{4} q^*$) were observed, indicative of hexagonally packed cylindrical PEO microdomains oriented normal to the film surface. Solvent annealing was performed to further refine the morphology. After water/THF (0.1 ml/0.2 ml) mixture solvent annealing for 2.5 h at 20 °C, the thin film surface morphologies were analyzed by Atomic Force Microscopy (AFM). As shown in **Figure 3.1.4**: the sample P4 showed quasi-hexagonally packed circular microdomains, which are characteristic of PEO cylindrical microdomains oriented perpendicular to the substrate, while P3 is in disordered state. The average center-to-center distance of adjacent cylinders in **Figure 3.1.4C** was calculated to be 50 nm, which was consistent with SAXS results (53 nm).

The high reactivity of activated esters to amines facilitates the functionalization of these thin films. To demonstrate the simple post-modification, thin films of PEO-*hν*-PPFPMA were treated with UV

irradiation ($\lambda = 365$ nm, 6 W) for 12 hours and then immersed in solutions of amines (hexamethylene diamine/cysteamine, molar ratio: 2/1) in methanol to remove the minor PEO block while simultaneously functionalizing the polymer matrix. The PFPMA matrix was reacted with two amines; the first a difunctional amine to crosslink the matrix and the second, cysteamine, introduced thiol moieties, as shown in **Figure 3.1.4**. The nanoporous morphology of the thin films remained after UV irradiation, methanol rinsing and amine modifications (**Figure 3.1.4**). This is remarkable considering the extensive post-modification applied to the films. The pore size is around 33 nm, which is similar to that before UV and methanol treatment (pore size around 35 nm). XPS measurements confirmed successful post-modification of the thin films. Firstly, the F1s peak at a binding energy of 686 eV (**S2 A**) from the pentafluorophenyl ester PFPMA-*h* ν -PEO completely disappeared after post-modification (**S2 B**); Moreover, N1s and S2p binding peaks appeared at 402 and 165 eV respectively, which means that the PFP ester was successfully converted to imide in the thin film. However, XPS is only useful for diagnosis of surface film layers and may not accurately describe the chemical composition in the bulk film. Although we do not have conclusive proof that the post-modification was complete throughout the entire film from XPS results, we speculate the conversion is high, as our previous studies have shown that thicker (more than 100 nm) PFPA-based polymer films could be converted quantitatively with amines, as characterized by FTIR spectroscopy.⁵⁷

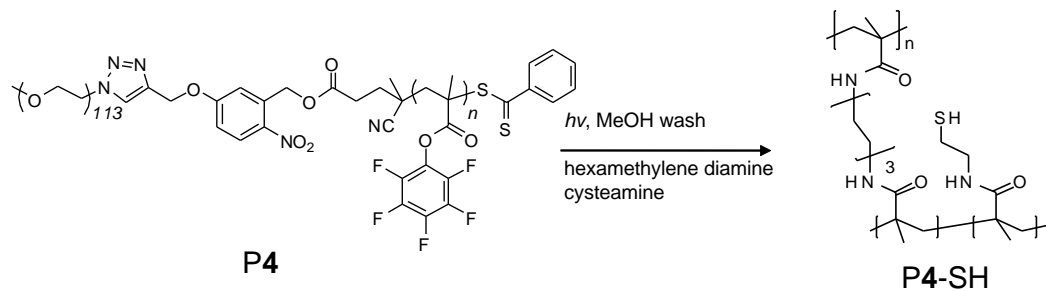
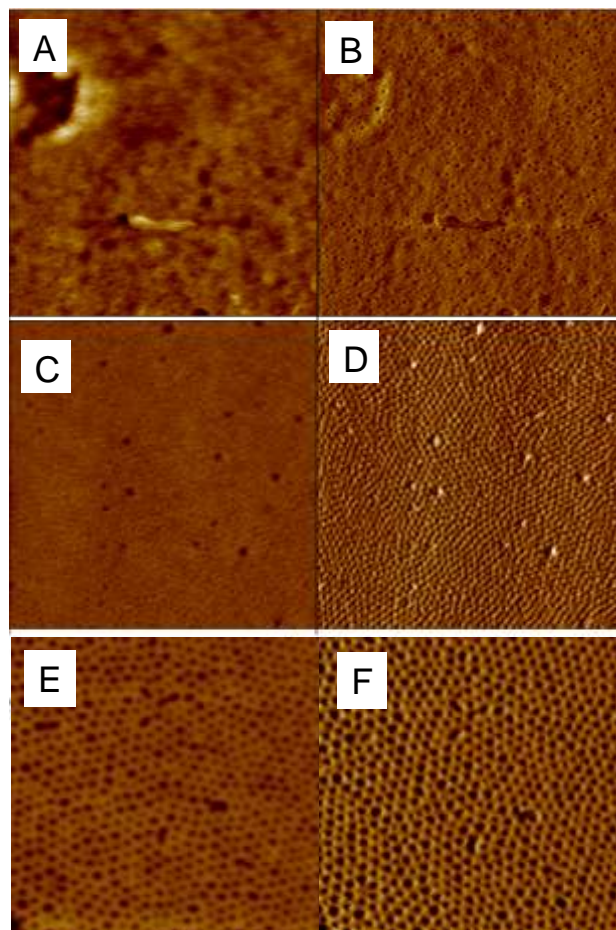


Figure 3.1.4 AFM images for PEO-*hv*-PPFPA (P3, 5k-18k, A: Height, B: Phase), PEO-*hv*-PPFPMA (P4, 5k-20k, B: Height, D: Phase) after water/THF annealing 2.5 h, 20°C, and image (E: Height, F: Phase) for PEO-*hv*-PPFPMA after UV and post-modification treatment with amines. Scale: 2 μm x 2 μm (A-D), 1 μm x 1 μm (E: Height, F: Phase).

Functionalized nanoporous fibers

Polymer nanofibers have attracted much interest for their varieties of applications, such as reinforcing component in composite systems,⁵⁸ templates for preparation of functional nanotubes,⁵⁹ biomedical and filter applications.⁶⁰ In a previous study, Boerner and coworkers showed

that the surface of PFP homopolymer nanofibers could be functionalized with suitable bioactive entities.⁶¹ Successful preparation of reactive nanoporous thin films based on PEO-*hν*-PPFPMA, encouraged us to make reactive and nanoporous fibers from PEO-*hν*-PPFPMA via electrospinning from a 1:4 (v:v) DMF/THF solution. As shown in **Figure 3.1.5A**, the diameter of the fibers ranged from 800 nm to 2 μm. After water/THF (0.1 ml/0.2 ml) annealing for 2 h, phase separation was observed by SEM and PEO cylinders were likely oriented parallel to the fiber direction due to the electro-spinning process.⁶³ Functionalized porous fibers were obtained by a similar procedure as that described above for the fabrication nanoporous thin films; UV irradiation followed by methanol rinsing and the reaction with an amine solution. In this case, a fluorescent amine, 4-nitro-7-(piperazin-1-yl)benzo[c][1,2,5]oxadiazole (NBD), was used for functionalization. As shown in SEM images **Figure 3.1.5 (C and D)**, the fiber structures remained completely intact and the surfaces displayed a nanoporous structure. The fluorescent confocal microscope image of the NBD-modified fibers showed a direct proof of successful dye-modification. Under 588 nm UV excitation, the fibers show strong green fluorescent emission (**Figure 3.1.5F**).

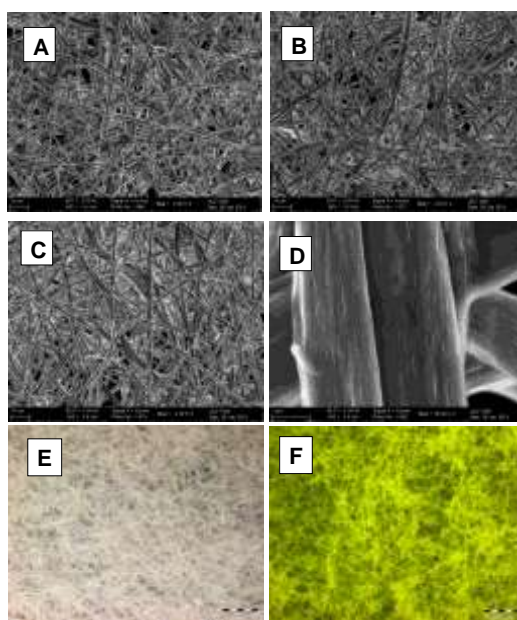


Figure 3.1.5 SEM images for fibers (A, B) before and (C, D) after THF/water annealing. Optical microscope image (E) and confocal microscope image (F) of NBD dye functionalized porous Fibers. Scales, A, B, C: 10 μm, D: 1 μm, E and F: 100 μm.

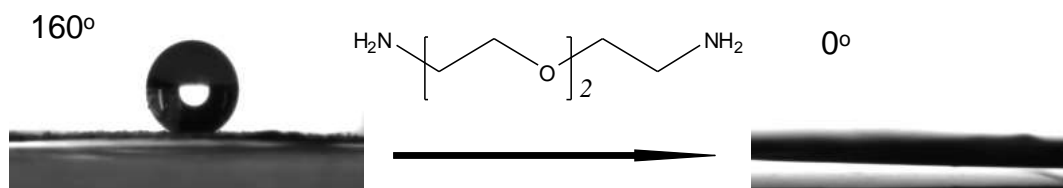


Figure 3.1.6 Contact angle of PPFMA-hv-PEO Fibers as electrospun and after UV irradiation, methanol washing and as 2,2'-(ethane-1,2-diylbis(oxy))diethanamine post-modification.

Electrospun polymer nanofibers films generally show superhydrophobic wetting behavior and therefore are used in special surface applications.⁶² Our PEO-*hv*-PPFPMA fiber mats indeed showed superhydrophobic behavior with static contact angles up to 160°. However, as shown in **Figure 3.1.6**, the fiber mats can be transformed to superhydrophilic by simple post-modification with Jeffamine. The measured water contact angle was zero after the fiber mats were allowed to react with 2,2'-(ethane-1,2-diylbis(oxy))diethanamine in a methanol solution at 30 °C for 12 h. FTIR indicated the reaction between the poly(FPMA) block and the amine was almost quantitative. The characteristic PFP ester band at 1780 cm⁻¹ nearly disappeared while an imide band at 1640 cm⁻¹ appeared (**S4**). This superhydrophobic to superhydrophilic transformation showed that our reactive fibers could have their properties significantly altered by this simple modification procedure, while featuring a porous structure. Further exploration of this dual porosity of fiber mats and porous fibers is currently underway.

Conclusions

In this work, photocleavable block copolymers featuring pentafluorophenyl ester moieties in one block were obtained by RAFT polymerization. Nanoporous thin films and nanofibers were prepared from PFP-containing photocleavable block copolymers. PFP-containing thin films and fibers show potential for making functional materials based on activated ester-amine substitution chemistry. The efficient post-modification of thin films and fibers was demonstrated by successful preparation of thiol-functionalized nanoporous thin films, and fluorescently labelled as well as superhydrophilic nanofibers.

3.2 Photocleavable Triblock Copolymers Featuring Activated Ester Middle Blocks: Synthesis and Application as Nanoporous Thin Film Templates

Introduction

Nanoporous thin films have attracted continued interest for their potential applications as templates,⁴⁵ separation materials,⁶⁴ and other advanced applications.⁶⁵ Placing reactive functional groups on the pore walls is critically important for allowing post-modification and host-guest interactions.⁶⁶ Several strategies have been developed for the fabrication of porous thin films featuring reactive pores. Russell and coworkers reported nanoporous thin films from polystyrene-*block*-poly(ethylene oxide) with a disulfide group as a junction.⁶⁷ Porous structures with thiol groups on the pore surfaces were formed after *D,L*-dithiothreitol treatment and methanol washing. This kind of diblock copolymer with a protected reactive junction group provided a facile method for fabricating reactive nanoporous thin films. However, the density of the pore surface functional groups introduced by this strategy is relatively low, which will hinder further advanced applications of the reactive thin films.

Higher density of pore surface functionality can be obtained from a triblock copolymer with a reactive middle block. However, the synthesis of triblock copolymers with reactive middle blocks has previously involved multiple synthetic steps, making it a synthetic challenge. For example, Hillmyer and coworkers once used a multiple-step synthesis to prepare polystyrene-*block*-poly(dimethylacrylamide)-*block*-polylactide, in which the midblock poly(dimethylacrylamide) was transformed to poly(acrylic acid) after hydrolysis.^{53a} Additionally, the reported functional groups on the pore walls in the thin films were only partially active and reacted under limited conditions. Hence, there is a strong demand for efficient and simple synthetic routes toward nanoporous thin films with a high density of reactive functional groups.

In this work, as shown in **Figure 3.2.1A**, a “one-step” synthesis route was developed to synthesize photocleavable triblock copolymers with a pentafluorophenyl ester containing middle block. Our approach is based on the well-known alternating copolymerization of styrene and maleimide.⁶⁸ By using an excess of styrene monomer, copolymerization with a given maleimide while using a poly(ethylene oxide) (PEO) chain transfer agent should produce a triblock copolymer with an activated ester middle block in one step. Our triblock copolymer system has three advantages: a) “one-pot and one-step” synthesis, avoiding multiple steps of polymerization, modification and purification; b) incorporating a photocleavable junction, an *o*-nitrobenzyl ester, between the PEO and poly(styrene-*co*-maleimide)-*b*-polystyrene, allowing the fabrication of highly-ordered nanoporous films under mild conditions,³⁵⁻³⁷ and c) the activated pentafluorophenyl ester is known to react with amines under very mild conditions, providing an efficient route to post-polymerization modification of the material.⁶⁹

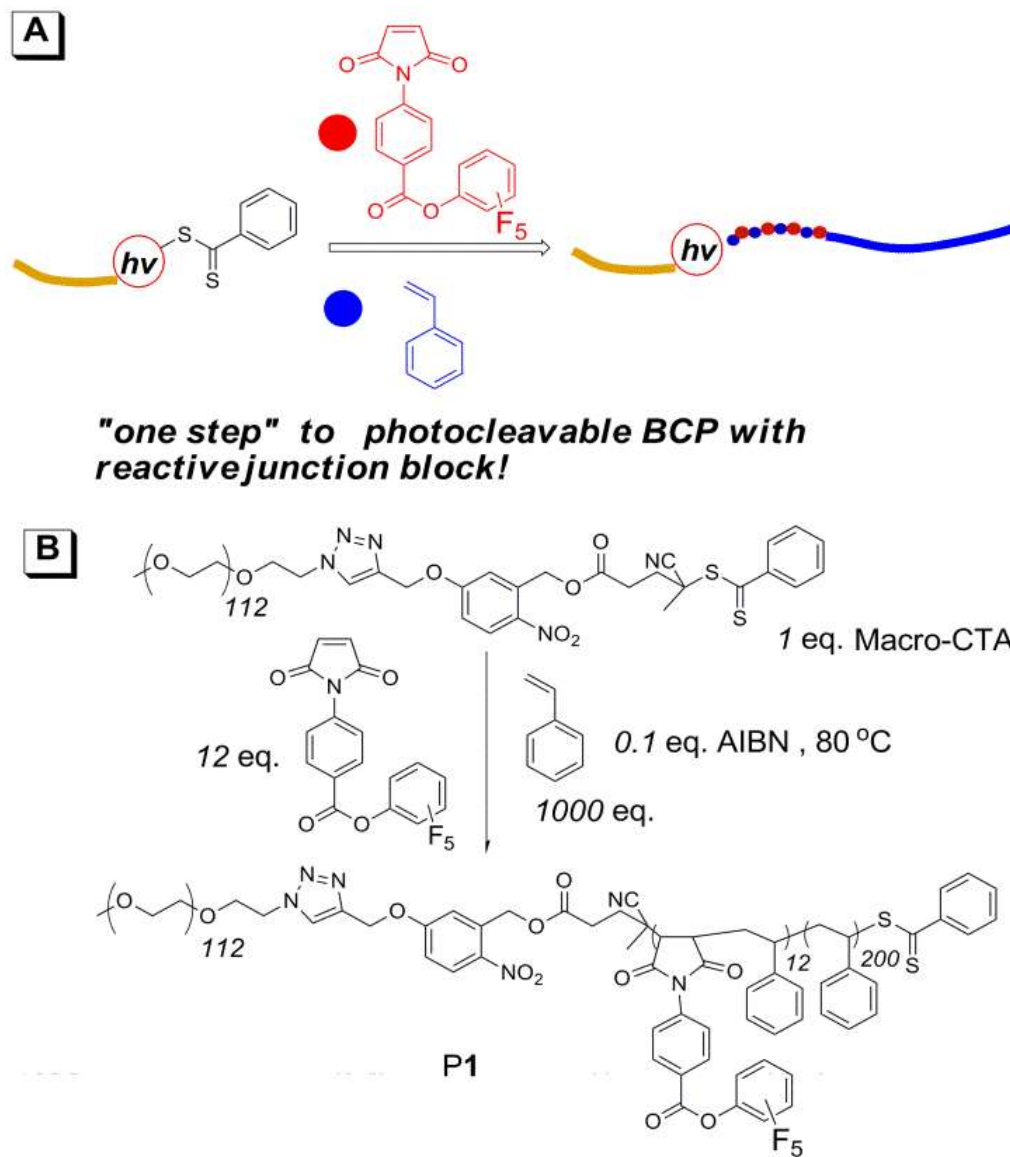


Figure 3.2.1 (A) Concept for “one-step” RAFT polymerization to produce reactive triblock copolymers. (B) Synthetic scheme for photocleavable triblock copolymers with a pentafluorophenyl ester middle block.

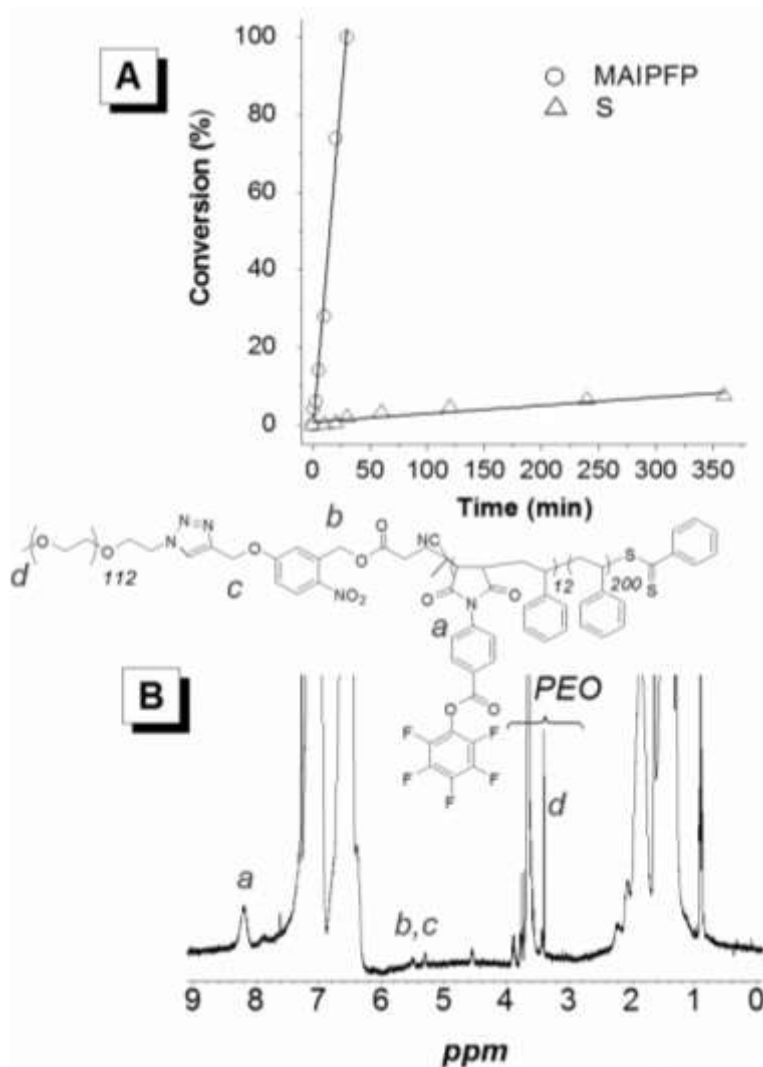


Figure 3.1.2 (A) Kinetic plots for polymerization of styrene (S) in the presence of pentafluorophenyl 4-maleimidobenzoate (MAIPFP), determined by ¹H NMR. (B) ¹H NMR of triblock copolymer PEO-*b*-P(S-co-MAIPFP)-*b*-PS (P1) in CDCl₃.

Results and Discussion

A poly(ethylene oxide) (PEO) chain transfer agent with an *o*-nitrobenzyl ester (ONB) junction (Macro-CTA) was synthesized by a CuAAC “click” reaction. Next, the RAFT polymerization of styrene in the presence of pentafluorophenyl 4-maleimidobenzoate (MAIPFP) and Macro-CTA was carried out in bulk at 80 °C under argon atmosphere with the ratio of [St]₀ / [MAIPFP]₀ / [Macro-CTA]₀ being 1000:12:1 (run 3 in Table 1). The polymerization kinetics was investigated by ¹H NMR measurements. The MAIPFP reached 100% conversion within 25 min, while the conversion of styrene at that time was 6%. Notably, while the polymerization rate of styrene is slow (the conversion reached around 20% after

16 hours), nevertheless, the polymerization was still living (**Figure 3.2.2A**). The polymerization kinetics clearly demonstrate that the MAIPFP was consumed at the very early stage during the polymerization. This indicates that the MAIPFP monomer was precisely incorporated as an alternating-structure middle block between the PEO and PS blocks. The length of middle block also can be controlled by changing the ratio between MAIPFP and CTA, provided styrene is used in large excess. For example, as shown in **Figure 3.2.2B**, the proton ratio between maleimide aromatic proton resonance *a* and the methyl ether end group of PEO *d* is 10:1, which corresponds to 15 MAIPFP units in the polymer. This value of MAIPFP units is in good agreement with the feed ratio between MAIPFP and Macro-CTA, which in this case was 12:1. Other data on middle block length are summarized in **Table 3.2.1**.

Table 3.2.1. RAFT polymerization of styrene and MAIPFP.^a

Run	MAIPFP repeat unit	MAIPFP repeat unit	M_n^b $g \cdot mol^{-1}$	M_w^b $g \cdot mol^{-1}$	\mathcal{D}^b
	<i>theory</i>	<i>NMR</i>			
1	3	4.5	30,300	35,800	1.17
2	9	11.5	27,300	32,300	1.16
3 (P1)	12	15.1	28,100	33,800	1.18
4	24	34.4	30,200	35,000	1.20

^a Bulk, 80 °C, 15 h, styrene conversion= 18-20%, MAIPFP conversion= 100% (at 25 min) determined by ¹H NMR in CDCl₃. ^b GPC in THF using linear PS standards.

Photocleavage was investigated by GPC measurements. P1 (10 mg/mL in THF) in a NMR tube exposed to a UV source (6 W, 365 nm) for 12 h. In **Figure 3.2.3**, GPC analysis shows the complete photocleavage of P1. After UV irradiation, the elution time peak associated with the block copolymer (33,800 *g/mol* in GPC) split into lower molecular weight peaks (20,100 *g/mol* and 7000 *g/mol* in GPC), which were assigned as cleaved P(MAIPFP-co-S)-*b*-PS and PEO from P1.

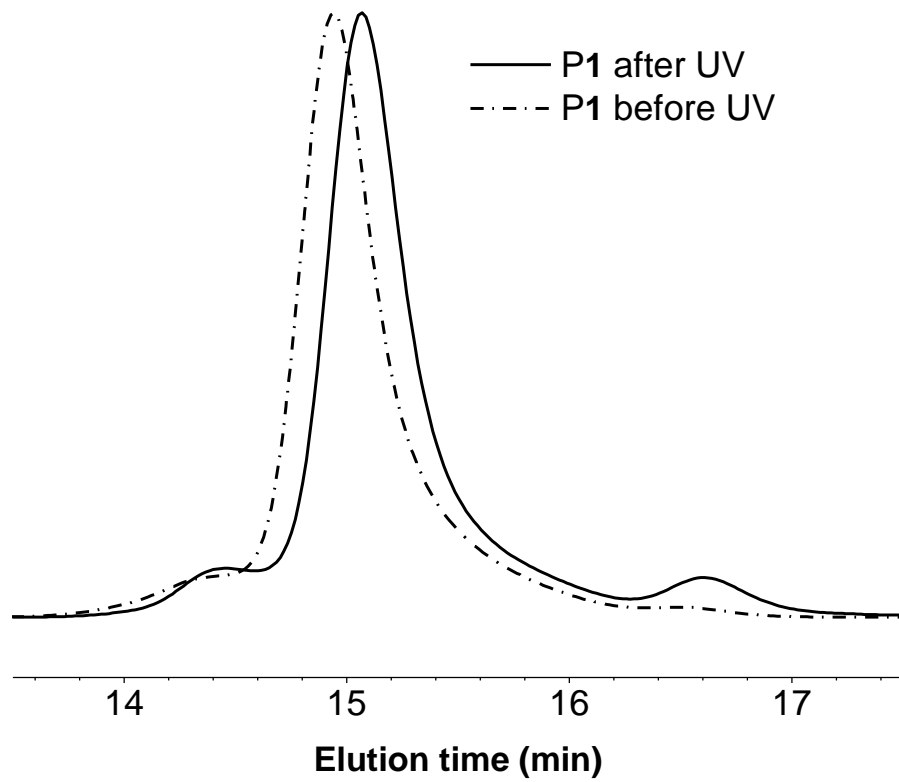


Figure 3.2.3 GPC trace for P1 before and after UV in THF.

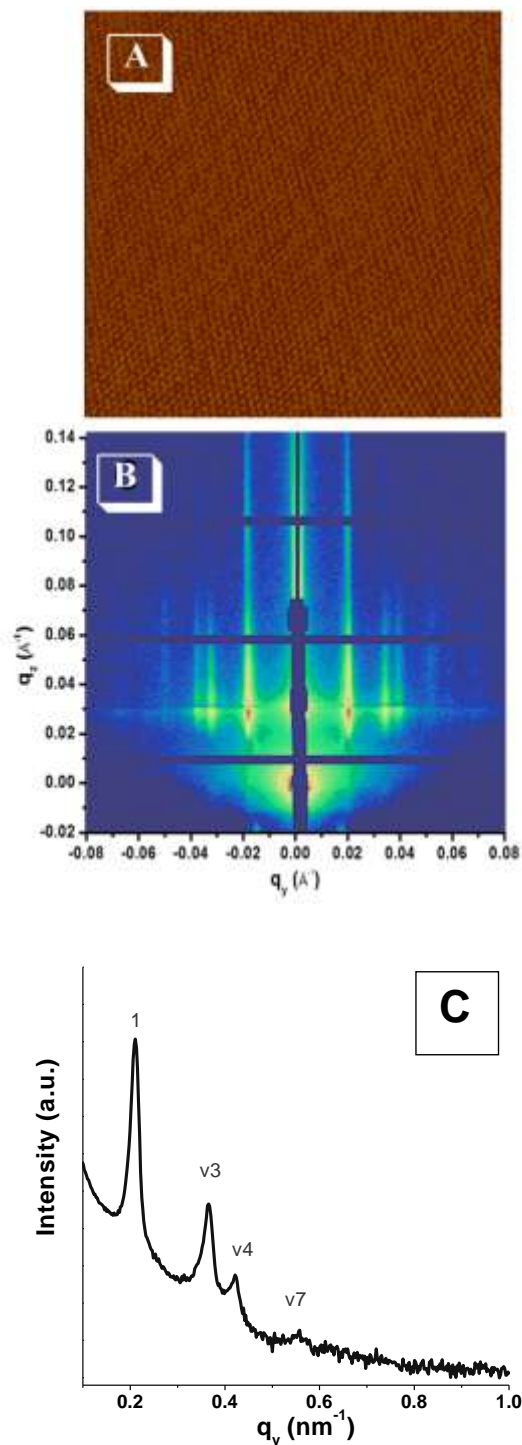


Figure 3.2.4 (A) AFM image for P1 thin film after water/THF annealing for 2.5 hours. (B) 2D GISAXS pattern for P1 thin film. (C) Intensity scans along q_y of the GISAXS patterns.

A 35 nm thick BCP thin film was prepared by spin-coating a solution of 0.8 wt % of P1 in toluene onto silicon substrates. Subsequently, the film was annealed in a THF/water vapor environment. The surface morphology of the annealed thin film was measured by atomic force microscopy (AFM) as

shown in **Figure 3.2.4A**. The highly ordered hexagonally packed arrays indicated that PEO cylinders were oriented normal to the substrate. Further, the static grazing incidence small-angle X-ray scattering (GISAXS) was used to characterize the thin films over a large area. An incidence angle of 0.2° , which is between the critical angle of polymer (0.16°) and silicon substrate (0.28°), was chosen so that the X-ray can penetrate into the film, where the scattering profiles are characteristic for the entire film. The corresponding 2D GISAXS pattern is shown in **Figure 3.2.4B**, in which, q_y represented the momentum transferred normal to the incident plane, i.e. parallel to the thin film surface while q_z is normal to the sample surface. Bragg rods (reflections extended along q_z) were seen, which was characteristic of cylindrical microdomains oriented normal to the film surface. The observed multiple order reflection peaks are characteristic of long-range ordering. A line scan in q_y is shown in **Figure 3.2.4C**. The first order reflection was at $q^* = 0.205 \text{ nm}^{-1}$ and the d spacing ($d = 2\pi/q^*$) was calculated to be 31 nm. Highly-ordered nanoporous thin films were formed after UV exposure and a successive methanol wash to selectively remove the PEO block. As can be seen from TEM images in **Figure 3.2.5A**, the nanoporous morphology is clear without need for any staining due to the large difference in electron density between the matrix and the empty pores. An average pore diameter of 16 nm and an average center-to-center distance between the pores of 35 nm were obtained, which is in good agreement with the GISAXS data.

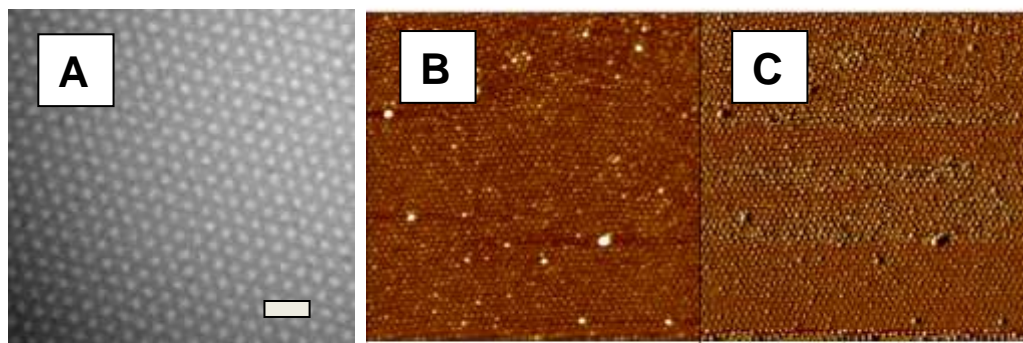


Figure 3.2.5. (A) TEM image of the nanoporous thin film from P1 after UV treatment and methanol wash, scale: 70 nm. (B) AFM phase image for iron oxide nanodots. (C) AFM height image for iron oxide nanodots. Scale for B and C: $2 \mu\text{m} \times 2 \mu\text{m}$.

To confirm the presence of reactive functional groups on the pore walls, the nanoporous film was immersed into a solution of 2-aminoethyl-ferrocene (Fc-amine) in ethanol, anchoring Fc-amine to the pore walls via the activated esters. The modified nanoporous films were then treated with oxygen plasma to remove the organics and convert Fc to iron oxide (Figure 3.2.5B and C). If, as we hypothesize, the reactive ester groups are located at the pore walls, iron oxide nanoring patterns should result. However, out of our expectation, as is shown in Figure 3.2.5B and C, we observed highly ordered nanodots with a diameter of around 20 nm. To explore the origin of nanodots formation rather than nanorings, TEM images were taken after Fc-amine modification and washing with methanol. As shown in Figure 3.2.6A, the Fc-amine appears to have aggregated in the center of the open pores rather than decorating the pore walls. This could be the result of unfavorable interactions between the hydrophilic Fc-amine and the hydrophobic pore walls. The aggregated Fc-amine can be removed after immersing the thin film into HCl solution (concentration: 0.1 M) for 3 hours (Figure 3.2.6B). However, no nanotorus was observed in the TEM after acid washing step. The electron density contrast between the Fc-amine functionalized pore walls and the PS matrix may not be sufficient enough to observe this sub-10 nm feature.

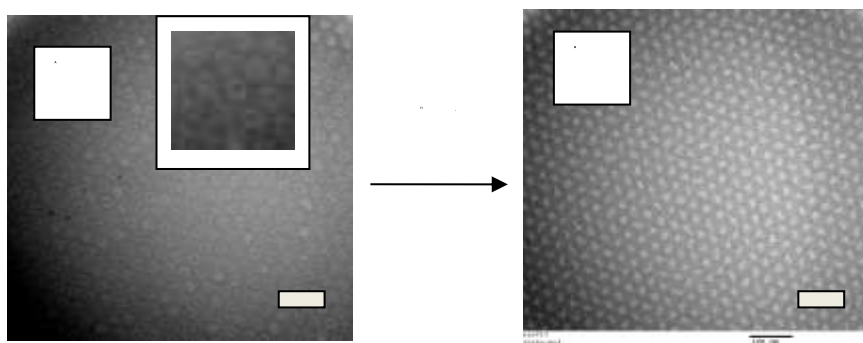


Figure 3.2.6 (A) TEM image of nanoporous P1 thin film after UV irradiation, Fc-amine post-modification, and methanol wash, scale: 70 nm. (B) TEM image for sample in **Figure 3.2.6A** after acid wash.

Finally, the sample as shown in **Figure 3.2.6B** was treatment with oxygen plasma, during which the functionalized porous thin film was transformed to iron oxide nanodonuts. The etching surface

morphology is shown in **Figure 3.2.7**. The average diameter of the torus was around 39 nm and their average height was around 1 nm. The torus had a minor radius 3.5 nm and a major radius 16 nm. These structures result from the activated esters located at the interface of the copolymer films that are exposed after PEO removal. The structure of the donuts supports our assertion that the alternating styrene-maleimide served a middle block between PEO and PS.

The resulting nanodonuts were further characterized by high resolution X-Ray photoelectron spectroscopy (XPS). The results are shown in **Figure 3.2.7D**. Two binding peaks can be seen at 725 and 710 eV, which were assigned to Fe 2p and Fe 2p_{1/2} in a γ -Fe₂O₃ sample, respectively. The XPS measurement once again demonstrates that we successfully postmodified the thin films with Fc-amine.

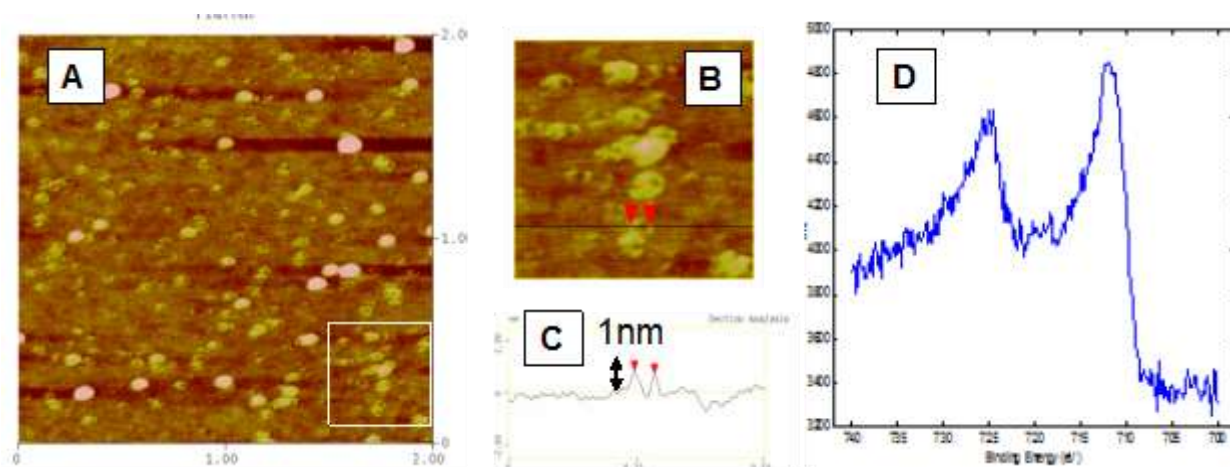


Figure 3.2.7 (A, B) AFM height images for iron oxide donuts. Scales: A, 2 μm x 2 μm ; B 0.5 μm x 0.5 μm . (C) Height profile in B, height scale is 2 nm. (D) High resolution XPS for sample shown in **Figure 6A**.

Conclusion.

In conclusion, we have demonstrated that activated ester-functionalized nanopores can be generated from photocleavable block copolymers with an activated ester middle block. The functionalities at the interface between the matrix and pore walls can then be used as handles to generate iron oxide nanodonuts. The results in this work present a unique example of a mild etching process and interface functionalization based on *o*-nitrobenzyl ester and activated ester chemistries. The method described here provides a broad range of possibilities, because the activated esters are reactive towards a large variety of amines that can lead to interesting applications in patterned materials.

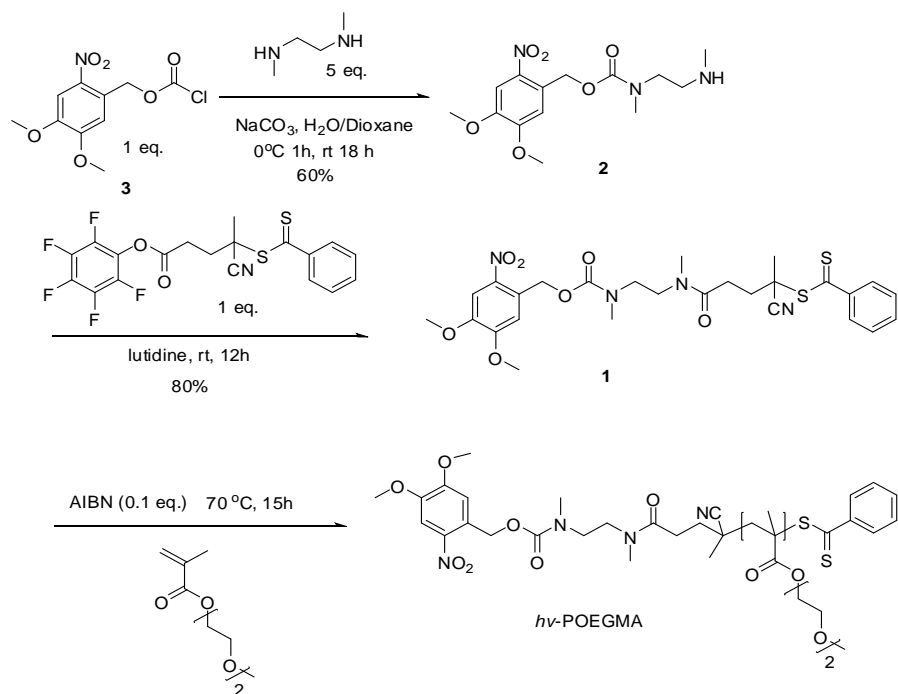
3.3 α -Photolabile Amine Semitelechelic Polymers for Light-induced Macromolecular Conjugation

Introduction

Increasing attention has been paid to block copolymers and biological/synthetic hybrid materials, causing a variety of strategies to be developed for synthesizing these materials using a macromolecular conjugation approach. Examples of these syntheses include copper catalyzed azide-alkyne cycloaddition (CuAAC),⁷⁰ thiol-ene and thiol-yne chemistries,^{71, 72} oxime formation,⁷³ Diels–Alder cycloaddition,⁷⁴ and the reaction of activated esters with amines.⁶⁹ Among conjugation approaches, UV light-induced macromolecular conjugation or surface-conjugation has attracted great interest as it can provide spatial and temporal control over these reactions that are not available to other chemistries. Until now, photo-triggered thiol-ene/yne has been explored by several groups.⁷⁵ Popik and coworkers reported selective labeling of living cells based on photo triggered acetylene-azide cycloaddition.⁷⁶ Barner-Kowollik and coworkers introduced UV light-induced Diels–Alder reactions for preparation of block copolymers and photo-patterning.⁷⁷

Activated ester-amine chemistry has many features of more conventional “click” chemistries, featuring metal free, mild condition reactions and a practically quantitative conversion. It has found wide application, including in peptide synthesis and preparation of well-defined reactive polymers and bio-hybrids.⁷⁸ However, there are only a few reports about light-triggered activated ester-amine chemistry, which would provide more spatial and temporal control about macromolecular conjugation. Recently, based on activated ester-amine chemistry, we synthesized a photolabile amine that can be successfully used for the preparation of reactive photopatternings.⁷⁹ These previous results encouraged us to develop a macromolecular conjugation chemistry based on this phototriggered activated ester-amine chemistry. In this work, we report an α -photolabile amine semitelechelic polymer that can be used for macromolecular conjugation based on light triggered activated ester-amine chemistry.

Results and Discussion



Scheme 3.3.1 Synthesis of photolabile amine CTA (1) and $h\nu$ -POEGMA.

Polymer Synthesis. Well-defined telechelic polymers featuring activated ester end groups have been previously studied.⁶⁹ The goal of our synthetic strategy was to place a photolabile amine at the end group of the polymer chain to enable a photo-triggered activated ester-amine conjugation. As shown in Scheme 3.3.1, an *o*-nitrobenzyl (ONB) protected amine functionalized chain transfer agent (**1**) was synthesized in two steps with a yield of around 50% (see experimental section for synthesis details). First the ONB mono-protected diamine (**2**) was synthesized via a one step reaction. Then the ONB protected amine CTA (**1**) was prepared by reaction of compound **2** with PFP-CTA under mild conditions. The CTA(**1**) was then successfully employed in the mediation of the RAFT polymerization of diethylene glycol methyl ether methacrylate (DEGMA) was mediated by CTA **1** in dioxane at 80 °C (Scheme 3.3.1). The kinetics of RAFT polymerization of DEGMA using CTA **1** are shown in Figure 3.3.1. A linear relationship was observed between the conversion of monomer (measured by proton

NMR) and time. After 4 hours, the monomer conversion reached about 40%. Additionally, the kinetics of polymerization were also examined by GPC. The molecular weight (M_n) measured by GPC increased linearly with time, with corresponding \bar{D} between 1.25 and 1.30 over the course of the reaction. Both the kinetic plots and low \bar{D} confirm that the polymerization follows controlled radical polymerization characteristics. The final polymer was purified by precipitation from n-hexane, and the ^1H NMR spectrum of the purified homopolymer is provided in Figure 3.3.2. As already shown in our previous studies, ONB of CTA normally remained intact after RAFT polymerization.³⁷ In Figure 3.3.2, the proton C was assigned to the resonance of end group ONB, which was clearly observed. The ratio between resonances C and B (phenyl from CTA) was around 1.15: 1.0. Therefore, we believe that the majority of ONB groups remained intact after RAFT polymerization.

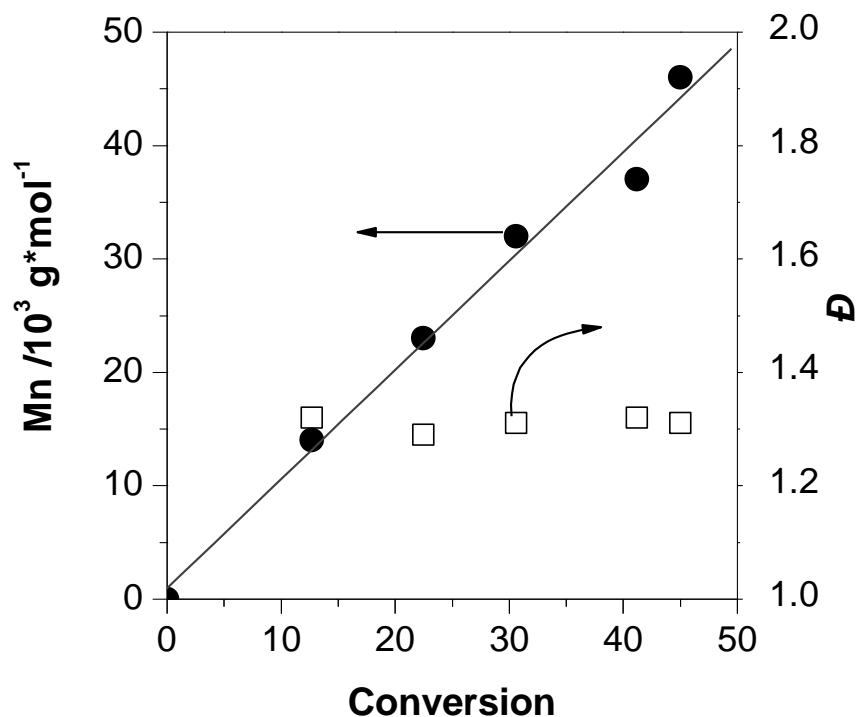


Figure 3.3.1 Kinetics of DEGMA RAFT polymerization as mediated by CTA **1** in dioxane at 80 °C. M_n and \bar{D} were measured by GPC using linear PS standards.

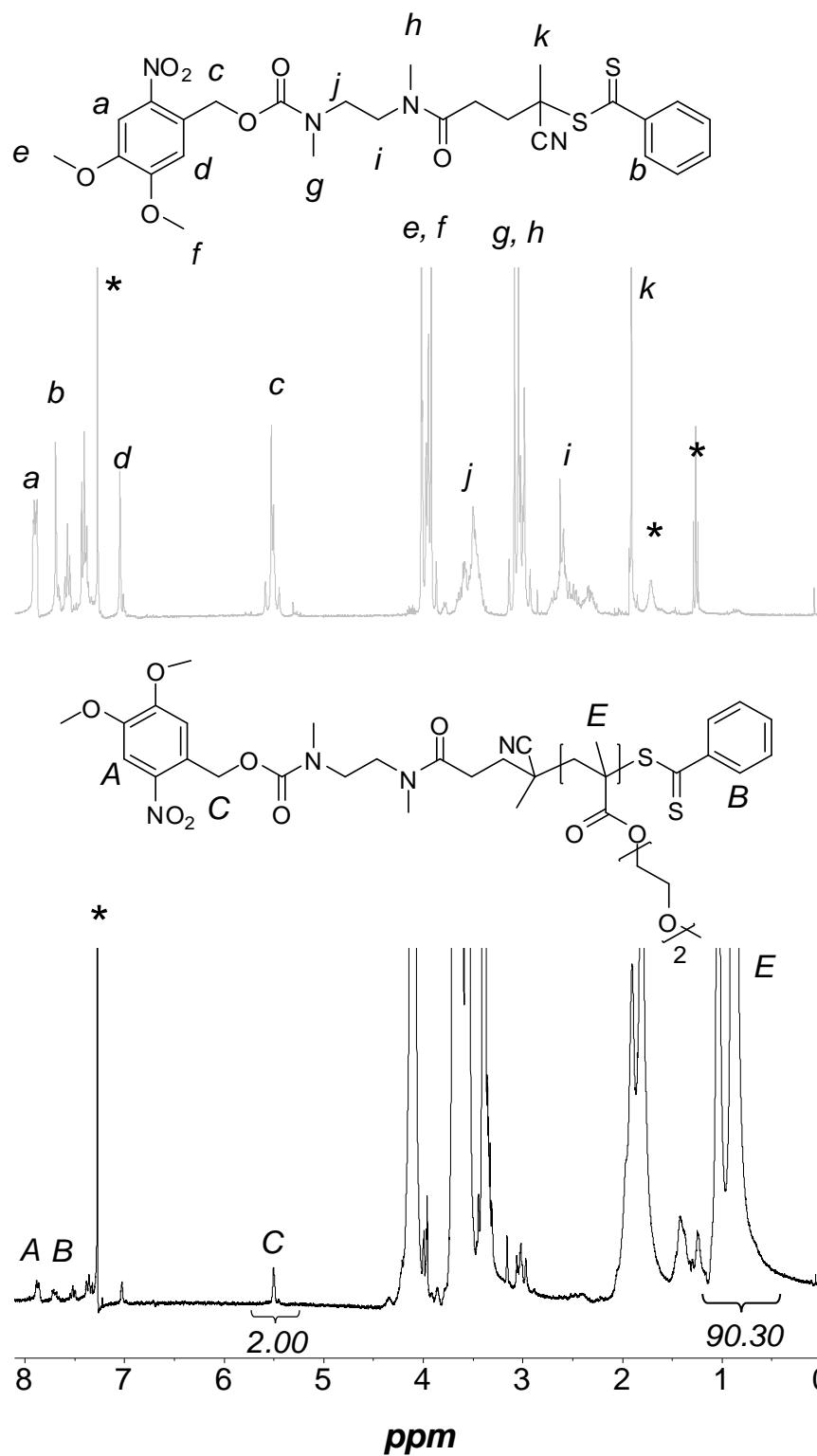


Figure 3.3.1 ^1H NMR of CTA 1 and $h\nu$ -Amine-PDEGMA in CDCl_3 .

Photolysis of Polymer with Photolabile Amine. Photolysis of the photolabile amine containing polymer was investigated by ^1H NMR and UV-Vis spectroscopy. Generally, CTA end group tend to react with amines, yielding thiol groups via an aminolysation. To avoid this side reaction, CTA end group was removed via treatment with an excess AIBN (ca. 30 equiv.) to the polymer P_0 in dioxane under $80\text{ }^\circ\text{C}$. As shown in Figure 3.3.2, the resonance at 7.72-7.36 ppm assigned to the aromatic group of the CTA end group disappeared completely (Figure 3.3.2), which indicated quantitative removal of the CTA end group. However, the resonances a, b and c assigned to the typical protons of the ONB protecting group⁸¹ were still observed after end group removal. Next, the photolysis reaction of the polymer P_0 in THF (ca. 30 mg/ml) was carried out in a NMR tube. The solution was irradiated using a UV lamp (6 W, wavelength = 365 nm) for 12 hours at room temperature. After the UV irradiation, the solution became deep yellow, which was the result of the formation of the *o*-nitrosobenzyl compound.⁸² The final product was purified by precipitating the crude solution from *n*-hexane three times. As shown in Figure 3.3.2, the proton resonance a, b and c in P_1 had completely disappeared, which indicated the complete removal of ONB protecting group. In early reports about ONB protected amines, there is often a side reaction⁸¹ between the coproduct *o*-nitrosobenzaldehyde and released amine. However, in our case, the released amine is a secondary amine, which is a poor substrate for this side reaction. There are no aromatic resonances in the ^1H NMR of P_2 , which further supports that the released amine did not react with *o*-nitrosobenzaldehyde. The photolysis reaction was also investigated by UV-Vis spectroscopy. The photocleavage of ONB proceeded rapidly under a high intensity 500 W UV source ($\lambda = 365\text{ nm}$), with complete photolysis within 30 min. As shown in Figure 3.3.3, the absorption intensity at 343 nm (associated with the *o*-nitrobenzyl moiety) decreased with increasing irradiation UV time. At the same time, additional peak appeared between 356 and 450 nm as the result of the formation of the *o*-nitrosobenzyl moiety (photochemistry shown in Figure 3.3.3).⁸⁰

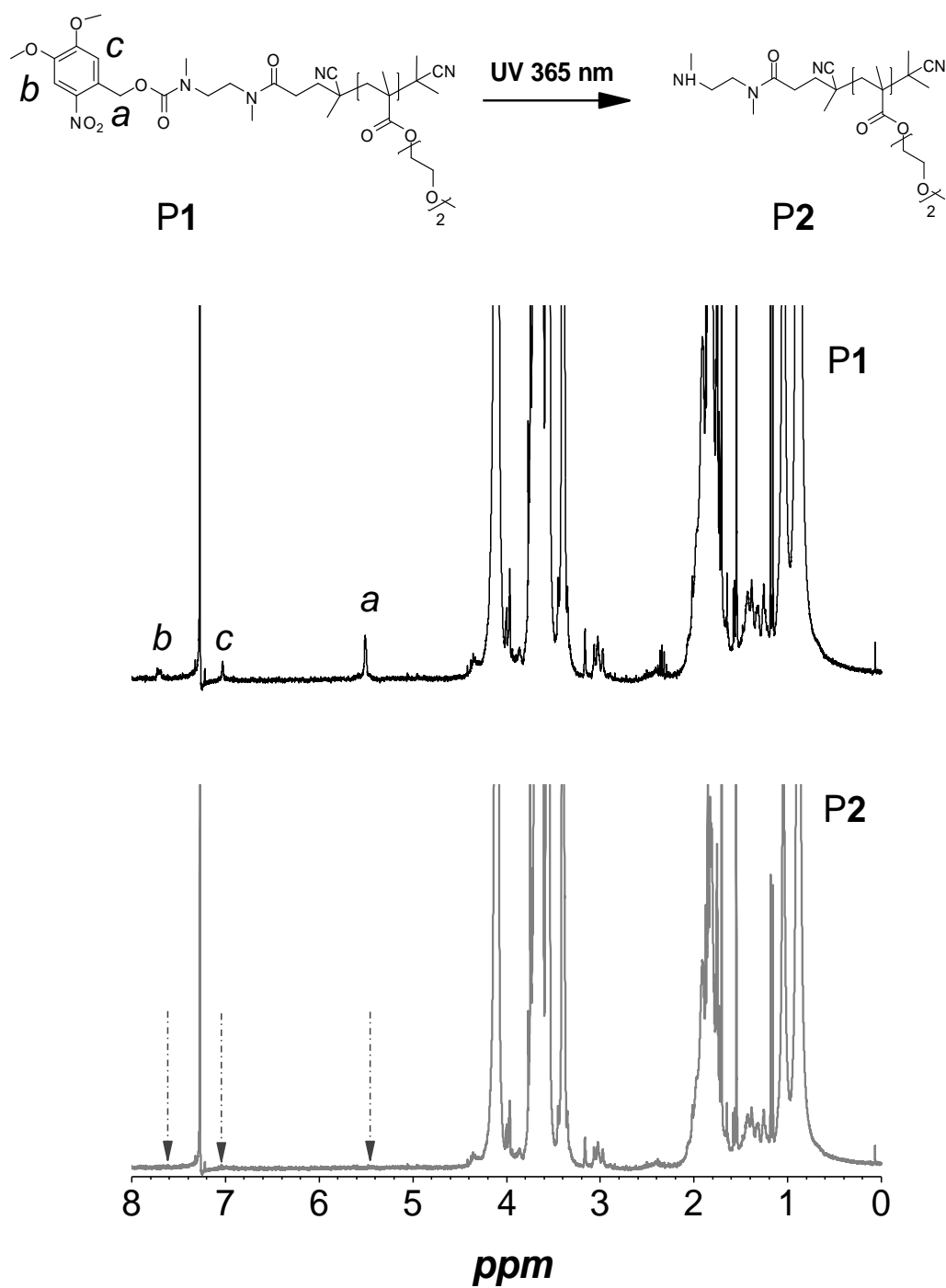


Figure 3.3.2. ¹H NMR of P1 and P2 in CDCl₃ showing disappearance of ONB protons after UV irradiation.

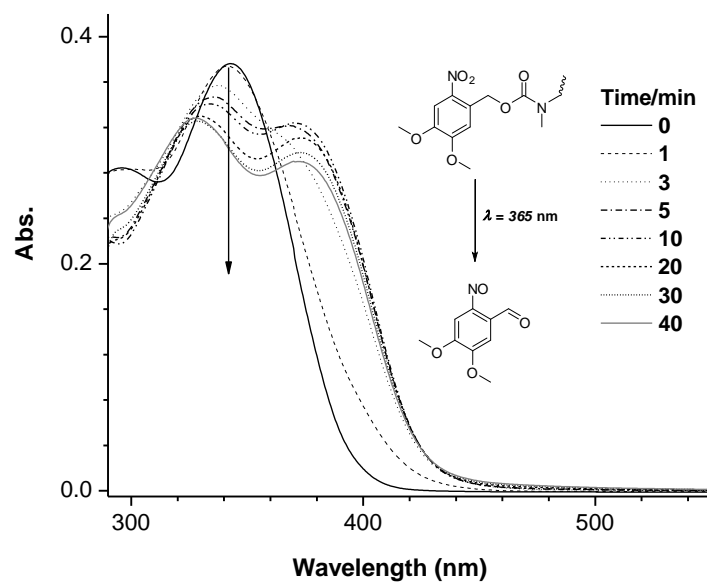
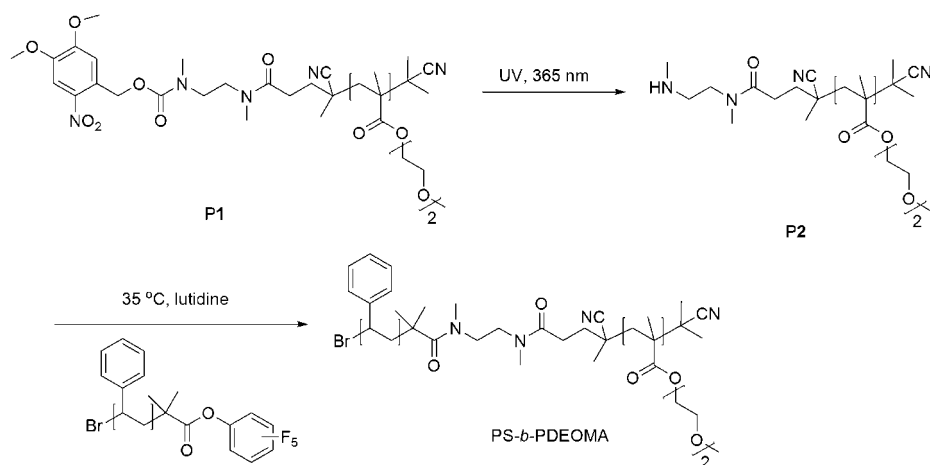


Figure 3.3.2. UV irradiation time dependent UV-Vis spectra of **P1** in THF (concentration: 0.02 mg/mL).

Macromolecular Conjugation. As shown in Scheme 3.3.2, macromolecular conjugation proceeded in two steps. First, photolysis of **P1** generated the free amine functionalized **P2**, followed by conjugation of **P2** to a PFP end functionalized polystyrene. A hydrophobic polystyrene was chosen as a the corresponding conjugation block, in order to simply purification and characterization of the obtained diblock copolymer.



Scheme 3.3.2 Synthesis of diblock copolymer **PS-*b*-PDEGMA** via light induced conjugation.

In this experiment, a molar ratio between **P2** and PS of 1.5: 1 was used. After stirring the solution at 40 °C for 24 hours, the final product was obtained by removing all solvent and washing the crude product with methanol three times to remove the excess of **P2**. The resulting material was characterized by ^1H NMR and GPC. The degree of polymerization (DP) of PS block was 130 units, which was calculated by both ^1H NMR and GPC using a linear PS as standard. The DP of DEGMA in **P2** was 30, which were calculated by monomer conversion (measured by ^1H NMR) and the ^1H NMR ratio between ONB group and main chain (see Figure 1). The DP of DEG could not be measured from GPC for there was not commercial available linear standard PDEGMA for GPC. DP of PDEGMA measured from GPC using a liner PS standard was around twice of which measured by ^1H NMR. As shown in Figure 3.3.4, the ratio between resonance *g* (phenyl groups in PS) and *a* (CH_3 group in PDEGMA main chain) was approximately 150: 89, which corresponds to a ratio of PS to PDEGMA was 1:1. This ^1H NMR result confirmed that the conjugation was successful. Further, GPC measurements were conducted to characterize the conjugation reaction. As shown in Figure 3.3.5, the GPC trace of PS-*b*-PDEOMA showed a narrow single peak, which was clearly shifted to higher molecular weights (15100), when compared to the GPC traces of PS (13500) and POEGMA (11000), confirming the successful conjugation

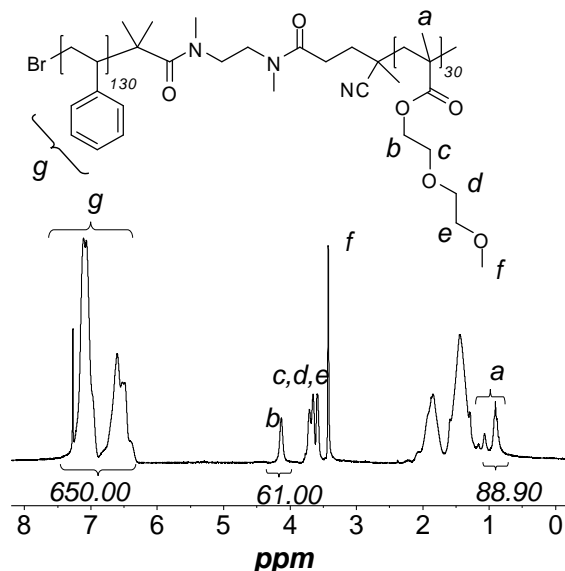


Figure 3.3.4 ^1H NMR of PS-PDEGMA in CDCl_3 .

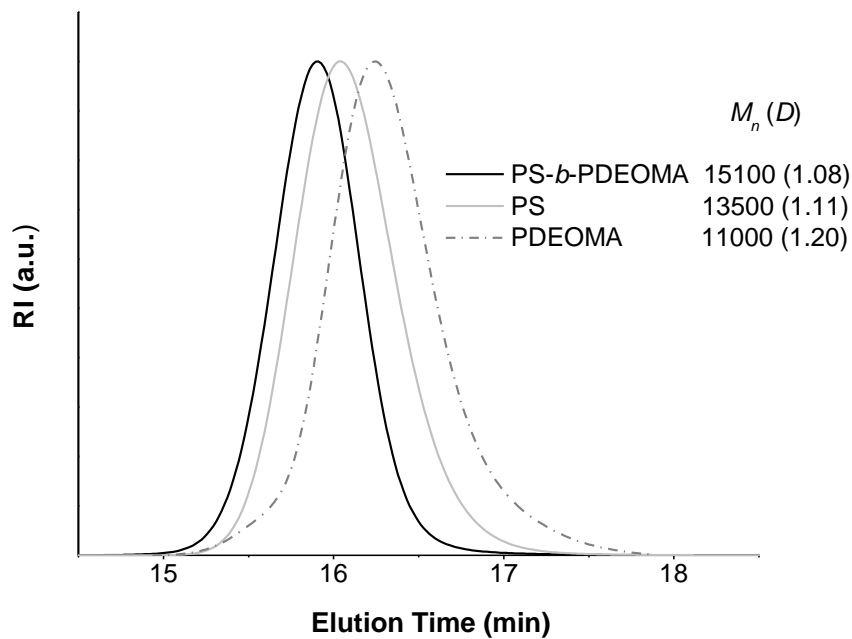
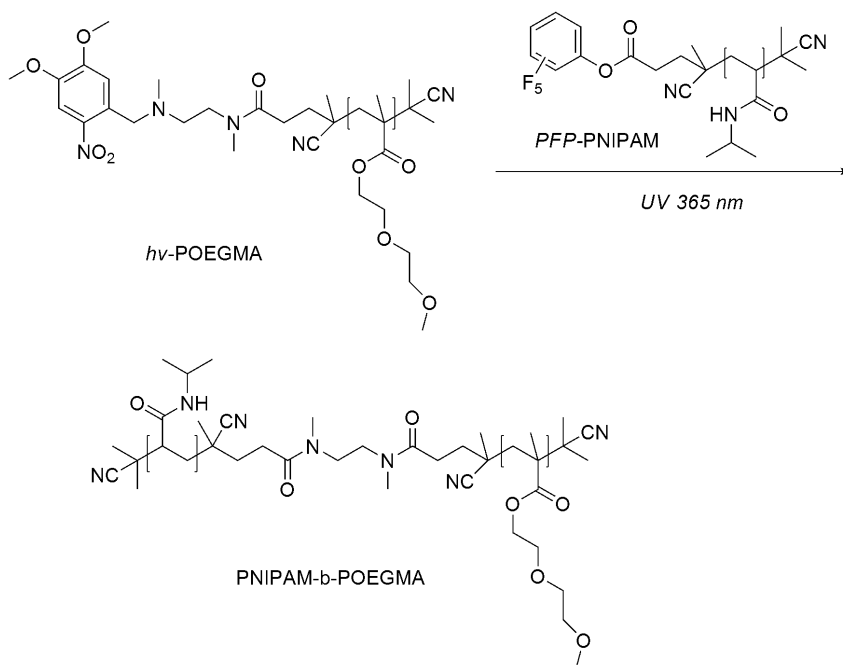


Figure 3.3.5 GPC trace in THF for PFP functionalized PS, ONB-amine functionalized POEGMA and diblock PS-*b*-POEGMA



Scheme 3.3.3 Synthesis of diblock copolymer PNIPAM-PDEGMA via light induced conjugation.

Additionally, a hydrophilic PNIPAM was used as conjugation block. As shown in Scheme 3.3.3, the block copolymer was produced in one step (molar ratio, PNIPAM/PDEGMA = 2/1, 20 °C in water, 12h). Both PNIPAM and PDEGMA are well-known thermal responsive polymers and accordingly, after irradiation for 12 hours under a 6 W UV source, the reaction solution was collected for further cloud point measurement. Figure 3.3.5 shows the LCST curve measured of PNIPAM, PEDOMA and PNIPAM-*b*-PDEOMA still containing the excess PNIPAM. The PNIPAM-*b*-PDEOMA in Figure 3.3.6 was the product of UV induced conjugation between P1 and PFP functionalized PNIPAM. As shown in Figure 3.3.6, the PNIPAM-*b*-PDEOMA/PNIPAM featured a LCST phase transition between 28 and 32 °C, which was attributed to be the phase separation occurring when both stimuli-responsive blocks collapsed. However, the temperatures below LCST of PNIPAM and above the LCST of PDEGMA, an amphiphilic block copolymer should be formed, which form micelles, as known for other block copolymers featuring two blocks with two different properties. To confirm the formation of micelles, dynamic light scattering (DLS) measurements were performed at different temperatures. Figure 3.3.7 shows the evolution of the D_h of the PNIPAM-*b*-PDEGMA/PNIPAM as the temperature was changed. At 20°C, all blocks in a hydrophilic state and hence the block copolymer was molecularly dissolved in water with an average D_h value of 6.0 nm. Upon increasing the temperature to 28°C, which is above the LCST of the PDEGMA block but below the LCST of the PNIPAM block, a significant change in the size and size distribution was observed. An average value of D_h of 70.0 nm was measured, indicating the formation of micelles due to the temperature induced collapse of PDEGMA block. Increasing temperature up to 33°C, which is above both blocks' LCST, a larger D_h value (around 800 nm) was observed due to collapse of the PNIPAM block and aggregation of micelles, which is also responsible for the turbidity measurement shown in Figure 3.3.6.

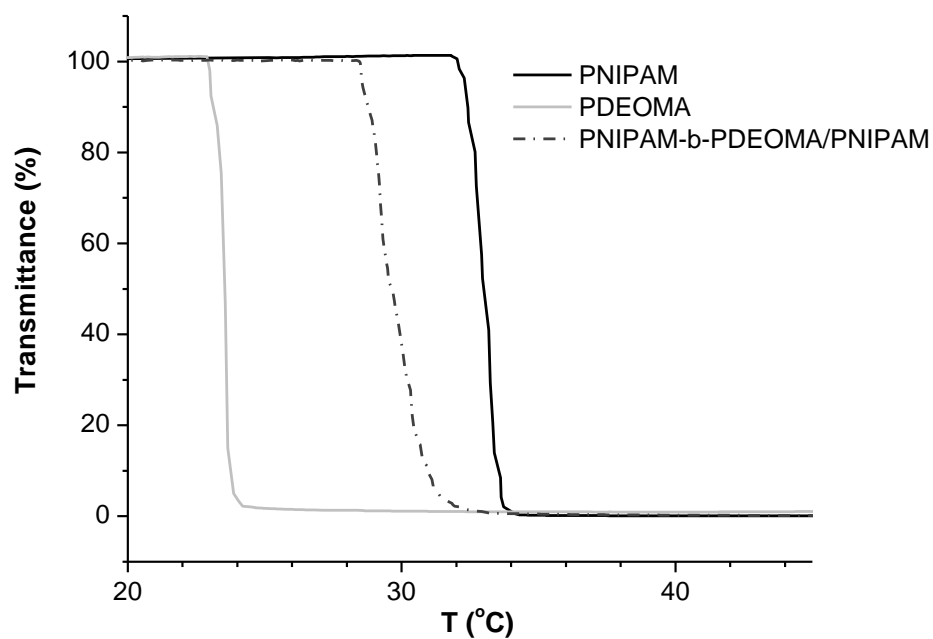


Figure 3.3.6 LCST heating curve of PNIPAM, PDEGMA and PNIPAM-b-PDEGMA/PNIPAM in water.

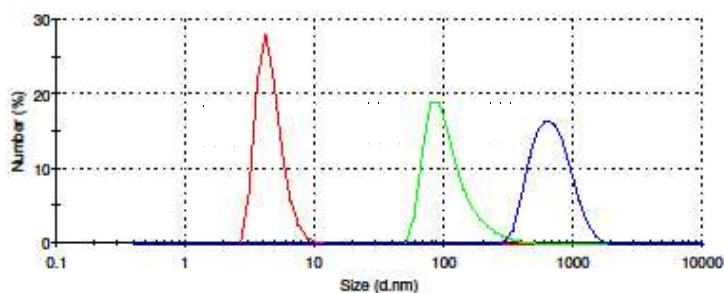


Figure 3.3.7 Temperature dependent change of the hydrodynamic diameter D_h of PNIPAM-*b*-PDEGMA/PNIPAM in water. Red line, measured at 20 °C; green line, measured at 28 °C and blue line, measured at 33 °C

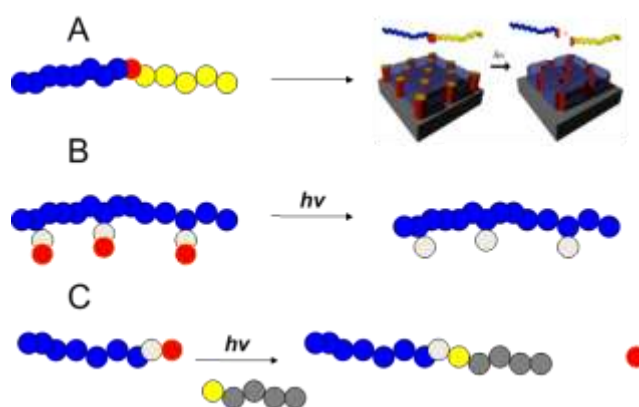
Conclusion.

In summary, we presented a facile synthetic method for light-induced macromolecular conjugation of an α -photolabile amine semitelechelic polymer based on activated ester-amine chemistry. The

successful conjugation of the α -photolabile amine semitelechelic polymer to PFP functionalized polymers was confirmed by ^1H NMR, GPC, LCST and DLC measurements. This work lays the foundation to conjugation of homopolymers by irradiation and thereby provides the precision and flexibility required in the area of bioconjugation and surface modification.

4 Overview of Results

As briefly illustrated in Scheme 4.1, the projects in this thesis include three parts. First, part A, the concept of nanoporous thin films from photocleavable BCPs will be introduced. Next, part B, the synthesis of well-defined polymers containing ONB in the side chains and applications as photopatterns will be introduced. Finally, part C, light-triggered macromolecular conjugation based on end group containing ONB polymers will be introduced.



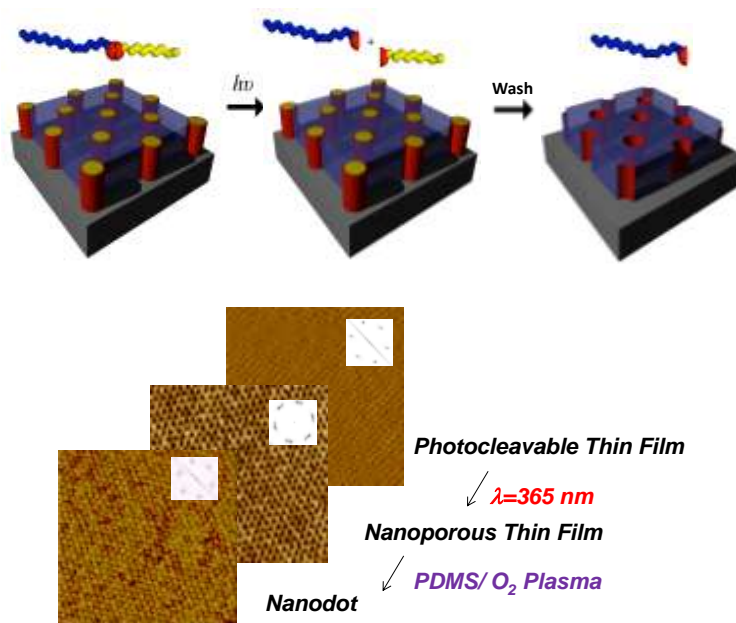
Scheme 4.1 Schematic representation of the photocleavable polymers and block copolymers projects in this work.

4.1 Nanoporous thin films from block copolymers featuring ONB junctions

4.1.1 Highly order thin films from PS-*b*-PEO with an ONB junction

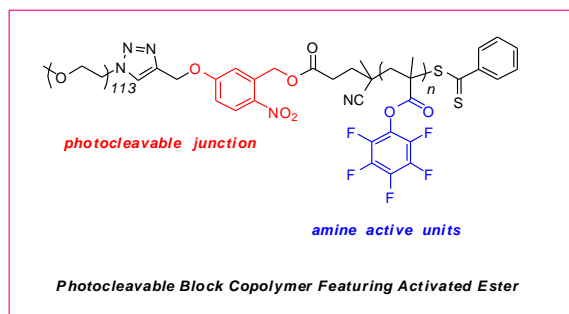
As discussed previously, establishing a synthetic method to produce block copolymers featuring photocleavable junctions is the first and key target for this thesis. In this work, we used PS-*b*-PEO as a model to demonstrate the synthetic methods for the preparation of BCPs with ONB junctions. PS-*h_v*-PEO with a photocleavable junction (*o*-nitrobenzyl ester) was synthesized by a combined RAFT polymerization and “click chemistry” approach and represents the first report utilizing this method for the synthesis of photocleavable block copolymers. After solvent annealing, highly ordered thin films were prepared from PS-*h_v*-PEO. Following a very mild UV exposure and successive washing with water,

PS- $h\nu$ -PEO thin films were transferred into highly ordered nanoporous thin PS films with pore diameters of 15~20 nm and long range ordering (over 2 $\mu\text{m} \times 2 \mu\text{m}$). Afterwards the pores were filled with PDMS by spin-coating in combination with capillary forces. After removal of the PS templates and treatment with oxygen plasma, highly ordered silica nanodots were obtained. This represents the first template application example from highly ordered nanoporous thin films derived from block copolymers featuring a photocleavable junction.



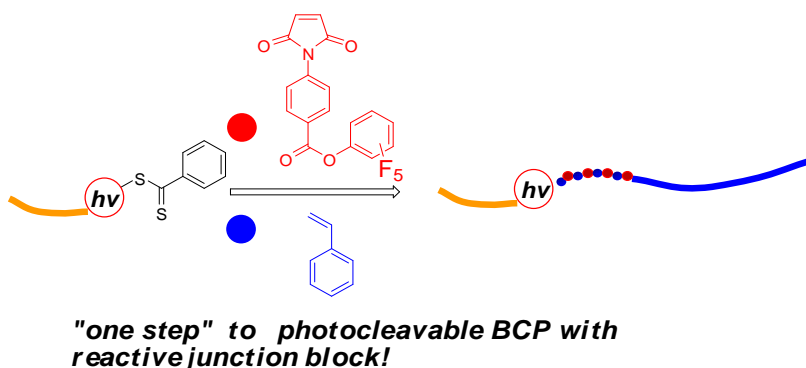
4.1.2 Functionalized thin films and fibers from PFPF(M)A- b -PEO with an ONB junction

In this work, we used the same concept as shown in the first publication to produce nanoporous structures. A series of poly(pentafluorophenyl-(methyl)-acrylates)-*block*-poly(ethylene oxide) with *o*-nitrobenzyl ester photocleavable junctions (PFPF(M)A- $h\nu$ -PEO) were synthesized by RAFT polymerization. The block copolymers were used to fabricate thin films and fibers by spincoating and electrospinning, respectively. After solvent annealing, UV exposure and washing with methanol/water to remove the minor block PEO, nanoporous structures were obtained. Both the porous thin films and fibers remained reactive to amine substitution of the pentafluorophenyl esters under mild conditions, which was confirmed by XPS, fluorescence confocal microscopy, FT-IR and contact angle measurements.



4.1.3 Photocleavable Triblock Copolymers Featuring Activated Ester Middle Blocks: Synthesis and Application as Nanoporous Thin Film Templates

In this part, photocleavable diblock copolymers were updated to photocleavable triblock copolymers. Polystyrene-*block*-poly(maleimide pentafluorophenyl ester-*co*-styrene)-*block*-poly(ethylene oxide) with an *o*-nitrobenzyl ester junction was synthesized by “one-step” RAFT polymerization. Highly ordered and reactive nanoporous thin films were obtained from the photocleavable triblock copolymer after spincoating, solvent annealing, UV exposure and washing with methanol/water to remove the minor PEO block. Iron oxide nanodots and nanodonuts were produced from these porous thin films after postmodification with amine functional ferrocene and treatment with oxygen plasma.

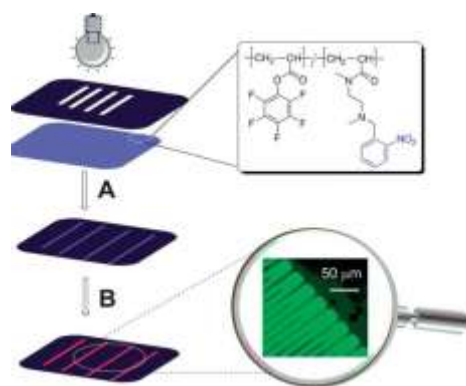


4.2 Photocleavable polymers featuring ONB as side chains or end groups

4.2.1 Copolymers Featuring Pentafluorophenyl Ester and Photolabile Amine Units: Synthesis and Application as Reactive Photopatterns

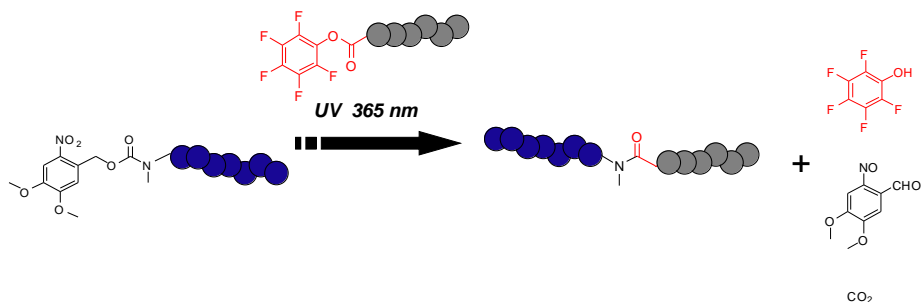
Polymers containing ONB in the side chains were introduced in the following part. Copolymers featuring pentafluorophenyl ester and *o*-nitrobenzyl (ONB) protected amine moieties have been prepared. Upon UV irradiation, the ONB protected amine group was released, which subsequently induced a crosslinking by a

spontaneous reaction with pentafluorophenyl esters, resulting in stable, reactive patterned thin films. Remaining esters were converted with a fluorescent dye.



4.2.2 α -Photolabile Amine Semitelechelic Polymer for Light-induced Macromolecular

Conjugation In this work, polymers featuring ONB as end group has been synthesized. The use of UV radiation as a reaction stimulus provides a facile means to obtain spatial and temporal control over polymer conjugation reactions. In this work, UV radiation was employed to induce an activated ester-amine conjugation of polymeric building blocks via the photo-induced deprotection of an amine and subsequent reaction with an activated ester. This is the first example of macromolecular conjugation using light triggered activated ester-amine chemistry.



5 Summary

In summary, a combined RAFT polymerization and “click chemistry” approach to synthesize block copolymers (BCPs) featuring photocleavable ortho-nitrobenzyl (ONB) junctions was successfully developed. Based on the developed synthetic method, three different kinds of BCPs featuring ONB junctions, polystyrene-*block*-poly(ethylene oxide) (PS-*hv*-PEO), poly(pentafluorophenyl-(methyl)acrylates)-*block*-poly(ethylene oxide) (PPFP(M)A-*hv*-PEO) and polystyrene-*block*-poly(maleimide pentafluorophenyl ester-*co*-styrene)-*block*-poly(ethylene oxide) (PS-*b*-(MAIPFP-*co*-PS)-*hv*-PEO), had been synthesized. After solvent annealing, highly ordered thin films were prepared from all above mentioned BCPs. Following a very mild UV exposure ($\lambda = 365\text{nm}$) and successive washing with water, BCPs thin films were transferred into highly ordered nanoporous thin films with pore diameters of 15~30 nm and long range ordering (over $2\ \mu\text{m} \times 2\ \mu\text{m}$). The resulting nanoporous thin films have been used for nanoscale templates: PS-*hv*-PEO, PPFPMMA-*hv*-PEO and PS-*b*-(MAIPFP-*co*-PS)-*hv*-PEO nanoporous thin films have been used to produce highly ordered silicon oxide nanodots, thiol functionalized nanoporous thin films and iron oxide nanodonuts, respectively.

Besides successful preparation of BCPs with ONB junctions, polymers featuring ONB protected amines were synthesized and have been described in this thesis. Photo-triggered activated ester-amine reactions have been developed based on the ONB functionalized polymers. The reaction has been used to produce reactive photopatterns or enable macromolecular conjugation.

Zusammenfassung

Es ist uns gelungen, einen kombinierten RAFT-Polymerisations- und "Klick-Chemie"-Ansatz zur Synthetisierung von BCPs mit ONB-Kreuzungen zu entwickeln. Auf Basis der etablierten Synthesemethode wurden drei verschiedene Arten von BCPs mit ONB-Übergängen, Polystyrol-*block*-Poly(Ethylenoxid) (PS-*hv*-PEO), Poly(pentafluorphenyl-(Methyl)-Acrylaten)-*block*-Poly(Ethylenoxid) (PPFP(M)A-*hv*-PEO) und Polystyrol-*block*-poly (Pentafluorphenylester Maleimid-*co*-Styrol)-*Block*-Poly(Ethylenoxid) (PS-*b*-(MAIPFP-*co*-PS)-*hv*-PEO), synthetisiert. Nach Lösemittelrelaxation wurden geordnete dünne Filme aus oben genannten BCPs hergestellt. Nach einer sehr milden UV-Exposition und sukzessivem Waschen mit Wasser wurden die dünnen Filme des BCP zu geordneten nanoporösen dünnen Filmen mit Porendurchmessern von 15 ~ 30 nm und Fernordnung (über 2 $\mu\text{m} \times 2 \mu\text{m}$) überführt. Die so erhaltenen nanoporösen dünnen Filme wurden für nanoskalige Vorlagen verwendet: PS-*hv*-PEO, PPFPMA-*hv*-PEO- und PS-*b*-(MAIPFP-*co*-PS)-*hv*-PEO nanoporöse dünne Filme wurden verwendet, um geordnete Silionoxid-Nanodonuts, bzw. Thiol-funktionalisierte nanoporöse dünne Filme und Eisenoxid-Nanodonuts zu erzeugen.

Neben der erfolgreichen Erstellung von BCPs mit ONB-Kreuzungen werden in dieser Arbeit Polymere mit ONB-geschützten Aminen synthetisiert. Durch Licht-Initiierung aktivierte Ester-Amin-Reaktionen wurden auf der Grundlage der ONB-funktionalisierten Polymere entwickelt. Die Reaktion wurde verwendet, um reaktive Fotomuster und makromolekulare Konjugation zu erstellen.

6 Experimental Part

This experimental part is related to chapter 3 and classified to 3 parts according to different sub-chapters in chapter 3.

6.1 Experimental part for chapter 3.1

Materials and Characterization

Pentafluorophenyl (methyl) acrylates (PFP(M)A) were synthesized according to reported methods.⁶³ 2,2'-Azobisisobutyronitrile (AIBN) was recrystallized from methanol. Triethylamine and dichloromethane (DCM) were distilled from calcium hydride. Tetrahydrofuran (THF) was distilled from sodium benzophenone. Monomethyl-PEO ($M_N = 5000$ g/mol) was purchased from Sigma Aldrich. All other reagents were purchased from commercial sources and used as received unless otherwise noted. ^1H NMR was measured on a Bruker 300 MHz NMR spectrometer using tetramethylsilane (TMS; $\delta = 0$ ppm) as internal standard. The average molecular weights (M_w and M_n) and dispersities (\mathcal{D}) of the polymers were estimated by a Waters Associates GPC system in chloroform against monodisperse polystyrene standards covering a molecular weight range of 10^3 – 10^7 Da. Scanning force microscopy was performed on a Digital Instruments Dimension 3100, operating in tapping mode. XPS analysis was performed in a Physical Electronics apparatus with a nonmonochromatic Mg K_{α} radiation source at a 45° take off angle. The sensitivity factors specified for the spectrometer were used for quantitative analysis. The pressure in the analysis chamber was less than 10^{-5} Pa. The spectrum collection time was kept under 10 min to minimize X-ray damage. To determine the bulk morphologies of the triblock copolymers, small-angle X-ray scattering (SAXS) was performed using a rotating anode with $\text{CuK}\alpha$ X-rays ($\lambda = 1.54$ Å). A sample-to-detector distance of 1.7 m was used to access the necessary q range.

Macro-CTA Synthesis PEO- N_3 and compound **1** were prepared according to previously published methods.⁶³ PEO- N_3 ($M_n = 5000$, $\mathcal{D} = 1.04$, 1 equiv.), compound **1** (1 equiv.), $\text{CuBr}/\text{PMDETA}$ (0.3 equiv./0.3 equiv.) and dioxane (2 ml) were loaded into a dry Schlenk tube. The reaction mixture was

degassed by three freeze-pump-thaw cycles and the flask was refilled with nitrogen. It was then stirred at room temperature for 48 h. The reaction solution was extracted 3 times with DCM/water; then all volatiles were removed under reduced pressure. The pink residue was dissolved in THF and precipitated three times into cold diethyl ether, and dried at 30 °C in vacuum. Yield: ~80%, End functionalization degree: ~90%. $^1\text{H NMR}$ (300 MHz, CDCl_3), δ (TMS, ppm): 8.21 (d, 1H, ONB), 7.92 (d, 2H, SS-ArH), 7.57 (t, 1H, SS-ArH), 7.39 (t, 2H, SS-ArH), 7.08 (d, 1H, ONB), 7.25 (d, 1H, ONB), 5.58 (s, 2H, ONB- CH_2 -O), 5.32 (s, triazole- CH_2 -ONB), 4.55 (t, 2H, triazole- CH_2 - CH_2 -O in PEG), 3.88-3.45 ((broad, CH_2 - CH_2 -O), 3.37 (s, O- CH_3 in PEG), 2.91-2.49 (m, OOC- CH_2 - CH_2), 1.98 (s, C(CN) CH_3). $M_{n, GPC} = 7000$, $D = 1.10$.

General Procedure for RAFT Polymerizations.

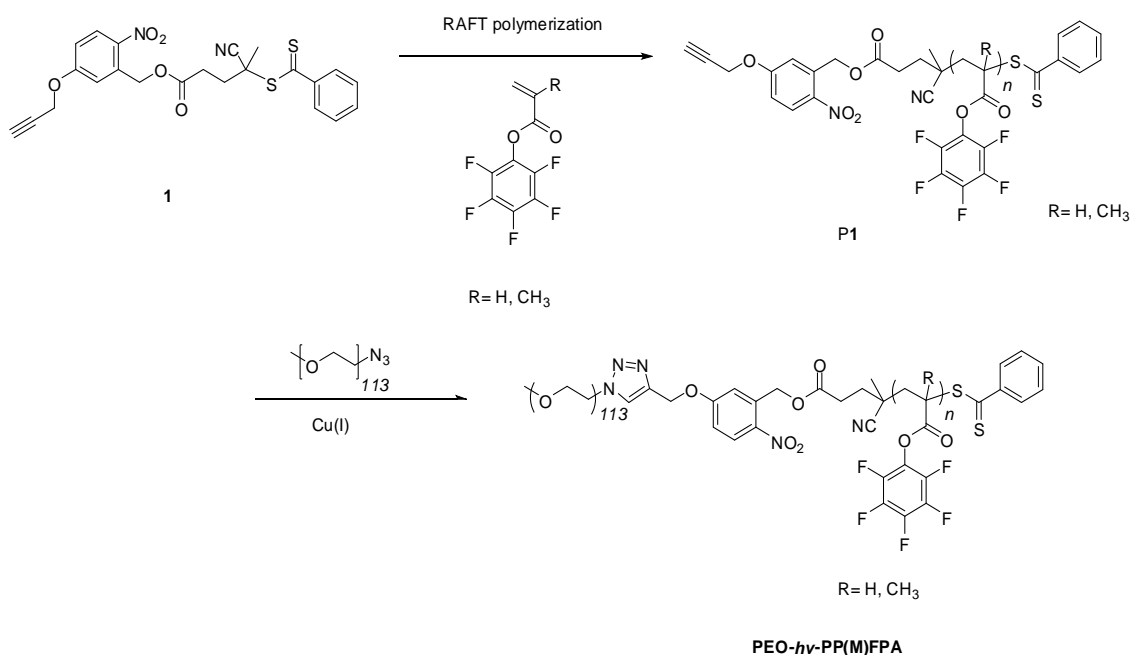
PPFMA, CTA (1 equiv.) and AIBN (0.125 equiv.) were loaded into a dry Schlenk tube. The reaction mixture was degassed by five freeze-pump-thaw cycles and the flask was refilled with nitrogen. It was then stirred in a preheated oil bath at 80 °C for 15 h. The pink product (conversion: 60%) was precipitated three times into cold hexane and dried at 30 °C in vacuum. $^1\text{H NMR}$ (300 MHz, CDCl_3), δ (TMS, ppm): 8.12 (d, ONB), 7.85 (broad, SS-ArH), 7.60-7.32 (broad, SS-ArH), 7.14-7.00 (broad, ArH in ONB), 5.47 (s, ONB- CH_2 -O), 5.24 (s, triazole- CH_2 -ONB), 4.48 (t, 2H, triazole- CH_2 - CH_2 -O in PEG), 3.88-3.45 (broad, CH_2 - CH_2 -O), 3.37 (s, O- CH_3 in PEG), 2.60-1.18 (broad, proton in PPFMA). Table 1, **P4**, $M_{n, GPC} = 25300$, $D = 1.31$.

General Procedures for Preparation of the Thin Films. The PPFMA-*h ν* -PEO BCPs were spin coated from toluene solutions onto silicon substrates and then annealed in a $\text{H}_2\text{O}/\text{THF}$ (0.1 ml/0.2 ml) atmosphere for 2.5 h at 20 °C. The film thickness was controlled by adjusting the solution concentration and the spinning speed. To cleave the PEO block and functionalize the film simultaneously, the block copolymer films were put in an amine/methanol solution under UV exposure at a wavelength of 365 nm

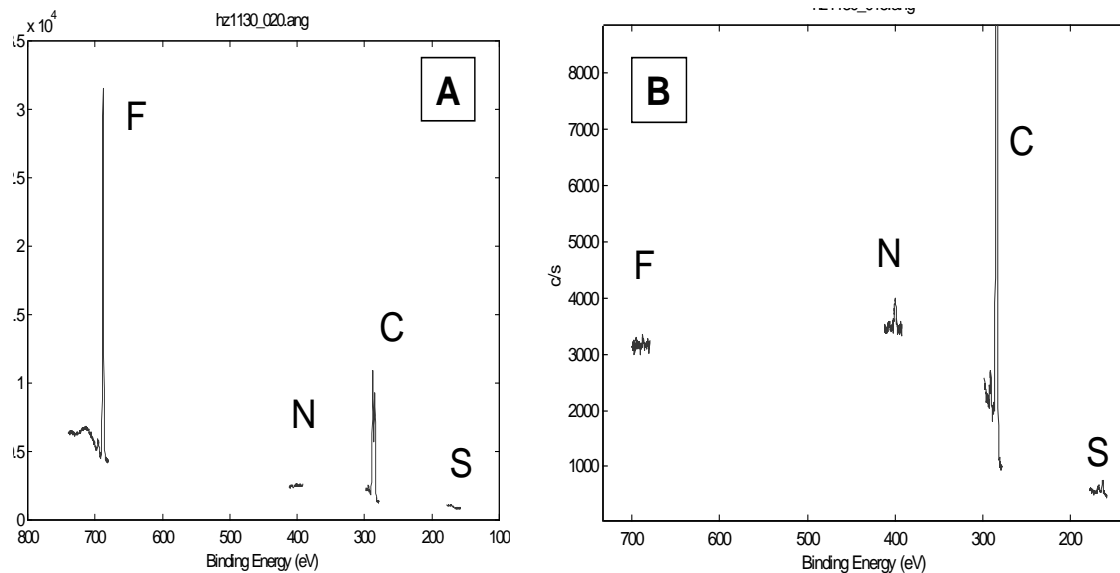
and a dose of 5.6 J cm^{-2} (Blak-Ray Model B, UVL-56) for 12 h; then the thin films were rinsed in methanol for 3h.

General Procedures for Preparation polymer nanofibers. The PFPMA-*hv*-PEO nanofibers were obtained from electrospinning a THF/DMF (4:1) solution (50 wt.% PFPMA-*hv*-PEO) onto aluminum foil in a horizontal setup. The polymer solution was fed at a rate of 1.5 mL/h by the syringe pump to the blunted needle tip with nominal inner diameter of 0.80 mm, where the voltage of 24 kV was applied. The spinning distance between tip and grounded collector was 12 cm.

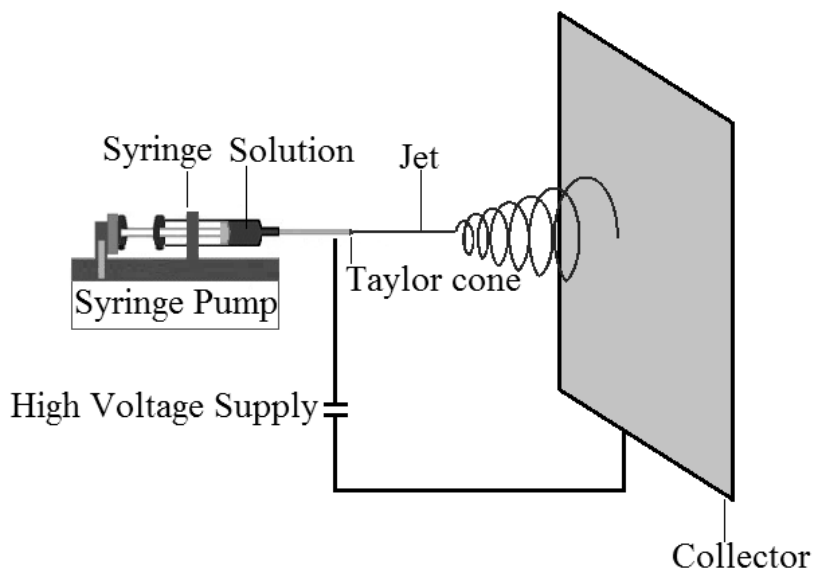
Supporting Information



S1. RAFT-Click method to photocleavable PEO-*hv*-PPFP(M)A.



S2. High resolution XPS for PEO-*hν*-PPFPMA (A) before and (B) after UV and amine post-modification treatment.



S 3. An electrospinning experiment with a horizontal setup arrangement of the electrodes.

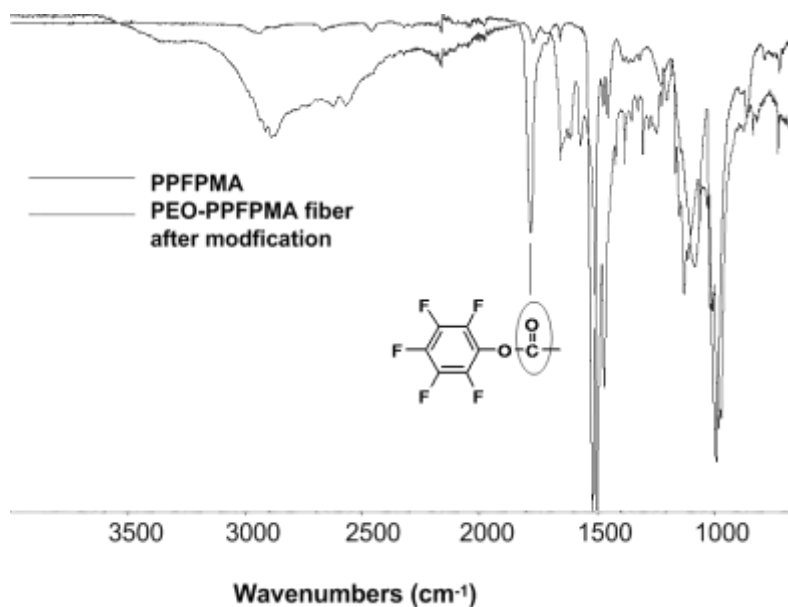


Figure S4. ATR-FIR for PPFMA and fibers after (purple, bottom spectra) Jeff amine post-modification.

6. 2 Experiental part for chapter 3.2

Materials and Characterization

Pentafluorophenyl 4-maleimidobenzoate (MAIPFP) was synthesized according to reported methods.⁸² 2,2'-Azobisisobutyronitrile (AIBN) was recrystallized from methanol. Tetrahydrofuran (THF) was distilled from sodium/benzophenone. Monomethyl ether-PEO ($M_n = 5000$ g/mol) was purchased from Sigma Aldrich. All other reagents were purchased from commercial sources and used as received unless otherwise noted. ¹H NMR was measured on a Bruker 300 MHz NMR spectrometer using tetramethylsilane (TMS; $\delta = 0$ ppm) as internal standard. The average molecular weights (M_w and M_n) and dispersities (\mathcal{D}) of the polymers were estimated by a Waters Associates GPC system in chloroform against monodisperse linear polystyrene standards covering a molecular weight range of 10^3 – 10^7 Da. Scanning force microscopy was performed on a Digital Instruments Dimension 3100 operating in tapping mode. XPS analysis was performed in a Physical Electronics apparatus with a nonmonochromatic Mg K_α radiation source at a 45° take off angle. The sensitivity factors specified for the spectrometer were used for quantitative analysis. The pressure in the analysis chamber was less than 10^{-5} Pa. The spectrum collection time was kept under 10 min to minimize X-ray damage. GISAXS

measurements were performed at the 8-ID-E beamline at the Advanced Photon Source (Argonne National Laboratory) with an X-ray wavelength of 1.664 Å. TEM studies were performed on a JEOL 100CX electron microscope operated at 100 kV. For the TEM measurements, the samples were prepared on silicon substrates with a thick layer of silicon oxide. The polymer film was then floated onto the surface of an aqueous solution containing 5 wt% HF, transferred to a water bath, and then retrieved with a Cu grid for TEM measurement.

Macro-CTA Synthesis. PEO-N₃ and compound **1** were prepared according to previously published methods.³¹ PEO-N₃ ($M_n = 5000$, $D = 1.04$, 1 equiv.), compound **1** (1 equiv.), CuBr/PMDETA (0.3 equiv./0.3 equiv.) and dioxane (2 ml) were loaded into a dry Schlenk tube. The reaction mixture was degassed by three freeze-pump-thaw cycles and the flask was refilled with nitrogen. It was then stirred at room temperature for 48 h. The reaction solution was extracted 3 times with DCM from water; then all volatiles were removed under reduced pressure. The pink residue was dissolved in THF and precipitated three times into cold diethyl ether, and dried at 30 °C in vacuum. Yield: ~80%, End functionalization degree: ~90%. ¹H NMR (300 MHz, CDCl₃), δ (TMS, ppm): 8.21 (d, 1H, ONB), 7.92 (d, 2H, SS-ArH), 7.57 (t, 1H, SS-ArH), 7.39 (t, 2H, SS-ArH), 7.08 (d, 1H, ONB), 7.25 (d, 1H, ONB), 5.58 (s, 2H, ONB-CH₂-O), 5.32 (s, triazole-CH₂-ONB), 4.55 (t, 2H, triazole-CH₂-CH₂-O in PEO), 3.88-3.45 ((broad, CH₂-CH₂-O), 3.37 (s, O-CH₃ in PEO), 2.91-2.49 (m, OOC-CH₂-CH₂), 1.98 (s, C(CN)CH₃). $M_{n,GPC} = 7000$, $D = 1.10$.

General Procedure for RAFT Polymerizations.

MAIPFP (12 equiv.), Styrene (1250 equiv.), Macro-CTA (1 equiv.) and AIBN (0.125 equiv.) were loaded into a dry Schlenk tube. The reaction mixture was degassed by five freeze-pump-thaw cycles and the flask was refilled with nitrogen. It was then stirred in a preheated oil bath at 80 °C for 15 h. The pink product (conversion: 20%) was precipitated three times into cold hexane and dried at 30 °C in vacuum. ¹H NMR (300 MHz, CDCl₃), δ (TMS, ppm): 8.20 (broad, MAIPFP) 8.12 (d, ONB), 7.85 (broad, SS-ArH), 7.60-7.32 (broad, SS-ArH), 7.14-7.00 (broad, ArH in ONB), 5.47 (s, ONB-CH₂-O),

5.24 (s, triazole-CH₂-ONB), 4.48 (t, 2H, triazole-CH₂-CH₂-O in PEO), 3.88-3.45 (broad, CH₂-CH₂-O), 3.37 (s, O-CH₃ in PEO), 2.60-1.18 (broad, proton in PPFMA). Table 1, **P1**, $M_{n, GPC} = 28100$, $\mathcal{D} = 1.18$.

General Procedures for Preparation of the Thin Films. The PEO-*b*-P(S-*co*-MAIPFP)-*b*-PS (**P1**) BCPs were spin coated from toluene solutions onto silicon substrates and then annealed in a H₂O/THF (0.1 ml/0.2 ml) atmosphere for 2.5 h at 20 °C. The film thickness was controlled by adjusting the solution concentration and the spinning speed. To cleave the PEO block and functionalize the film simultaneously, the block copolymer films were put in a methanol solution under UV exposure at a wavelength of 365 nm and a dose of 5.6 J cm⁻² (Blak-Ray Model B, UVL-56) for 12 h; then the thin films were rinsed in methanol for 3h.

Iron Nanodots and Nanodots from Nanoporous Thin Films Template The nanoporous film was immersed into a methanol solution of amine functional Fc (Ferrocene, (2-aminoethyl)-, 10 mg/mL) at 35 °C for 12 hours. Nanodots were produced after methanol washing and oxygen plasma treatment. Nanodons were produced after acid (HCl, 0.1 M in water) washing and oxygen plasma treatment.

6. 3 Experiental part for chapter 3.3

Materials and Characterization

Styrene was filtered through basic aluminum oxide before polymerization, and 2,-2'-azobisisobutyronitrile (AIBN) was recrystallized from methanol. Triethylamine and Dichloromethane (DCM) were distilled from calcium hydride. Tetrahydrofuran (THF) was distilled from sodium benzophenone ketyl. All other reagents were purchased from commercial sources and used as received unless otherwise noted. ¹H NMR was measured on a Bruker 300 MHz NMR spectrometer using tetramethylsilane (TMS; $\delta = 0$ ppm) as internal standard. The average molecular weights (M_w and M_n) and dispersities (\mathcal{D}) of the polymers were estimated by a Waters Associates GPC system in chloroform. A set of monodisperse linear polystyrene standards covering molecular weight range of 10³–10⁷ was

used for the molecular weight calibration. PFP end group functionalized PS and PNIPAM were synthesized according to literature procedure.⁷⁸

Synthesis

4,5-dimethoxy-2-nitrobenzyl methyl(2-(methylamino)ethyl)carbamate (2). Into a 250 mL round-bottom flask were placed 3.08 g (35 mmol) of *N*¹,*N*²-dimethylethane-1,2-diamine in dioxane/water 50/50 (volume) mL. The solution was cooled in an ice bath. 2 g (7.3 mmol) of 4,5-dimethoxy-2-nitrobenzyl carbonochloridate in dioxane was slowly added to the amine solution over the course of 1 hour. The resulting solution was stirred at room temperature for 48 h. After filtration, the solution was extracted three times by DCM/water followed by removal of DCM in vacuum. The residue was collected and purified on a silica gel column using chloroform as eluent. A viscous liquid (1.4 g, yield~60%) was obtained after drying 48h in vacuum at 30°C. ¹H NMR (300 MHz, CDCl₃), δ (TMS, ppm): 7.71 (s, ArH in ONB), 7.04 (s, ArH in ONB), 5.53 (s, ONB-CH₂-O), 3.98 (s, CH₃ in ONB), 3.97 (s, CH₃ in ONB), 3.48 (board, (CH₃)(CO)NCH₂-CH₂-), 3.08-2.99 (d, (CH₃)(CO)NCH₂-CH₂-), 2.78 (board, (CH₃)(CO)NCH₂-CH₂-), 2.50 (d, (CH₃)(CO)NCH₂-CH₂-N(CH₃)H).

2-cyano-5-((2-(((4,5-dimethoxy-2-nitrobenzyloxy)carbonyl)(methylamino)ethyl)(methylamino)-5-oxopentan-2-yl benzodithioate (1). Into a 50 mL round-bottom flask were placed 650 mg (2 mmol) of compound **2**, 990 mg (2.2 mmol) of compound **3**, 235 mg (2.2 mmol) of lutidine, and 20 mL DCM. The resulting solution was stirred at room temperature for 16 h. The residue was purified on a silica gel column using chloroform as eluent. A pink highly viscous compound was obtained in 80% yield (1.1 g). ¹H NMR (300 MHz, CDCl₃), δ (TMS, ppm): 7.90 (d, 1H, ONB), 7.69 (d, 2H, SS-ArH), 7.57 (t, 1H, SS-ArH), 7.44 (t, 2H, SS-ArH), 7.05 (s, 1H, ONB), 5.53 (s, 2H, ONB-CH₂-O), 4.03-3.92 (m, 6H, CH₃-ONB), 3.50 (b, 2H, ONB(CH₃)(CO)NCH₂-CH₂-), 3.14-2.92 (m, 6H, -(CH₃)(CO)NCH₂-CH₂N(CO)(CH₃)-), 2.59 (d, 2H, ONB(CH₃)(CO)NCH₂-CH₂-), 1.90 (s, 3H, C(CN)CH₃).

General Procedure for RAFT Polymerizations

DEGMA, CTA (1 equivalent) and AIBN (0.125 equivalent) were loaded into a dry Schlenk tube. The reaction mixture was degassed by three freeze-pump-thaw cycles and the flask was refilled with nitrogen. It was then stirred in a preheated oil bath at 80 °C. For isolation of the polymer, the pink product was precipitated three times into cold hexane and dried at 30 °C in vacuum. ¹H NMR (300 MHz, CDCl₃), δ (TMS, ppm): 7.88 (d, ONB), 7.72 (broad, SS-ArH), 1.51-1.39 (broad, main chain in POEGMA), 1.05-0.85 (broad, CH₃ linking to main chain).

7 References and notes

- (1) Bates, F. S.; Hillmyer, M. A.; Lodge, T. P.; Bates, C.M.; Delaney, K. T.; Fredrickson, G. H. *Science* **2012**, *336*, 434.
- (2) Toombes, G. E. S. PhD *thesis* **2007** August
- (3) Olson, D. A.; Chen, L.; Hillmyer, M. A. *Chem. Mater.*, **2008**, *20*, 871.
- (4) Xu, T.; Kim, H. C.; DeRouchey, J.; Seney, C.; Levesque, C.; Martin, P.; Stafford, C. M.; Russell, T. P. *Polymer* **2001**, *42*, 9091.
- (5) Guarini, K. W.; Black, C. T.; Yeung, S. H. I. *Adv. Mater.* **2002**, *14*, 1290.
- (6) Urbas, A. M.; Maldovan, M.; DeRege, P.; Thomas, E. L. *Adv. Mater.* **2002**, *14*, 1850.
- (7) (a) Labet, M. and Wim Thielemans, W. *Chem. Soc. Rev.*, **2009**, *38*, 3484. (b) Carlotta, D. *J. Polym. Env.*, **2001**, *9*, 63.
- (8) Ndoni, S.; Vigild M. E.; Berg, R. H. J. *Am. Chem. Soc.* **2003**, *125*, 13366.
- (9) Costache, M. C.; Wang, D. Y.; Heidecker, M. J.; Manias, E.; Wilkie, C. A. *Polym. Adv. Technol.* **2006**, *17*, 272.
- (10) Hedrick, J. L; Miller, R. D.; Hawker, C. J.; Carter, K. R.; Volksen, W.; Yoon, D. Y.; Trollsas, M. *Adv. Mater.* **1998**, *10*, 1049.
- (11) Philippides, A.; Budd, P. M.; Price, C.; Cuncliffe, A. V. *Polymer* **1993**, *34*, 3509.
- (12) Li, M.; Douki, K.; Goto, K.; Li, X.; Coenjarts, C.; Smilgies, D. M.; Ober, C. K. *Chem. Mater.* **2004**, *16*, 3800.
- (13)(a) Liu, G.; Ding, J.; Hashimoto, T.; Kimishima, K.; Winnik, F. M.; Nigam, S. *Chem. Mater.* **1999**, *11*, 2233. (b) Liu, G.; Ding, J.; Herfort, M.; Bezett-Jones, D. *Macromolecules* **1997**, *30*, 1850. (c) Ludwigs, S.; Schmidt, K.; Krausch, G. *Macromolecules* **2005**, *38*, 2376.

- (14) Njikang, G.; Han, D. H.; Wang, J.; Liu, G. J. *Macromolecules* **2008**, *41*, 9727–9735. (b) Dupont, J.; Liu, G. J.; Niihara, K.; Kimoto, R.; Jinnai, H. *Angew. Chem. Int. Ed.* **2009**, *48*, 6144–6147. (c) Taribagil, R. R.; Hillmyer, M. A.; Lodge, T. P. *Macromolecules* **2010**, *43*, 5396–5404.
- (15) (a) Schmalz, H.; Knoll, A.; Muller, A. J.; Abetz, V. *Macromolecules* **2002**, *35*, 10004. (b) Balsamo, V.; de Navarro, C. U.; Gil, G. *Macromolecules* **2003**, *36*, 4507.
- (16) Gadzinowski, M.; Sosnowski, S. *J. Polym. Sci. Part A: Polym. Chem.* **2003**, *41*, 3750.
- (17) (a) Wang, J.; Matyjaszewski, K. *J. Am. Chem. Soc.* **1995**, *117*, 5614. (b) Kato, M.; Kamigaito, M.; Sawamoto, M.; Higashimura, T. *Macromolecules* **1995**, *28*, 1721.
- (18) Chiefari, J.; Chong, Y. K.; Ercole, F.; Krstina, J.; Jeffery, J.; Le, T. P. T.; Mayadunne, R. T. A.; Meijs, G. F.; Moad, C. L.; Moad, G.; Rizzardo, E.; Thang, S. H. *Macromolecules* **1998**, *31*, 5559–5562.
- (19) Barner-Kowollik, C. *Handbook of RAFT Polymerization* **2008**, Wiley-VCH Weinheim, ISBN: 9783527319244.
- (20) (a) Batz, H. G.; Franzmann, G.; Ringsdorf, H. *Angew. Chem. Int. Ed.* **1972**, *11*, 1103. (b) Ferruti, A.; Bettelli, A.; Fere, A. *Polymer* **1972**, *13*, 462.,
- (21) Theato P. *J. Polym. Sci.: Part A: Polym. Chem.* **2008**, *46*, 6677.
- (22) Barltrop, J. A.; Plant, J.; Schofield, P. *Chem. Commun.* 1966, *22*, 822
- (23) Patchornik, A.; Amit, B.; Woodward, R. B. *J. Am. Chem. Soc.* **1970**, *92*, 6333.
- (24) Il'ichev, Y. V.; Schworer, M. A.; Wirz, J. *J. Am. Chem. Soc.* **2004**, *126*, 4581.
- (25) Johnson, J. A.; Finn, M. G.; Koberstein, J. T.; Turro, N. J. *Macromolecules* **2007**, *40*, 3589.
- (26) Jay, S. M.; Saltzman, W. M. *Nature Biotechnol.* **2009**, *27*, 451. (b) Lutolf, M. P. *Nature Mater.* **2009**, *8*, 451. (c) Blow, N. *Nature Methods* **2009**, *6*, 619.
- (27) (a) Tibbitt M. W.; Kloxin, A. M.; Dyamenahalli, K. U.; Anseth, K. S. *Soft Matter* **2010**, *6*, 5100. (b) Kloxin, A. M.; Tibbitt, M. W.; Anseth, K. S. *Nature Protoc.* **2010**, *5*, 1867.
- (28) Jiang, J.; Tong, X.; Morris, D.; Zhao, Y. *Macromolecules* **2006**, *39*, 4633.

- (29) Iizawa, T.; Kudou, H.; Nishikubo, T. *J. Polym. Sci., Part A: Polym. Chem.* **2008**, *46*, 6677.
- (30) Choi, O. J.; Chung, M. K.; Ryu, Y.; Lee, M.-H. *Polymer (Korea)*, **1991**, *29*, 1875.
- (31) Doh, J.; Irvine, D. J. *J. Am. Chem. Soc.* **2004**, *126*, 9170.
- (32) Zhao, B.; Moore, J. S.; Beebe, D. J. *Science* **2001**, *291*, 1023.
- (33) Kim, H.-C.; Park, S.-M.; Hinsberg, W. D. *Chem. Rev.* **2010**, *110*, 146.
- (34) (a) Chen, D.; Jiang, M. *Acc. Chem. Res.* **2005**, *38*, 494. (b) Bang, J.; Jeong, U.; Ryu, D. Y.; Russell, T. P.; Hawker, C. J. *Adv. Mater.* **2009**, *21*, 4769.
- (35) Kang, M.; Moon, B. *Macromolecules* **2009**, *42*, 455.
- (36) Schumers, J. M.; Gohy, J. F. and Fustin, C. A. *Polym. Chem.*, **2010**, *1*, 161.
- (37) Zhao, H.; Gu, W.; Sterner, E.; Russell, T. P.; Coughlin, E. B. Theato, P. *Macromolecules* **2011**, *44*, 6433.
- (38) (a) Furukawa, H.; Yaghi, O. M. *J. Am. Chem. Soc.* **2009**, *131*, 8875. (b) Chen, Q.; Luo, M.; Hammershoj, P.; Zhou, D.; Han, Y.; Laursen, B. W.; Yan, C.-G.; Han, B.-H., *J. Am. Chem. Soc.* **2012**, *70*, 134, 6084.
- (39) Wood, C. D.; Tan, B.; Bradshaw, D.; Stoeckel, E.; Trewin, A.; Rosseinsky, M. J.; Cooper, A. I. *Adv. Mater.* **2008**, *20*, 1916.
- (40) (a) Shi, Z.; Zhou, Y.; Yan, D. *Macromol. Rapid Commun.* **2006**, *27*, 1265. (b) Li, G.; Yang, X.; Wang, B.; Wang, J.; Yang, X. *Polymer* **2008**, *49*, 3436. (c) Yang, X.; Chen, L.; Huang, B.; Bai, F.; Yang, X. *Polymer* **2009**, *50*, 3556. (d) Abidian, M. R.; Kim, D. H.; Martin, D. C. *Adv. Mater.* **2006**, *18*, 405. (e) Duan, H.; Kuang, M.; Zhang, G.; Wang, D.; Kurth, D. G.; Möhwald, H. *Langmuir* **2005**, *21*, 11495.
- (41) Pulko, I.; Wall, J.; Krajnc, P.; Cameron, N. R. *Chem. Eur. J.* **2010**, *16*, 2350.
- (42) Kimmins, S. D.; Cameron, N. R. *Adv. Funct. Mater.* **2011**, *21*, 211.
- (43) Hu, X.; Li, G.; Li, M.; Huang, J.; Li, Y.; Gao, Y.; Zhang, Y. *Adv. Funct. Mater.* **2008**, *18*, 575.

- (44) (a) Uehara, H.; Kakiage, M.; Sekiya, M.; Sakuma, D.; Yamonobe, T.; Takano, N.; Barraud, A.; Meurville, E.; Ryser, P. *ACS Nano* **2009**, *3*, 924. (b) Yang, S. Y.; Ryu, I.; Kim, H. Y.; Kim, J. K.; Jang, S. K.; Russell, T. P. *Adv. Mater.* **2006**, *18*, 709. (c) Yang, S. Y.; Yang, J. A.; Kim, E. S.; Jeon, G.; Oh, E. J.; Choi, K. Y.; Hahn, S. K.; Kim, J. K. *ACS Nano* **2010**, *4*, 3817. (d) Yang, S. Y.; Park, J.; Yoon, J.; Ree, M.; Jang, S. K.; Kim, J. K. *Adv. Funct. Mater.* **2008**, *18*, 1371. (e) Lv, Y. Q.; Hughes, T. C.; Hao, X. J.; Hart, N. K.; Littler, S. W.; Zhang, X. Q.; Tan, T. W. *Macromol. Rapid Commun.* **2010**, *31*, 1785.
- (45) (a) Tseng, W. H.; Chen, C. K.; Chiang, Y. W.; Ho, R. M.; Akasaka, S.; Hasegawa, H. *J. Am. Chem. Soc.* **2009**, *131*, 1356. (b) Jones, B. H.; Lodge, T. P. *Chem. Mater.* **2010**, *22*, 1279. (c) Crossland, E. J. W.; Kamperman, M.; Nedelcu, M.; Ducati, C.; Wiesner, U.; Smilgies, D. M.; Toombes, G. E. S.; Hillmyer, M. A.; Ludwigs, S.; Steiner, U.; Snaith, H. J. *Nano Lett.* **2009**, *9*, 2807. (d) Melde, B. J.; Burkett, S. L.; Xu, T.; Goldbach, J. T.; Russell, T. P.; Hawker, C. J. *Chem. Mater.* **2005**, *17*, 4743. (e) Crossland, E. J. W.; Ludwigs, S.; Hillmyer, M. A.; Steiner, U. *Soft Matter* **2007**, *3*, 94.
- (46) Fasolka, M. J.; Mayes, A. M. *Ann. Rev. Mater. Res.* **2001**, *31*, 323.
- (47) Park, S.; Wang, J. Y.; Kim, B.; Xu, J.; Russell, T. P. *ACS Nano* **2008**, *2*, 766.
- (48) Leiston-Belanger, J. M.; Russell, T. P.; Drockenmuller, E.; Hawker, C. J. *Macromolecules* **2005**, *38*, 7676.
- (49) Hirao, A.; Nakahama, S. *Macromolecules* **1988**, *21*, 274.
- (50) (a) Thurn-Albrecht, T.; Steiner, R.; DeRouchey, J.; Stafford, C. M.; Huang, E.; Bal, M.; Tuominen, M.; Hawker, C. J.; Russell, T. P. *Adv. Mater.* **2000**, *12*, 787. (b) Bang, J.; Kim, S. H.; Drockenmuller, E.; Misner, M. J. Russell, T. P. and Hawker, C. J. *J. Am. Chem. Soc.* **2006**, *128*, 7622.
- (51) Schumers, J. M.; Vald, A.; Huynen, S.; Gohy J. F. and Fustin, C. A. *Macromol. Rapid Commun.* **2011**, *3*, 199.
- (52) Olson, D. A.; Chen, L.; and Hillmyer M. A. *Chem. Mater.* **2008**, *20*, 869.

- (53) (a) Rzaev, J.; Hillmyer, M. A. *J. Am. Chem. Soc.*, **2005**, *127*, 13373. (b) Johnson, B. J. S.; Wolf, J. H.; Zalusky, A. S.; and Hillmyer, M. A. *Chem. Mater.*, **2004**, *16*, 2909. (c) Chen, L.; Hallinan, D. T.; Elabd, Y. A.; and Hillmyer, M. A. *Macromolecules* **2009**, *42*, 6075. (d) Rodwogin, M. D.; Spanjers, C. S.; Leighton, C.; and Hillmyer, M. A. *ACS Nano*, **2010**, *4*, 725.
- (54) Gamys, C.G.; Schumers, J. M.; Vlad, A.; Gohy J. F. and Fustin, C. A *Soft Matter*, **2012**, *8*, 4486.
- (55) (a) Theato, P. *J. Polym. Sci. Part A. Polym. Chem.*, **2008**, *46*, 6677. (b) Theato, P. and Klok, H.A. (Ed.) “*Functional Polymer by Post-polymerization on Modification: Concepts, Guideline and Application*”, **2012**, Wiley-VCH, Weinheim. (c) Guenay, K. A.; Theato, P.; Klok, H.A. *J. Polym. Sci. Part A. Polym. Chem.*, **2013**, *51*, 1.
- (56) (a) Zhao, H.; Sterner, E.; Coughlin, E. Theato, P. *Macromolecules*, **2012**, *45*, 1723. (b) Zhao, Y. *Macromolecules* **2012**, *45*, 3647. (c) Han, D.; Tong, X.; Zhao, Y. *Macromolecules* **2011**, *44*, 437. (d) Gumbley, P.; Koylu, D.; Thomas, S. W. *Macromolecules* **2011**, *44*, 7956. (e) Smith, Z. C.; Pawle, R. H.; Thomas, S. W. *ACS Macro Lett.* **2012**, *1*, 825. (f) Zhao, H.; Theato, P. *Polym. Chem.* **2013**, *4*, 891.
- (57) Kessler, D.; Roth, P. J.; Theato, P. *Langmuir* **2009**, *25*, 10068.
- (58) Bergshoef, M. M.; Vancso, G. J. *Adv. Mater.* **1999**, *11*, 1362.
- (59) Bognitzki, M.; Hou, H.; Ishaque, M.; Frese, T.; Hellwig, M.; Schwarte, C.; Schaper, A.; Wendorff, J. H.; Greiner, A. *Adv. Mater.* **2000**, *12*, 637.
- (60) Huang, L.; McMillan, R. A.; Apkarian, R. P.; Pourdeyhimi, B.; Conticello, V. P.; Chaikof, E. L. *Macromolecules* **2000**, *33*, 2989.
- (61) Gentsch, R.; Pippig, F.; Nilles, K.; Theato, P.; Kikkeri, R.; Maflinao, M.; Lepenies, B.; Seeberger, P. H. And Boerner, H. G. *Macromolecules*, **2010**, *43*, 9239.
- (62) Ruotsalainen, T.; Turku, J.; Hiekkataipale, P.; Vainio, U.; Serimaa, R.; Brinke, G.; Harlin, A.; Ruokolainen, J.; Ikkala, O. *Soft Mater* **2007**, *3*, 978.
- (63) Eberhardt, M. and Theato, P. *Macromol. Rapid Commun.* **2005**, *26*, 1488–1493.

- (64) (a) Jackson, E. A.; Hillmyer, M. A. *ACS Nano* **2010**, *4*, 3548. (b) Wang, X.; Husson, S. M.; Qian, X.; Wickramasinghe, S. R. *J. Membr. Sci.* **2010**, *365*, 302. (c) Phillip, W.; Rzyayev, J.; Hillmyer, M.; Cussler, E. *J. Membr. Sci.* **2006**, *286*, 144.
- (65) (a) Pulko, I.; Wall, J.; Krajnc, P.; Cameron, N. R. *Chem. Eur. J.* **2010**, *16*, 2350. (b) Kimmins, S. D.; Cameron, N. R. *Adv. Funct. Mater.* **2011**, *21*, 211. (c) Zhang, Y.; Wang, S.; Eghtedari, M.; Motamedi, M.; Kotov, N. A. *Adv. Funct. Mater.* **2005**, *15*, 725.
- (66) Wu D.; Xu, F.; Sun, B.; Fu, R.; He, H.; Matyjaszewski, K. *Chem. Rev.* **2012**, *112*, 3959.
- (67) Ryu, J. H.; Park, S.; Kim, B.; Klaikherd, A.; Russell, T. P.; Thayumanavan, S. *J. Am. Chem. Soc.* **2009**, *131*, 9870.
- (68) (a) Alfrey, T.; Lavin, E. J. *Am. Chem. Soc.* 1945, *67*, 2044. (b) Pfeifer, S.; Lutz, J.-F. *J. Am. Chem. Soc.* **2007**, *129*, 9542. (c) Weiss, J.; Li, A.; Wischerhoff, E.; Laschewsky, A. *Polym. Chem.* **2012**, *3*, 352.
- (69) (a) Theato, P. *J. Polym. Sci. Part A. Polym. Chem.*, **2008**, *46*, 6677. (b) Theato, P. and Klok, H.A. (Ed.) "Functional Polymer by Post-polymerization on Modification: Concepts, Guideline and Application", **2012**, Wiley-VCH, Weinheim. (c) Guenay, K. A.; Theato, P.; Klok, H.A. *J. Polym. Sci. Part A. Polym. Chem.*, **2013**, *51*, 1.
- (70) Narumi, A.; Fuchise, K.; Kakuchi, R.; Toda, A.; Satoh, T.; Kawaguchi, S.; Sugiyama, K.; Hirao, A.; Kakuchi, T. *Macromol. Rapid Commun.* **2008**, *29*, 1126.
- (71) Shin, J.; Nazarenko, S.; Hoyle, C. E. *Macromolecules* **2009**, *42*, 6549.
- (72) Chan, J. W.; Shin, J.; Hoyle, C. E.; Bowman, C. N.; Lowe, A. B. *Macromolecules* **2010**, *43*, 4937
- (73) Wu, Z.; Liang, H.; Lu, J. *Macromolecules* **2010**, *43*, 5699.
- (74) Bousquet, A.; Barner-Kowollik, C.; Stenzel, M. H.; *J. Polym. Sci., Part A: Polym. Chem.* **2010**, *48*, 1773.

- (75) (a) Mansfeld, U.; Pietsch, C.; Hoogenboom, R.; Becer, R.; Schubert U. *Polym. Chem.*, **2010**, *1*, 1560. (b) Iha, R. K.; Wooley, K. L.; Nystroem, A. M.; Burke, D. J.; Kade, M. J.; Hawker, C. J. *Chem. Rev.* **2009**, *109*, 5620.
- (76) Poloukhine, A. A.; Mbua, N. E.; Wolfert, M. A.; Boons, G. J.; Popik, V. V. . *J. Am. Chem. Soc.* **2009**, *131*, 15769.
- (77) Gruending, T.; Oehlenschlaeger, K. K.; Frick, E.; Glassner, M.; Schmid, C.; Barner-Kowollik, C. *Macromol. Rapid Commun.* **2011**, *32*, 807.
- (78) (a) Wiss, K. T.; Krishna, O. D.; Roth, P. J.; Kiick, K. L.; Theato, P. *Macromolecules* **2009**, *42*, 3860. (b) Roth, P. J.; Wiss, K. T.; Zentel, R.; Theato, P. *Macromolecules* **2008**, *41*, 8513. (c) Mcrae, S.; Chen, X. J.; Kratz, K.; Samanta, D.; Henchey, E.; Schneider, S.; Emrick, T. *Biomacromolecules*, **2012**, *13*, 2099.
- (79) Zhao, H.; Theato, P. *Polym. Chem.* **2013**, *4*, 891.
- (80) (a) Zhao, H.; Sterner, E.; Coughlin, E. Theato, P. *Macromolecules*, **2012**, *45*, 1723. (b) Zhao, Y. *Macromolecules* **2012**, *45*, 3647. (c) Han, D.; Tong, X.; Zhao, Y. *Macromolecules* **2011**, *44*, 437. (d) Gumbley, P.; Koylu, D.; Thomas, S. W. *Macromolecules* **2011**, *44*, 7956. (e) Smith, Z. C.; Pawle, R. H.; Thomas, S. W. *ACS Macro Lett.* **2012**, *1*, 825.
- (81) Pauloehrl, T.; Delaittre, G.; Bruns, M.; Meißler, M.; Bçrner, H. G.; Bastmeyer, M.; Barner-Kowollik, C. *Angew. Chem. Int. Ed.* **2012**, *51*, 9181.
- (82) Kakuchi, R.; Zamfir, M.; Lutz, J. F.; Theato, P. *Macromolecular Rapid Communication* **2012**, *33*, 54.

8 Appendix (published work)

8.1 Highly-ordered Nanoporous Thin Films from Photocleavable Block Copolymers

Hui Zhao,¹ Weiyin Gu,² Elizabeth Sterner,² Thomas P. Russell,² E. Bryan Coughlin,^{2*} Patrick Theato^{1, 3, 4*}

¹ Institute of Organic Chemistry, University of Mainz, Duesbergweg 10-14,
D-55099 Mainz, Germany

² Department of Polymer Science & Engineering, University of Massachusetts, 120 Governors Drive,
Amherst MA, 01003-4530

³ World Class University (WCU) program of Chemical Convergence for Energy &
Environment (C₂E₂), School of Chemical and Biological Engineering, College of Engineering, Seoul
National University (SNU), Seoul, Korea

⁴ present address: Institut für Technische und Makromolekulare Chemie, Universität Hamburg, Bundesstr.
45, 20146 Hamburg, Germany

Published on Macromolecules **2011**, *44*, 6433-6400.

* Corresponding authors. E-mails: theato@chemie.uni-hamburg.de and Coughlin@mail.pse.umass.edu.

ABSTRACT: Poly(styrene-*block*-ethylene oxide) (PS-*hv*-PEO) with a photocleavable junction (*o*-nitrobenzyl ester) was synthesized by a combined RAFT polymerization and “click chemistry“ approach and represents the first report utilizing this method for the synthesis of photocleavable block copolymers. After solvent annealing, highly ordered thin films were prepared from PS-*hv*-PEO. Following a very mild UV exposure and successive washing with water, PS-*hv*-PEO thin films were transferred into highly ordered nanoporous thin PS films with pore diameters of 15~20 nm and long range ordering (over 2 μm x 2 μm). Afterwards the pores were filled with PDMS by spin-coating in combination with capillary forces. After removal of the PS templates and treatment with oxygen plasma, highly ordered silica nanodots were obtained. This represents the first template application example from highly ordered nanoporous thin films derived from block copolymers featuring a photocleavable junction.

Introduction

Highly-ordered nanoporous thin films through self-assembly of block copolymers (BCPs) have received continuous attention since they are a promising platform for a "bottom-up" fabrication of nanostructured materials and devices.¹ However, several challenges have to be addressed before nanoporous thin films can be used for fabrication of advanced templates and devices. One of the most severe challenges is the selective removal of one domain under very mild and technological compatible conditions. Until now, diverse methods have been developed for the selective removal of one domain, such as chemical etching,² ozonolysis,³ and UV degradation.⁴ However, most of these methods work under relatively harsh conditions or are limited to specific kinds of degradable polymers, such as poly(methyl methacrylate), poly(1,4-isoprene) and poly(lactic acid). To overcome these drawbacks, the approach of introducing an efficiently cleavable linker between the two blocks has been developed and received considerable attention.^{5,6} In particular, the strategy based on photocleavable junctions is a very promising platform for the synthesis of nanoporous materials (Figure 1).⁶

Among the many photocleavable groups available, *o*-nitrobenzyl (ONB) alcohol derivatives have gained tremendous attention in the area of synthetic organic chemistry.⁷ Moon and coworkers were the first to demonstrate the possibility to achieve photocleavable BCP thin films based on ONB.^{6a} They synthesized a photocleavable polystyrene-*block*-poly(ethylene oxide) diblock copolymer by ATRP using an ONB-functional PEO macroinitiator. Recently, Fustin and coworkers developed a one pot ATRP–CuAAC “Click” method to synthesize photocleavable BCPs.^{6b} The pioneering work of Moon and Fustin shows that the introduction of an ONB junction to BCPs is a very promising method to prepare nanoporous thin films.

RAFT polymerization is generally considered to have certain potential benefits over ATRP in the controlled polymerization of functional monomers.⁸ However, the synthesis of RAFT chain transfer agents (CTAs) is difficult, in particular for macromolecular CTAs, which often requires multiple steps

of end-group modification. Developing CTAs suitable for the synthesis of photocleavable BCPs based on ONB remains a challenge that has not yet been addressed, in particular by combining RAFT polymerization and “Click” chemistry⁹ for this purpose. A combined “RAFT-Click” method has two advantages: a) it can avoid the synthesis of a macro-CTA, which is very difficult to purify since they often need multiple steps of macromolecular reactions (Scheme 1, Route A); and b) it represents a platform method capable to provide easy access to series of different photocleavable BCPs.

In this work, we successfully developed a “RAFT-Click” method to synthesize photocleavable BCPs (Scheme 1, Route B) and compared it to the sequential route using a macro-CTA approach. The resulting photocleavable BCPs were then used to prepare highly ordered thin films. Following exposure to UV light and washing step with water is expected to lead to highly ordered nanoporous thin films (see figure 5.1.1). As a demonstration of the utility of the nanoporous array a replication technique resulting in silica nanodots will be investigated using a simply spin coating procedure with polydimethylsiloxane and treatment with oxygen plasma.

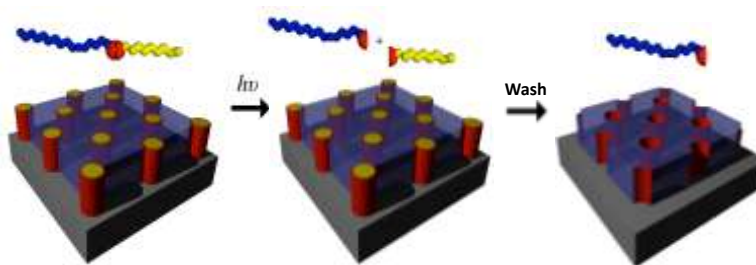


Figure 1. Schematic representation of the self-assembly of photocleavable block copolymers and the subsequent removal of one domain after UV irradiation.

Results and Discussion

Polymer Synthesis and Photolysis in Solution

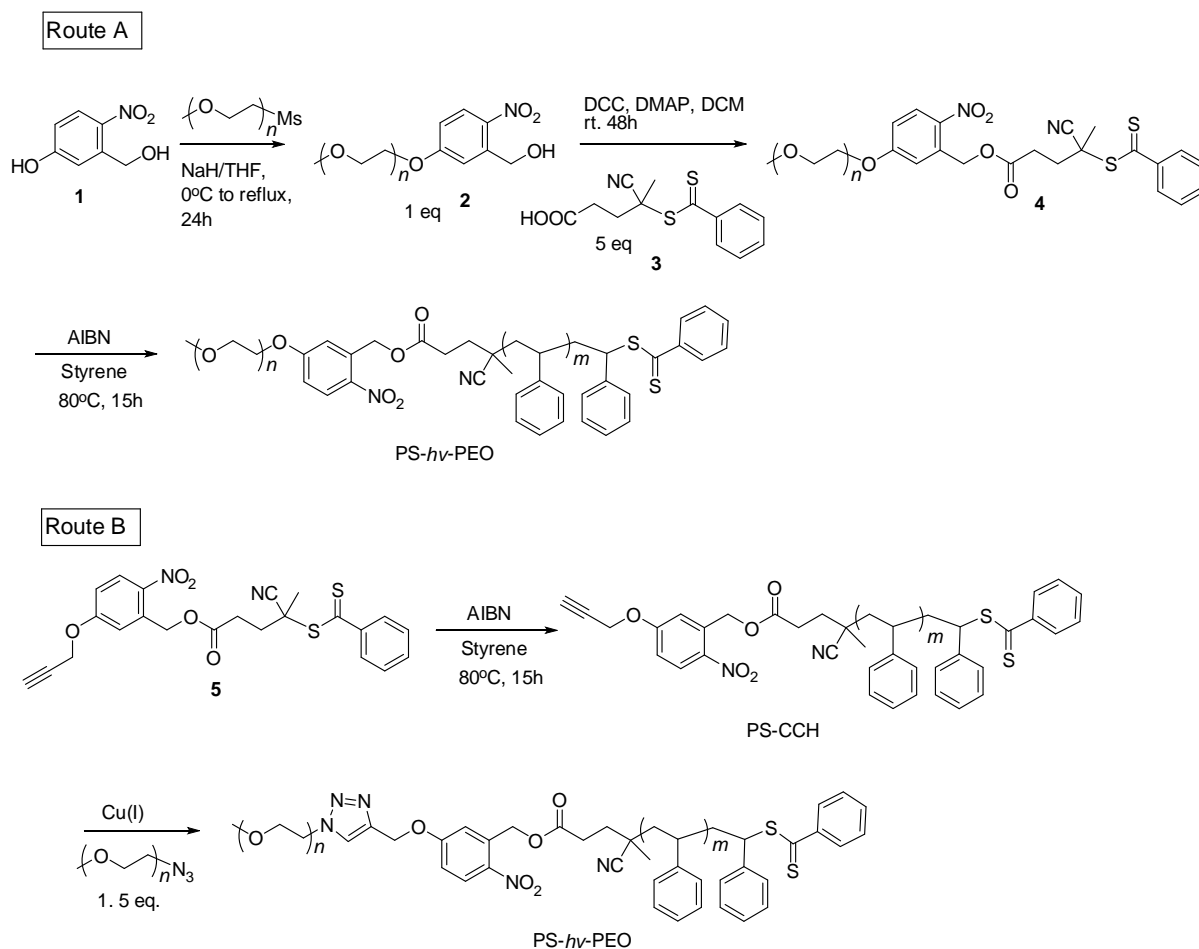
To demonstrate the versatility of the “RAFT-Click” approach yielding photocleavable BCPs, two different routes involving RAFT polymerization yielding PS-*hν*-PEO have been investigated. We have

employed the nomenclature of “*hv*” in place of the common italic “*b*” to denote a BCP with a photocleavable junction point between the two blocks. In the first route, the traditional RAFT polymerization utilizing a macro-CTA (Scheme 1, Route A) and in the second route) a combined RAFT polymerization-“click chemistry” approach (Scheme 1, Route B). For Route A, a macromolecular chain transfer agent (**4**) was synthesized in two steps from monomethoxy polyethyleneoxide, 3-hydroxymethyl-4-nitrophenol (**1**) and 4-cyano-4-(phenylcarbonothioylthio)pentanoic acid (**3**). The overall yield of **4** was very low due to multiple reactions on macromolecular end-groups and an unexpected disulfide dimer (**9**) was found to be present in the final product (see supporting information, Scheme S1). A mechanism for this dimerization yielding polymeric disulfides was proposed (Scheme S1) and verified by an obvious GPC change after adding (*DL*-dithiothreitol, DTT) due to the reductive cleavage of the proposed disulfide bond (Scheme S2 and Figure S1). It is very difficult to remove the polymeric disulfide **9** from the desired CTA **4** due to the small difference in molecular weight (29k vs 16k) and their very similar hydrophilic properties. Accordingly, all attempts to use the mixture for a RAFT polymerization of styrene resulted in a poor control over the polymerization (PDI >1.5).

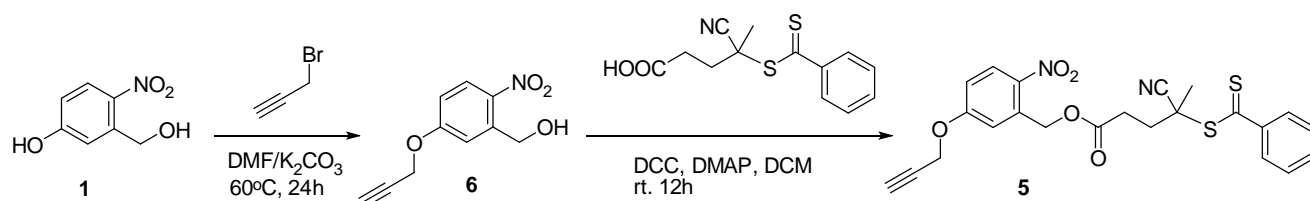
Compared with route A, the advantages of route B are: a) straight forward synthesis of CTA in high yields (Scheme 2); (b) RAFT polymerization using CTA (**5**) is well controlled (Table 1 and Figure S3); and (c) the “RAFT-Click” method represents a versatile platform for the production of photocleavable BCPs, which can be easily prepared by replacing PEO-N₃ with other polymers featuring an azide end-group as well as replacing styrene with other functional monomers during the RAFT polymerization. The RAFT polymerization of styrene and “Click” coupling with PEO-N₃ were successful and the resulting polymers were characterized by ¹H NMR and GPC. Polystyrene **P4** (Table 1, PS, $M_{n,GPC}$ = 15700) and the resulting block copolymer **P4-*hv*-PEO** will exemplarily be discussed in the following as typical representative for all synthesized block copolymers.

¹H NMR spectra of the photocleavable RAFT agent **5**, PS (**P4**) and **P4-*hv*-PEO** are shown in Figure 1. All protons of compound **5** could be assigned (see Figure 1A). Polystyrene with ONB end group was prepared by RAFT polymerization using CTA **5**. The ¹H NMR spectrum of **P4** (see Figure 1B) revealed

besides the signals for PS at 1.17~2.0 ppm (main chain) and at 6.30~7.50 ppm (side chain phenyl group) that the alkyne end-group (Figure 1B, peak 11) remained intact after RAFT polymerization. After the “Click” reaction with PEO-N₃, the peak 11 disappeared in the ¹H NMR (see Figure 1C). Further, the chemical shift of the methylene protons (peak 12 in Figure 1B) close to the triple bond shifted from 4.76 ppm to 5.29 ppm (peak 17 in Figure 1C) due to the presence of the electron-withdrawing 1,2,3-triazole ring. According to ¹H NMR, the yield of “Click” coupling between PEO-N₃ and alkyne end functionalized PS was nearly quantitative.



Scheme 1 Two RAFT polymerization routes for the synthesis of photocleavable PS-*hν*-PEO.



Scheme 2 Synthesis of CTA 5.

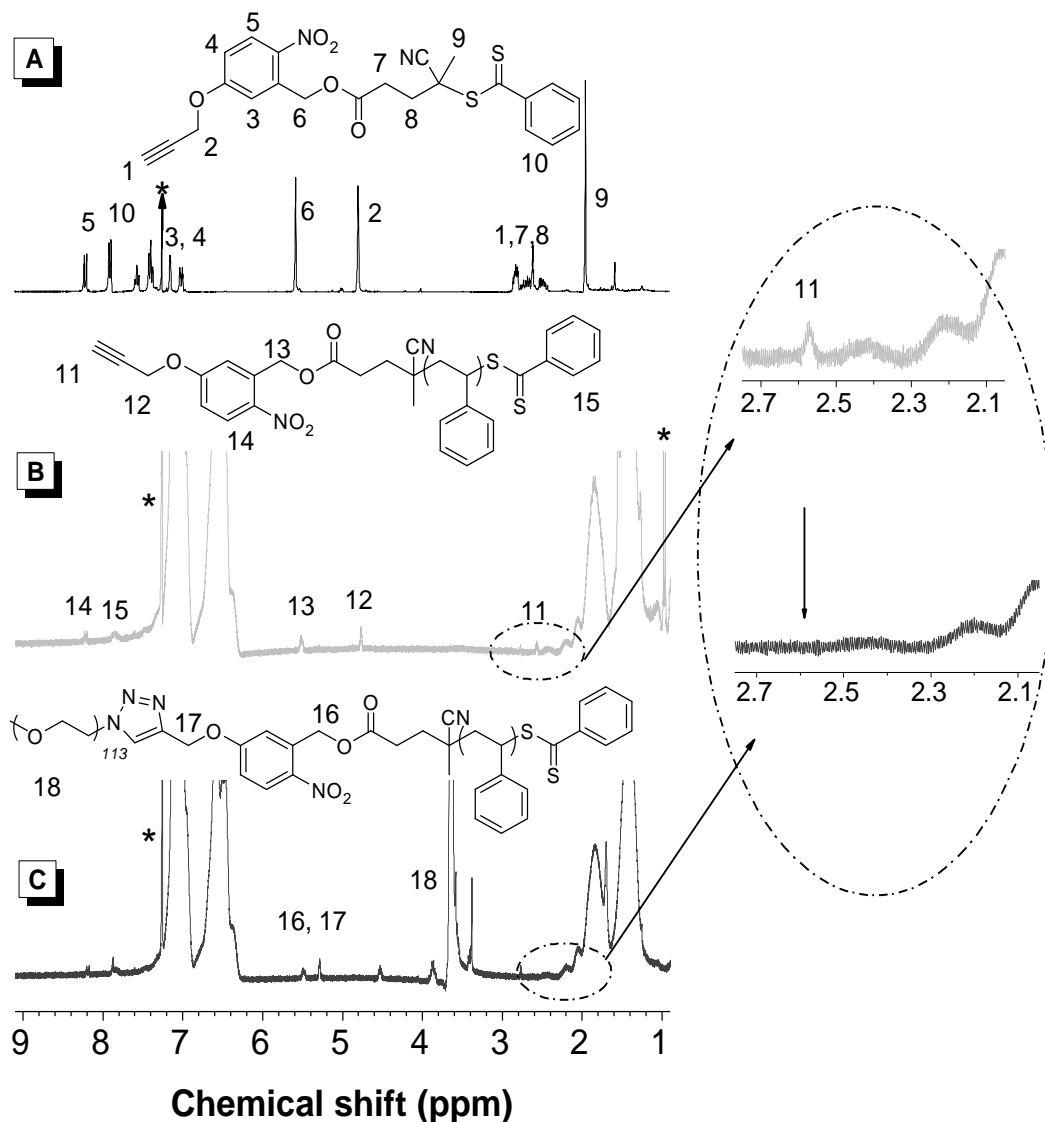


Figure 1. ¹H NMR (all in CDCl₃) (A) CTA 5, (B) alkyne end-group functionalized polystyrene (P4) prepared by RAFT polymerization, (C) PS-*hν*-PEO (P4-*hν*-PEO) by “click” chemistry with PEO-N₃.

As summarized in table 1, PS with different molecular weights (5 kDa to 27 kDa, $M_w/M_{n,GPC}$ below 1.20) were prepared by RAFT polymerization utilizing CTA 5. The polymerization was carried out at 80°C in both bulk and dioxane as a solvent with a ratio [AIBN]:[CTA] of 1:8. The highest conversion in the bulk was nearly the same as that in dioxane (about 20 %). Given the fact that nitrobenzene can act as an inhibitor for radical polymerization, ONB might effect RAFT polymerization. To check the ONB effect on the polymerization, a polymerization was performed in the presence of CTA (4-cyano-4-(phenylcarbonothioylthio) pentanoic acid) using the same polymerization conditions as with CTA 5. The

conversion of polymerization in the presence of CTA (4-cyano-4-(phenylcarbonothioylthio) pentanoic acid) is also approximately 20%. Thus, we concluded the ONB did not affect on the RAFT polymerization, which is in accordance to the ^1H NMR data shown in figure **1B**.

Table 1 Synthesis of the alkyne end-group functionalized polystyrenes (PS-C \equiv CH) and block copolymers (PEO-*h* ν -PS) bearing a photocleavable ONB junction.^a

PS and PEO	[St] ₀ /[CTA]	$M_{n,GPC}$ (g/mol ⁻¹)	$M_w/M_{n,GPC}$	PS- <i>h</i> ν -PEO	$M_{n,GPC}$ (g/mol ⁻¹)	$M_w/M_{n,GPC}$
PS-C \equiv CH(P1)	240	5200	1.17	P1-<i>h</i>ν-PEO	15000	1.30
PS-C \equiv CH(P2)	480	12000	1.12	P2-<i>h</i>ν-PEO	22000	1.22
PS-C \equiv CH(P3)	600	14400	1.13	P3-<i>h</i>ν-PEO	24000	1.23
PS-C \equiv CH(P4)	720	15700	1.12	P4-<i>h</i>ν-PEO	27000	1.22
PS-C \equiv CH(P5)	1080	23700	1.19	P5-<i>h</i>ν-PEO	33000	1.30
PS-C \equiv CH(P6)	1200	26800	1.20	P6-<i>h</i>ν-PEO	37000	1.30
PEO-N ₃	-	9500	1.04			

^a RAFT polymerization was carried out at 80 °C with a ratio [AIBN]:[CTA] of 1:8, conversion of styrene was around 20%; “Click” coupling between PEO-N₃ and PS (PS-C \equiv CH) was carried out at room temperature in the presence of CuBr/PMDETA (*N,N,N',N',N''*-pentamethyldiethylenetriamine) (molar ratio: 1/1).

Next, “Click” coupling between PEO-N₃ and **P4** (PS-C \equiv CH) was carried out at room temperature in the presence of CuBr/PMDETA (*N,N,N',N',N''*-pentamethyldiethylenetriamine) (molar ratio: 1/1) as catalyst. As amines tend to trigger an aminolysis of the dithioester end-group of RAFT polymers resulting often in disulfide dimerization, polymers obtained by RAFT polymerization are often treated with AIBN to replace the dithioester end-group which would avoid this side reaction.^{9g} However, this adds one more step to the synthesis. To keep the synthesis route as short as possible, we omitted the step

of AIBN radical substitution of the dithioester. Given CuBr/PMDETA as the catalyst, we tried to reduce the amount of catalyst in the “Click” coupling to prevent the use of any excess of PMDETA to eliminate side reactions. When the ratio between CuBr/PDEDTA and PS-C≡CH was 0.3:1 (or lower), the “Click” coupling worked very well (Table 1, Figure 2). The PDI of the resulting PS-hv-PEO diblock copolymers were between 1.22 to 1.30 with almost no indication of polymer dimerization. Even though a small tailing towards higher molecular weights was still observed in the GPC (see figure 2), it did not have an effect on the organization behavior of the diblock copolymers within thin films.

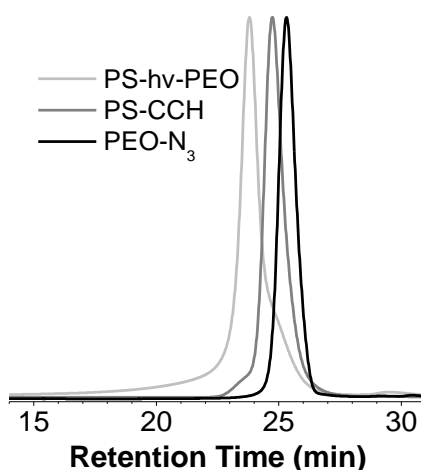


Figure 2 GPC trace of P4-hv-PEO ($M_{n, GPC} = 27000$, PDI = 1.22), PS-CCH (P4, $M_{n, GPC} = 15700$, PDI = 1.12), and PEO-N₃ ($M_{n, GPC} = 9500$, PDI = 1.04) in chloroform using linear PS standards.

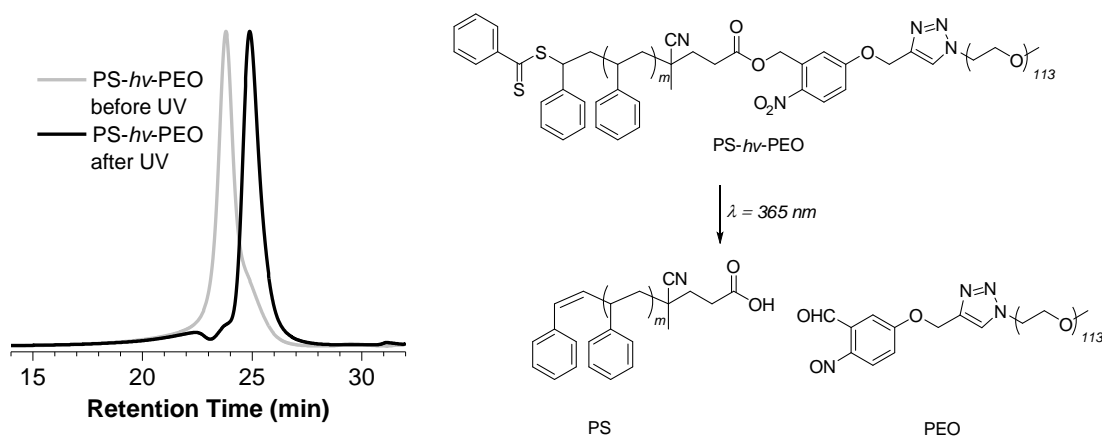


Figure 3 GPC trace in chloroform of PS-hv-PEO (P4-hv-PEO) before and after UV exposure using linear PS standard (Left). Photolysis for PS-hv-PEO in solution (Right).

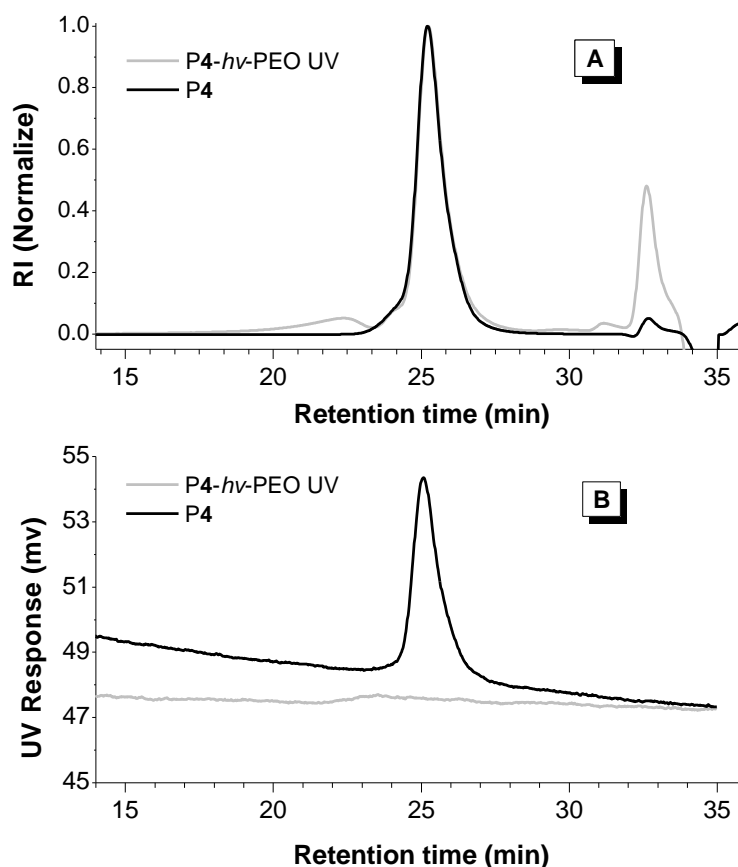


Figure 4 GPC-RI (A) and GPC-UV (wavelength = 512 nm, at dithio ester absorbance peak) (B) trace of **P4** and **P4-hv-PEO** after UV exposure using linear PS as standard sample.

P4-hv-PEO was selected as an example to demonstrate the photolysis of the prepared photocleavable block copolymers in solution. Photolysis of **P4-hv-PEO** in dioxane was carried out in a NMR tube under UV light exposure using a common UV lamp ($\lambda=365$ nm, 1.3 mW/cm²). After 12 hours, the cleaved polystyrene was then collected by precipitating into MeOH. GPC analysis showed that **P4-hv-PEO** was cleaved completely under UV exposure resulting in PS (Figure 3, Left). However, the PS obtained from photolysis of **P4-hv-PEO** was white (**P4** and **P4-hv-PEO** were pink), indicating that the CTA end group might also be cleaved under UV exposure (Figure 3, Right). GPC with refractive index (IR) and UV-Vis (UV) (wavelength = 512 nm, at dithio ester absorbance peak) detection were used in combination to detect the **P4-hv-PEO** and **P4** to prove this hypothesis (Figure 4). If the CTA was intact after UV

exposure, the GPC-IR and GPC-UV should result in overlapping GPC traces. As can be seen from Figure 4, the PS collected from P4-*hν*-PEO after UV irradiation was nearly the same as P4 in GPC-IR (Figure 4A). But the UV-Vis GPC trace measured after UV exposure had no peak, showing clearly that the CTA group was also cleaved during the UV exposure. These results indicate that UV exposure is also a simple, non-chemical method for removing CTA groups from RAFT polymers, which is in agreement with the literature.¹⁴

Highly Ordered Nanoporous Thin Film and Application as Nanodots Template

PS-*b*-PEO BCPs have attracted considerable attention for the generation of highly-ordered microphase separated thin films of nanocylinders oriented perpendicular to the substrate.¹ However, the PEO block is not easily removable by simple etching processes, limiting potential applications.¹⁰ Russell and coworkers introduced PS-*b*-PMMA-*b*-PEO triblock system, in which PMMA could be degraded by short-wave UV exposure.^{4b} Venkataraman and coworkers reported a PS-*b*-PEO system with an acid-sensitive trityl ether linkage, which can be cleaved by acid treatment.^{5d} All these methods can selectively remove the PEO block and result in highly ordered nanoporous thin films, but they require harsh cleavage conditions: PS-*b*-PMMA-*b*-PEO undergoes cleavage at high-intensity short-wave UV irradiation; PS-*b*-PEO with the trityl ether junction requires exposure to strong acid. As demonstrated above, photolysis of PS-*hν*-PEO is successful under mild UV irradiation conditions. Accordingly, PS-*b*-PEO featuring an ONB cleavable junction seems a strong candidate for highly ordered nanoporous thin films. So far, only one example of thin films prepared from PS-*b*-PEO with an ONB junction has been reported^{6a}, however, the morphology of thin films was not highly ordered, limiting its potential application. We therefore tried to find the best condition of solvent annealing to get highly ordered morphology in the thin film, which will lead to highly ordered templates after UV cleavage of the ONB junction.

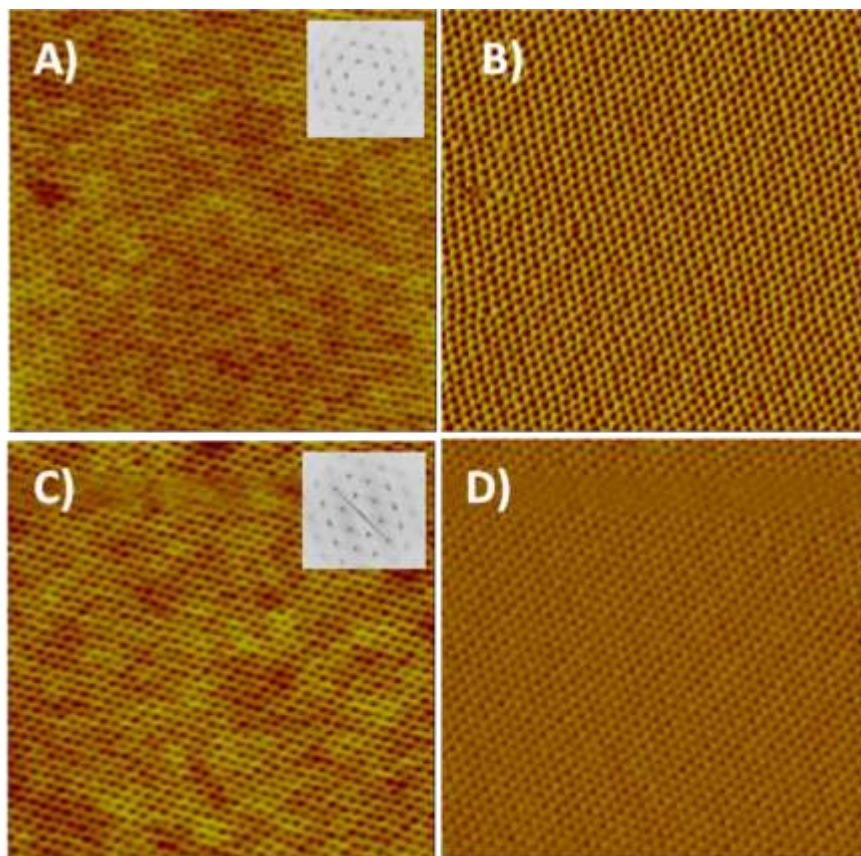


Figure 5 AFM height (A, C) and phase (B, D) images for PS-*hv*-PEO thin films (film thickness ~30 nm) after annealing for 2.5 h in H₂O/THF atmosphere. A and B: P5-*hv*-PEO (5k-24K); C and D: P6-*hv*-PEO (5K-26.8K). Scale: 1 μm x 1 μm . The insets in A and C show the corresponding 2D Fourier transform.

PS-*hv*-PEO was spin-coated from toluene solution onto silicon wafers and a highly ordered morphology for these PS-*hv*-PEO thin films was obtained after annealing for 2.5 h at 20°C in a H₂O/THF atmosphere. In particular, highly ordered hexagonally packed cylinders oriented perpendicular to the substrate were obtained for the block copolymers P5-*hv*-PEO and P6-*hv*-PEO (see figure 5). The Fourier transforms of the AFM images are shown in the insets of Figure 5A and 5C. Six-point patterns, with multiple higher-order reflections are clearly seen, which is characteristic for a long-range lateral ordering.¹¹ This highly ordered morphology of PS-*hv*-PEO is a prerequisite for highly-ordered nanoporous thin films.

The next step was the selective removal of the PEO block from the PS-*hν*-PEO thin film in simple two-step procedure, first UV exposure (365 nm for 12 h) to promote photocleavage and subsequent removal of the PEO by a washing step with water. This mild procedure maintains the highly ordered morphology. As can be seen from AFM images in figure 6, highly ordered nanoporous thin films with six point FT patterns were obtained after UV exposure and a successive water washing step. The pores in the film were around 15~20 nm in diameter, similar to the diameter of the original PEO cylinders, and had very narrow domain size distributions. TEM images also showed highly ordered nanoporous morphology in the resulting PS thin film (see figure 7). Noteworthy, the contrast between bright and dark domains was enhanced noticeably after UV exposure and washing with water, which indicates the enhanced electron contrast due to the removal of the PEO domain. The highly ordered array morphology was of long range order (over 2 μm x 2 μm) as seen from TEM (see supporting information, figure S6).

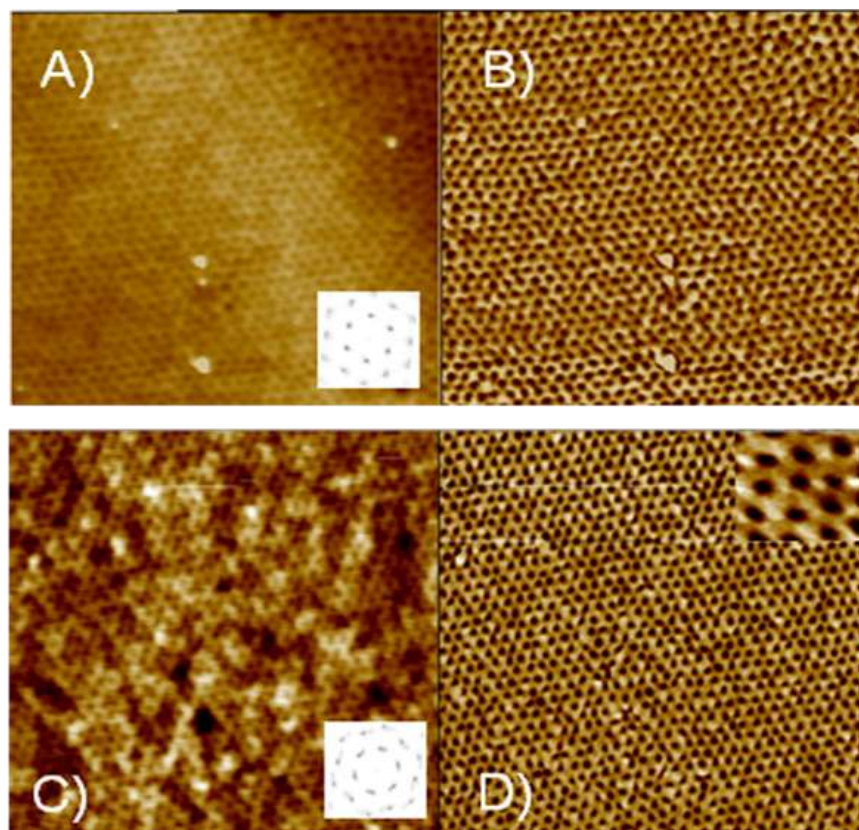


Figure 6 AFM height (A, C) and phase (B, D) images for PS-*hν*-PEO thin film (film thickness ~30 nm) after UV exposure and washing with water. A and C: P5-*hν*-PEO (5K-24K); B and D: P6-*hν*-PEO

(5K-26.8K). The insets in A and C show the corresponding Fourier transform. Inset in D shows a magnified image at 100 nm x 100 nm. A-D scale: 1 μm x 1 μm .

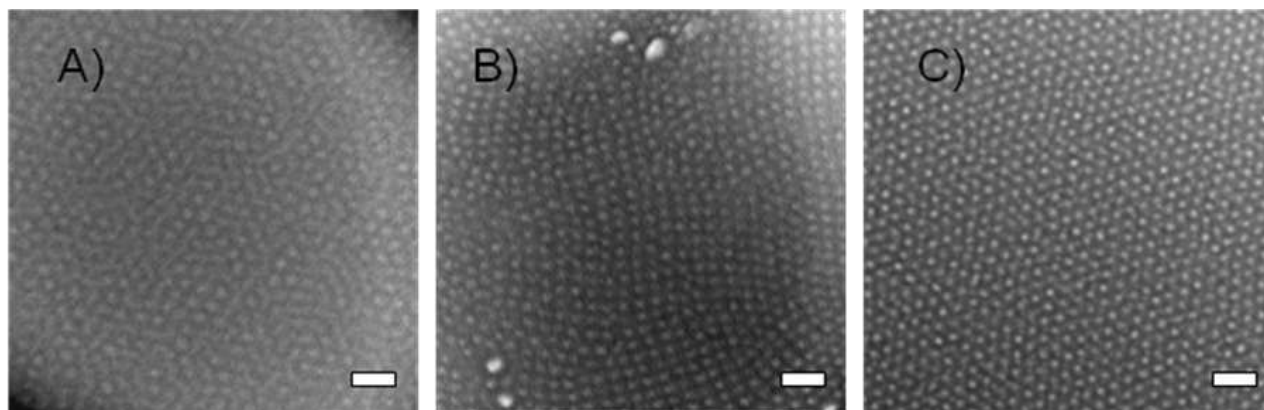


Figure 7 TEM images for PS-*h ν* -PEO thin film before (A, P5-*h ν* -PEO) and after UV exposure and water wash (B, P5-*h ν* -PEO; C, P6-*h ν* -PEO). Scale bar: 100 nm.

To prove that our nanoporous structures were not a result from a potential reconstruction of the thin film by drawing PEO to the surface of the film¹¹ but are rather a result of the PEO removal, high-resolution X-ray Photoelectron Spectroscopy (XPS) was performed. First, XPS measurements were performed on PEO, PS-*h ν* -PEO and PS-*h ν* -PEO after UV treatment at the bottom surface of the thin films at 75°. There were at least eight kinds of carbon related bonds in PS-*h ν* -PEO: for the PS block, C-C, C-H bond in backbone and C-C, C-H bond in phenyl side group; for the PEO block, C-C bond and C-O, C-C, C-H bonds in backbone. A shoulder was observed at 286-284 eV (C-O bond) for PS-*h ν* -PEO before UV irradiation, which vanished almost completely after UV irradiation (see supporting information figure S4). Next, the nanoporous thin films (PS-*h ν* -PEO films post-UV treatment) were analyzed at the top surface by XPS at 15° (see supporting information, figure S5). The spectra obtained from the surface were the same as the spectra from the bottom surface, allowing us to conclude that the holes are resulted from PEO remove and throughout from surface to bulk in the film.

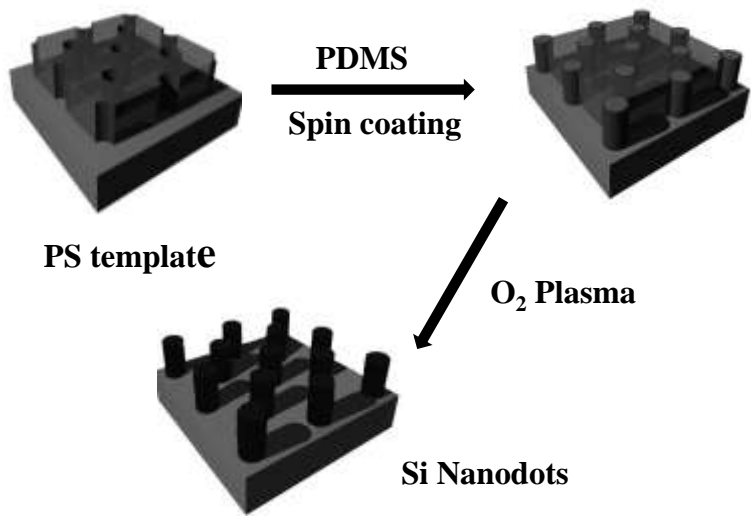


Figure 8 Schematic illustration for preparation of silica nanodots from a nanoporous PS template. Filling the pores with PDMS by spin-coating and subsequent conversion into silica nanodots by oxygen plasma treatment.

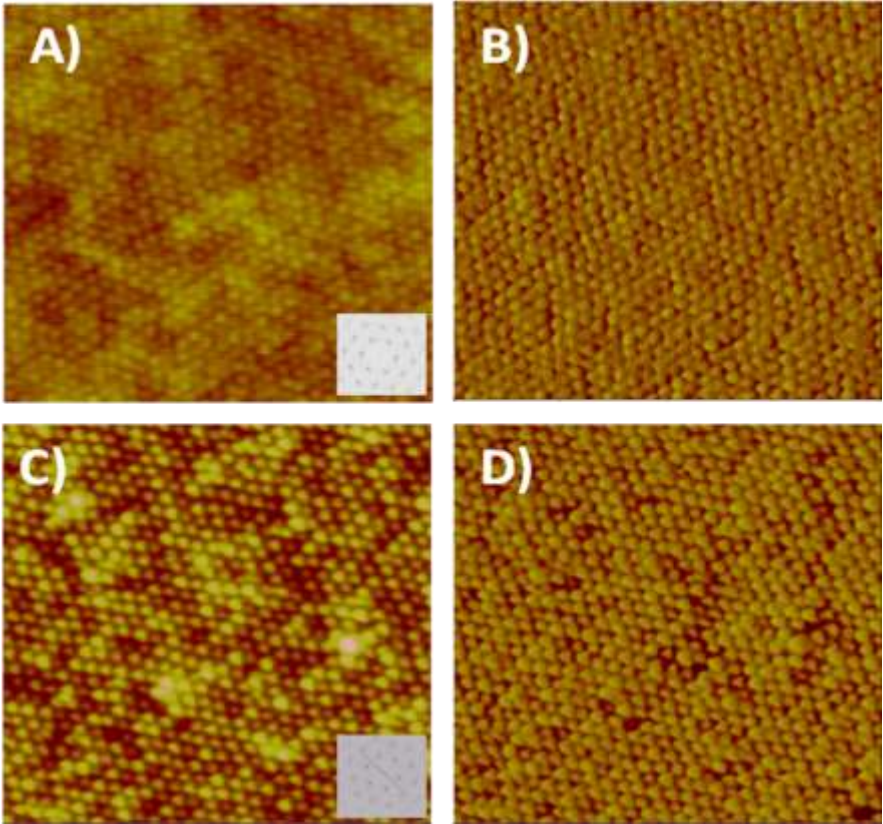


Figure 9 AFM height (A, C) and phase (B, D) images of silica nanodots obtained from PDMS by oxygen plasma treatment. The insets in A and C show the corresponding Fourier transform. Scale: 1 μm x 1 μm .

The highly-ordered morphology in the nanoporous thin film makes it a good candidate to be used as a nanoscale template. As a proof of concept, silica nanodot array were produced utilizing the PS template. As illustrated in figure 8, silica nanodots were prepared using a PS template in two steps: a) spin-coating PDMS from heptane solution on the nanoporous thin film; b) removing the PS template and oxidizing PDMS by treatment with an oxygen plasma (1 hour, 30 W, 0.2 bar O₂). The resulting SiO₂ nanodots were then imaged by AFM. It should be noted that the morphology of the resulting nanodots persisted a long-range lateral order transferred from the mother template, as can be evidenced by the Fourier transform patterns, demonstrating these PS-*hν*-PEO block copolymers are good candidates for the preparation and utilization as nanotemplates with long range order.

Conclusions

In this work, we demonstrated the development of a versatile method to produce photocleavable block copolymers via “RAFT-Click” combination, which is a platform methodology that allows the fabrication of highly ordered arrays of nanopores via the self-assembly of photocleavable block copolymer thin films. Under mild UV treatment and subsequent washing with water, almost perfect hexagonal arrays of ~15 nm diameter holes were obtained. Highly ordered silica nanodots were then prepared utilizing these nanoporous thin films, which showed that the high degree of order of the nanoporous films can be transferred from the template into nanodot array.

Experimental Section

Materials and Characterization

Styrene was filtered through basic aluminum oxide before polymerization, and 2, 2'-azobisisobutyronitrile (AIBN) was recrystallized from methanol. Triethylamine and Dichloromethane (DCM) were distilled from calcium hydride. Tetrahydrofuran (THF) was distilled from sodium benzophenone ketyl. Monomethoxy PEO (5000 g/mol) was purchased from Sigma Aldrich. All other

reagents were purchased from commercial sources and used as received unless otherwise noted. The ^1H NMR was measured on a Bruker 300 MHz NMR spectrometer using tetramethylsilane (TMS; $\delta = 0$ ppm) as internal standard. The average molecular weights (M_w and M_n) and polydispersity indices (PDIs) of the polymers were estimated by a Waters Associates GPC system in chloroform. A set of monodisperse polystyrene standards covering molecular weight range of 10^3 – 10^7 was used for the molecular weight calibration mode. Films for transmission electron microscopy (TEM) were prepared on silicon substrates having a thick layer of silicon oxide. These films were floated off the surface with a 5 wt % HF solution, transferred to a water bath, and then picked up on a Cu grid. A JEOL 100CX electron microscope operating at 100 kV was used to examine the morphology. Scanning force microscopy was performed on a Digital Instruments Dimension 3100, operating in tapping mode. The XPS analysis was carried out in a Physical Electronics apparatus with a nonmonochromatic Mg K α radiation source at 15° and 75° take off angle. The sensitivity factors specified for the spectrometer were used for quantitative analysis. The pressure in the analysis chamber was less than 10^{-5} Pa. The spectrum collection time was kept under 10 min to minimize X-ray damage.

CTA Synthesis 3-Hydroxymethyl-4-nitrophenol (**1**), PEO-ONB-OH (**2**), Compound **3**, PEO-MS, PEO-N₃ and compound **6** were prepared according to previously published methods.^{6, 12, 13}

Macromolecular CTA (4). Into a 250 mL round-bottom flask were placed 2 g (0.4 mmol) of PEO-ONB-OH (**2**), 1.1 g (4 mmol) of compound **3**, 400 mg (2 mmol) of 1,3-dicyclohexylcarbodiimide (DCC), 50 mg (0.4 mmol) of 4-dimethyl-aminopyridine (DMAP) and 150 mL DCM. The resultant mixture solution was stirred at room temperature for 48 h. After filtration, the solution was extracted three times by DCM/water followed by removal of DCM in vacuum. The residue was diluted with DCM and precipitated from diethylether. A slightly pink powder (1 g, yield~50%) was obtained after filtration and dried one night in vacuum at 30°C . ^1H NMR (300 MHz, CDCl_3), δ (TMS, ppm): 8.20 (d, ArH), 7.90 (d, ArH), 7.60-7.31 (m, ArH), 7.05 (s, ArH), 6.95 (d, ArH), 5.5 (s, $-\text{CH}_2\text{O}$), 4.20-3.38 (CH_2O in PEO), 3.35 (s, OCH_3), 2.15 (s, $\text{C}(\text{CN})\text{CH}_3$).

ONB-CTA (5). Into a 50 mL round-bottom flask were placed 830 mg (4 mmol) of compound **6**, 1.2 g (4.4 mmol) of compound **3**, 800 mg (4 mmol) of 1, 3-dicyclohexylcarbodiimide (DCC), 50 mg (0.4 mmol) of 4- dimethyl-aminopyridine (DMAP) and 20 mL DCM. The resultant mixture solution was stirred at room temperature for 16 h. DCM was removed under reduced pressure and the residue was collected and purified by a silica gel column using chloroform as eluent. A pink highly viscous compound was obtained in 83% yield (1.5 g). ¹H NMR (300 MHz, CDCl₃), δ (TMS, ppm): 8.24 (d, 1H, ONB), 7.92 (d, 2H, SS-ArH), 7.60 (t, 1H, SS-ArH), 7.43 (t, 2H, SS-ArH), 7.15 (s, 1H, ONB), 7.03 (d, 1H, ONB), 5.58 (s, 2H, ONB-CH₂-O), 4.80 (s, 2H, HCC-CH₂-ONB), 2.86-2.43 (m, 5H, OOC-CH₂-CH₂, HCC-CH₂-ONB), 1.95 (s, 3H, C(CN)CH₃). ¹³C NMR (300 MHz, CDCl₃), δ (TMS, ppm): 219.5 (C(=S)S), 170.8 (C(=O)C), 161.6 (C-O, phenyl of ONB), 144.4 (C-C(=S)S), 140.8 (C-NO₂), 134.9 (C-CH₂, phenyl of ONB), 133.9 (*p*-C-C(=S)S), 128.6 (*m*-C-C(=S)S), 128.0 (*o*-C-C(=S)S), 126.6 (CN), 118.4 (*o*-C-C-NO₂, phenyl of ONB), 114.8 (*o*-C-C-O, *m*-C-C-NO₂, phenyl of ONB), 113.9(*o*-C-C-O, *o*-C-C-CH₂, phenyl of ONB), 63.6 (CC, alkyne group), 56.4 (CCH, alkyne group), 45.7 (CH₃-C-CN), 33.3 (C-C-C(-CN, -CH₃)), 29.8 (C-C-C(=O)), 24.2 (CH₃).

General Procedure for RAFT Polymerizations

Styrene, CTA (1 equivalent) and AIBN (0.125 equivalent) were put in a dry Schlenk tube. The reaction mixture was degassed by three freeze-pump-thaw cycles and the flask refilled with nitrogen. It was then stirred in a preheated oil bath at 80 °C for 15 h. For isolation of the polymer, the pink product (conversion: 20%) was precipitated three times into cold hexane and dried at 30 °C in vacuum. ¹H NMR (300 MHz, CDCl₃), δ (TMS, ppm): 8.24 (d, ONB), 7.86 (broad, SS-ArH), 7.60-7.43 (broad, SS-ArH), 7.33-7.29 (broad, ArH in PS), 5.53 (s, ONB-CH₂-O), 4.77 (s, HCC-CH₂-ONB), 2.58 (s, HCC-CH₂-ONB), 2.44-1.20 (broad, OOC-CH₂-CH₂, C(CN)CH₃, CH-CH₂ backbone in PS).

Click Reactions PS-C≡CH(1 equivalent), PEO-N₃ (2 equivalent), CuBr/PMEDTA (0.3 equivalent/0.3 equivalent) and dioxane (2 ml per 1g PS) were put in a dry Schlenk tube. The reaction mixture was degassed by three freeze-pump-thaw cycles and the flask was refilled with nitrogen. It was then stirred at room temperature for 48 h. The reaction solution was extracted 3 times by DCM/water; then all the

solvents were removed under reduced vacuum. The pink residue was washed more than 5 times by methanol (100 ml per 1 g product) and dried at 30 °C in a vacuum oven. Yield: ~80%. ¹H NMR (300 MHz, CDCl₃), δ (TMS, ppm): 8.24 (d, 1H, ONB), 7.88 (s, CH=C in triazole), 7.85 (broad, 1H, SS-ArH), 7.60-7.43 (broad, 2H, SS-ArH), 7.33-7.29 (broad, ArH in PS), 5.50 (s, ONB-CH₂-O), 5.30 (s, triazole-CH₂-ONB), 4.53 (broad, triazole-CH₂-CH₂-O), 3.88 (broad, triazole-CH₂-CH₂-O), 3.70-3.45 ((broad, CH₂-CH₂-O), 3.38 (s, O-CH₃), 2.44-1.20 (broad, OOC-CH₂-CH₂, C(CN)CH₃, CH-CH₂ backbone in PS).

General Procedures for Preparation of the Thin Films The PS-*h_v*-PEO BCPs were spin coated from toluene solutions onto silicon substrates and then annealed in a H₂O/THF atmosphere for 2.5 h. The film thickness was controlled by adjusting the solution concentration and the spinning speed. To cleave the PEO block, the block copolymer films were put in a methanol solution under UV exposure with a wavelength of 365 nm at a dose of 5.6 J cm⁻² (Blak-Ray Model B, UVL-56) for 12 h; then rinsed in water for 2h.

Silicon Nanodots from Nanoporous Thin Films Template Polydimethylsiloxane (PDMS, Aldrich, *M_w* =62 000 g/mol) dissolved in heptane was spin-coated onto the films, annealed at 50 °C for 1 h to enhance the mobility of PDMS and draw the PDMS into the interstitial regions (Chart 2). Finally, the PDMS was transformed into silica by oxygen plasma treatment (1 hour, 30 W, 0.2 bar O₂), while PS template was completely degraded.

Acknowledgement. Financial support from the German Science Foundation (DFG) under grant TH 1104/4-1, and an International Collaboration in Chemistry award from the National Science Foundation (CHE 0924435) is gratefully acknowledged. This research was partly supported by WCU (World Class University) program through the National Research Foundation of Korea funded by the Ministry of Education, Science and Technology (R31-10013). The authors thank J. Hirsch (UMass, Amherst) for XPS measurement and helpful discussion.

Supporting Information. The mechanism of dimerization RAFT polymer and GPC trace before and after adding a reductive agent (DL-Dithiothreitol, DTT); ¹H NMR of compound **2** and **4** in CDCl₃;

RAFT polymerization kinetics based on CTA **5**. XPS spectra of nanoporous thin films; TEM image of nanoporous thin film with large scale (over 2 μm x 2 μm).

References and Notes

- (1) Leiston-Belanger, J. M.; Russell, T. P.; Drockenmuller, E.; Hawker, C. J. *Macromolecules* **2005**, *38*, 7676–7683.
- (2) Lee, J. S.; Hirao, A.; Nakahama, S. *Macromolecules* **1988**, *21*, 274–276.
- (3) (a) Thurn-Albrecht, T.; Steiner, R.; DeRouchey, J.; Stafford, C. M.; Huang, E.; Bal, M.; Tuominen, M.; Hawker, C. J.; Russell, T. P. *Adv. Mater.* **2000**, *12*, 787–791. (b) Bang, J.; Kim, S. H.; Drockenmuller, E.; Misner, M. J. Russell, T. P. and Hawker, C. J. *J. Am. Chem. Soc.* **2006**, *128*, 7622–7629.
- (4) (a) Coursan, M.; Desvergne, J.P.; Deffieux, A. *Macromol. Chem. Phys.* **1996**, *197*, 1599–1608. (b) Goldbach, J. T.; Russell, T. P. Penelle, J. *Macromolecules* **2002**, *35*, 4271–4276. (c) Yurt, S.; Anyanwu, U. K.; Scheintaub, J. R.; Coughlin, E. B. and Venkataraman, D. *Macromolecules* **2006**, *39*, 1670-1672. (d) Zhang, M.; Yang, L.; Yurt, S.; Misner, M. J.; Chen, J. T.; Coughlin, E. B.; Venkataraman, D. and Russell T. P. *Adv. Mater.* **2007**, *19*, 1571–1576.
- (5) (a) Kang, M. and Moon, B. *Macromolecules*, **2009**, *42*, 455-458. (b) Schumers, J. M.; Gohy J. F. and Fustin, C. A. *Polym. Chem.*, **2010**, *1*, 161–163.
- (6) (a) Mayer, G. and Heckel, A. *Angew. Chem. Int. Ed.* **2006**, *45*, 4900–4921. (b) Bochet, C. G. *J. Chem. Soc. Perk. T.* **2002**, *2*, 125-142.
- (7) (a) Eberhardt, M. and Theato, P. *Macromol. Rapid Commun.* **2005**, *26*, 1488–1493. (b) Rowe-Konopacki, M. D. and Boyes, S. G. *Macromolecules*, **2007**, *40*, 879-888.
- (8) “Click” chemistry has obtained great success in macromolecule science, in particular, postfunctionalization of preformed polymers through polymer reactions. See: (a) Golas, P. L.; Matyjaszewski, K. *Chem. Soc. Rev.* **2010**, *39*, 1338-1354. (b) Liu, J. Z.; Lam, J. W. Y.; Tang, B. Z. *Chem. Rev.* **2009**, *109*, 5799. (c) Qin, A.; Lam, J. W. Y.; Tang, B. Z. *Chem. Soc. Rev.*, **2010**, *39*, 2522–2544. (d) Hawker, C. J.; Wooley, K. L. *Science* **2005**, *309*, 1200. (e) Helms, B.; Mynar, J. L.; Hawker, C. J.; Frechet, J. M. J. *J. Am. Chem. Soc.* **2004**, *126*, 15020-15201. (f) Quemener, D.; Davis, T. P.; Barner-Kowollik, C.; Stenzel, M. H. *Chem. Commun.*, **2006**, 5051–5053. (g) Wiss, K. T. and Theato, P. *J. Poly. Sci.: Part A: Poly. Chem.* **2010**, *48*, 4758–4767. (h) Mansfeld, U.;

Pietsch, C.; Hoogenboom, R.; Remzi Becer, R. C. and S. Schubert, U. S. *Polym. Chem.*, **2010**, *1*, 1560–1598.

(9) Mao, H.; Hillmyer, M. A. *Soft Matter*, **2006**, *2*, 57. (b) Mao, H.; Hillmyer, M. A. *Macromolecules* **2005**, *38*, 4038.

(10) Park, S.; Kim, B.; Xu, J.; Hofmann, T.; Ocko, B. and Russell, T. P. *Macromolecules* **2009**, *42*, 1278-1284.

(11) Thang, S. H.; Chong, Y. K.; Mayadunne, R. T. A.; Moad, G. and Rizzado, E. *Tetradron Letters* **1990**, *40*, 2435-2438.

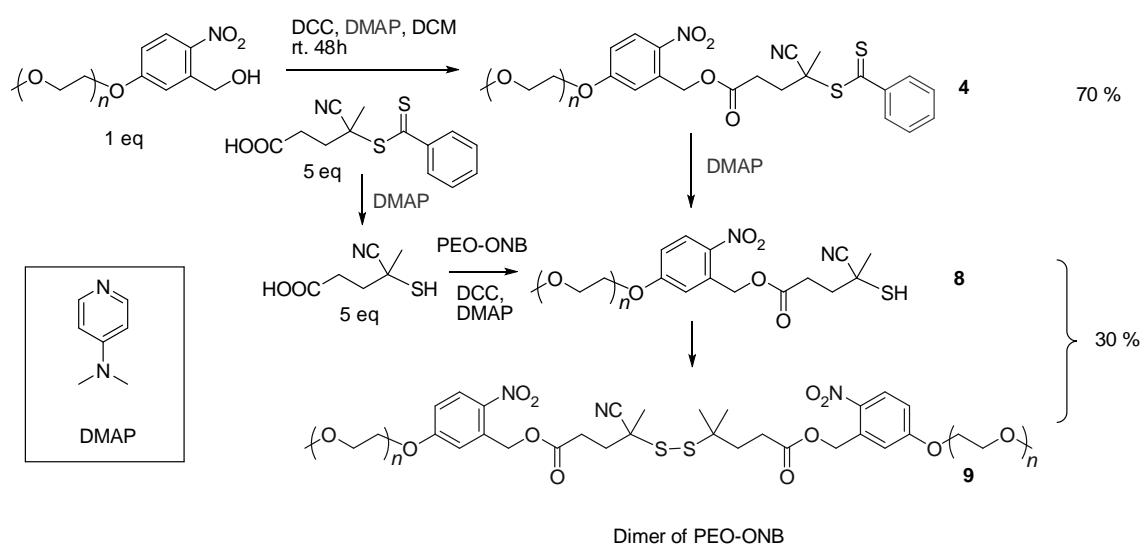
(12) Fishman, A.; Farrah, M. E.; Zhong, J. H.; Paramanatham, S.; Carrera, C. and Lee-Ruff E. *J. Org. Chem.* **2003**, *68*, 9843-9846.

(13) (a), Barner-Kowollic, C. *Handbook of RAFT polymerization* Wiley-VCH 2008, (b) Willcock, H. and O'Reilly, R. K. *Polym. Chem.*, **2010**, *1*, 149–157.

Supporting Information

Highly-ordered Nanoporous Thin Films From Photocleavable Block Copolymers

Scheme S1



Scheme S2

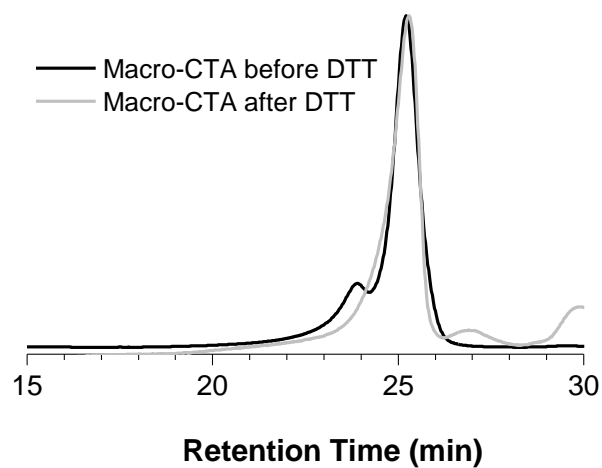
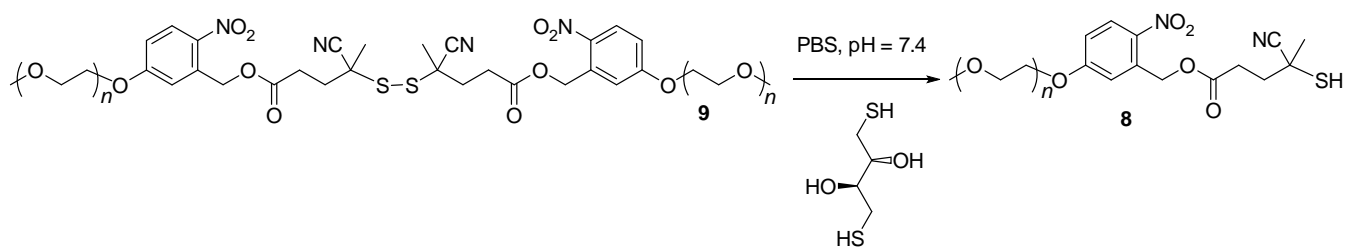


Figure S1. GPC trace of Macro-CTA before and after adding DTT in chloroform.

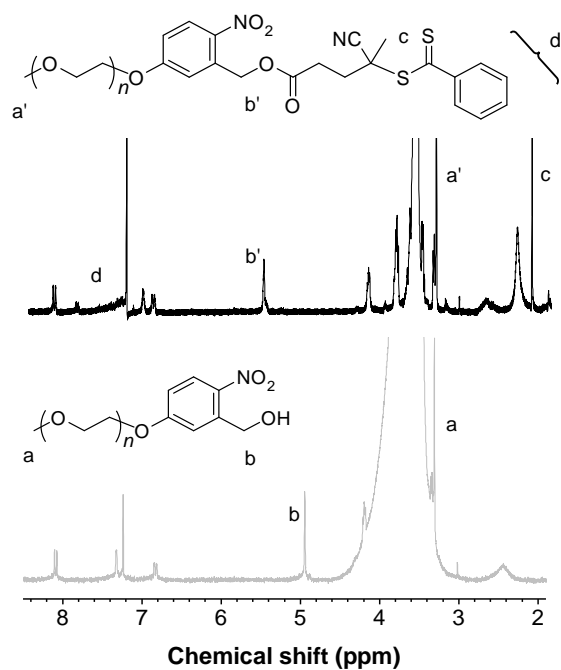


Figure S2. ¹H NMR of compound 2 and 4 in CDCl₃.

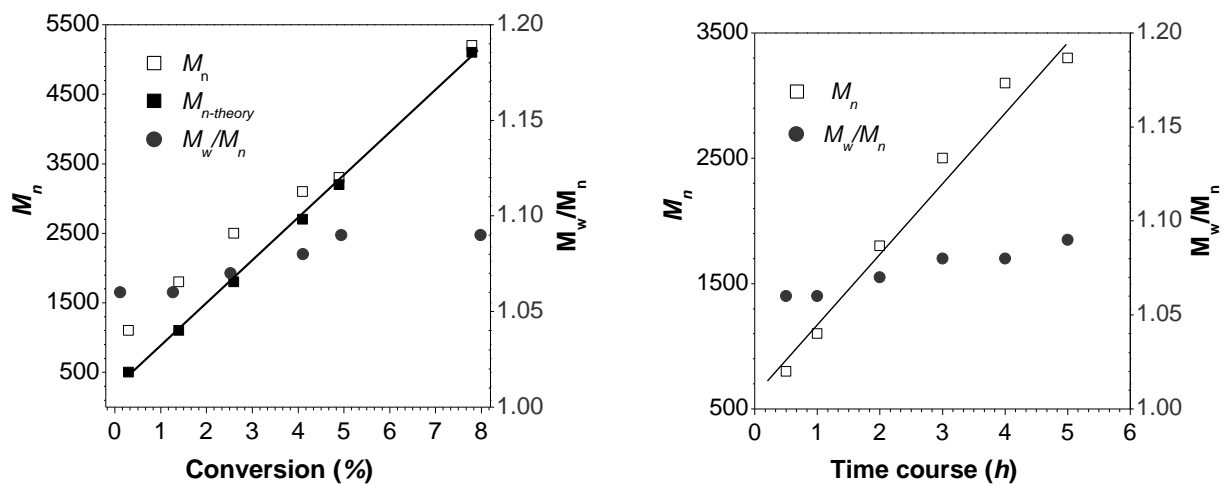


Figure S3. RAFT polymerization kinetics based on CTA 5.

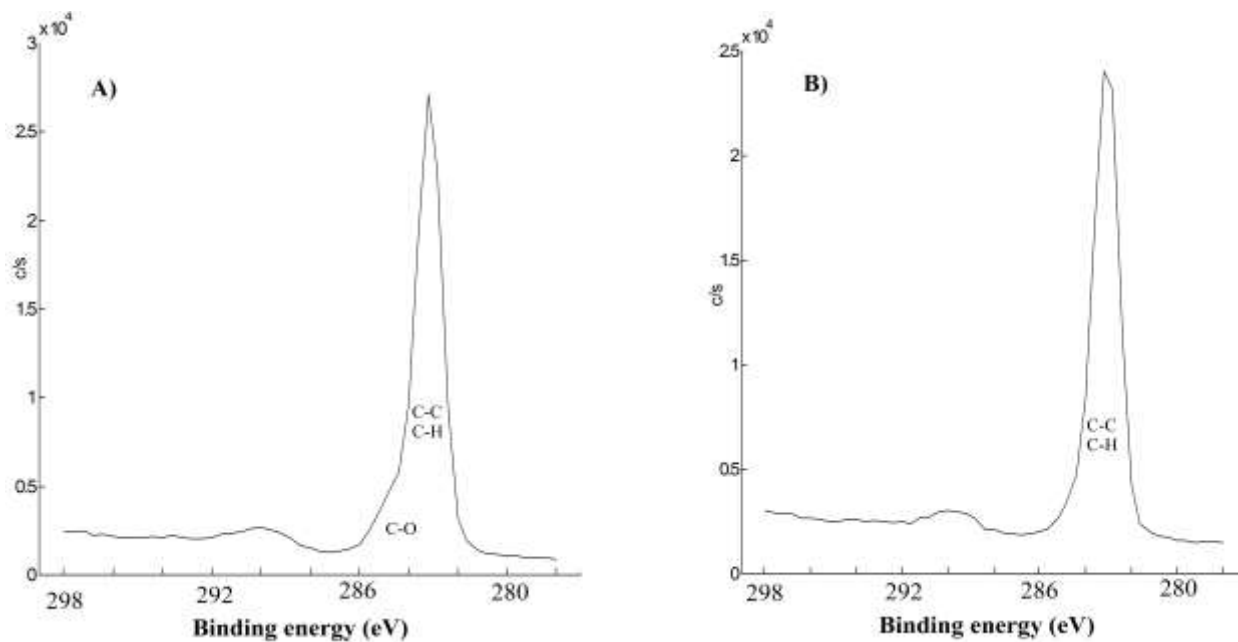


Figure S4. C1s high-resolution XPS spectra of thin film at 75 deg (bottom of film) taken off angle: A) PS-*hν*-PEO; B) PS-*hν*-PEO after UV exposure and water wash.

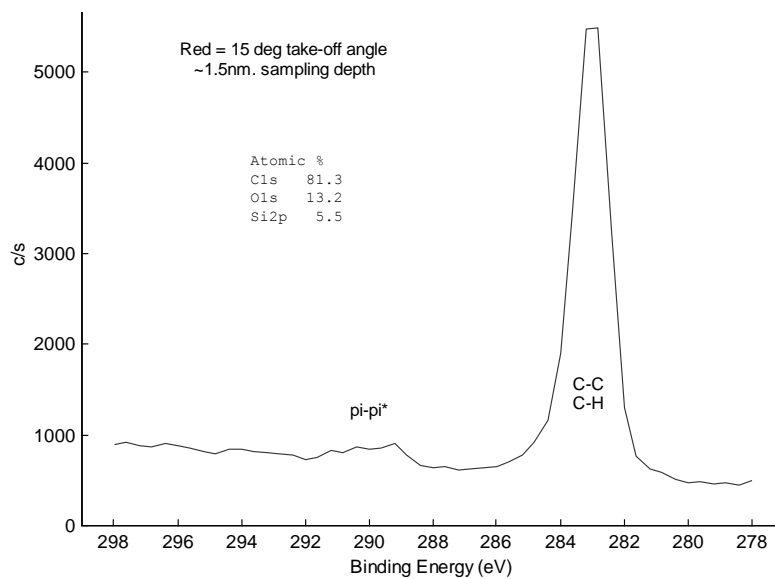


Figure S5. C1s high-resolution XPS spectra of thin film (PS-*hν*-PEO after UV exposure and water wash) at 15 deg taken off angle.

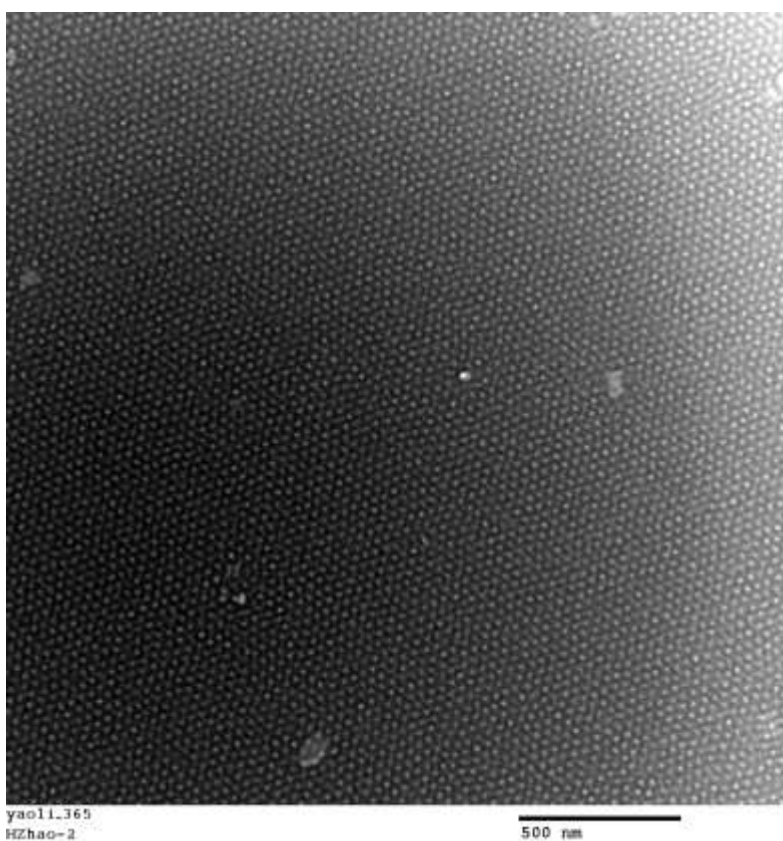


Figure S6. TEM images for PS-*hν*-PEO (P6-*hν*-PEO) thin film after UV exposure and water wash.

8.2 Copolymers Featuring Pentafluorophenyl Ester and Photolabile Amine Units: Synthesis and Application as Reactive Photopatterns

Hui Zhao and Patrick Theato

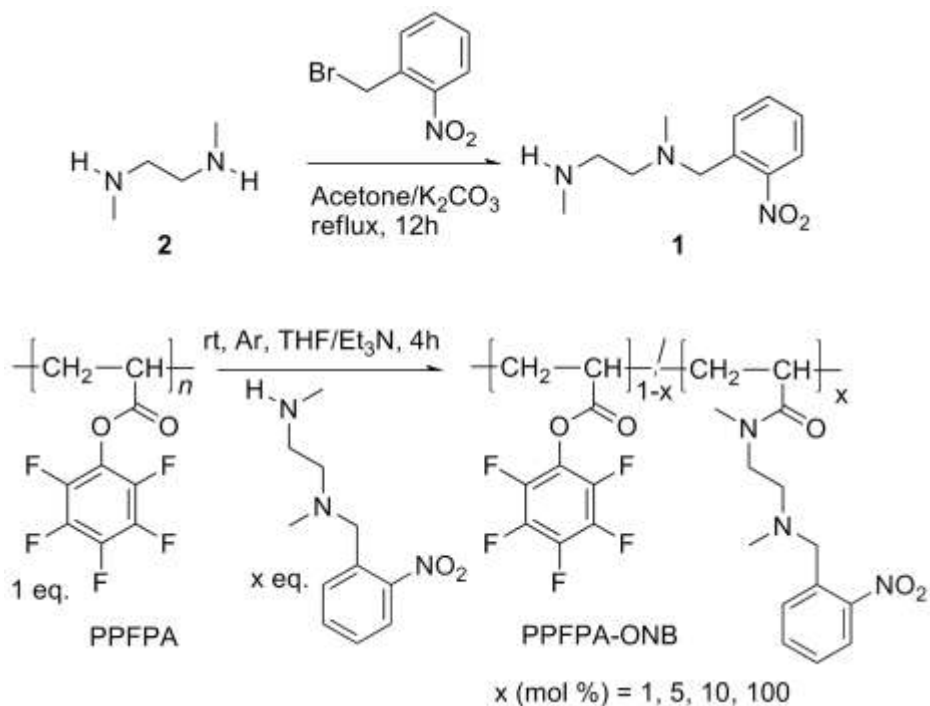
Published on Polymer Chemistry 2013, 4, 891-894.

ABSTRACT: Copolymers featuring pentafluorophenyl ester and *o*-nitrobenzyl (ONB) protected amine moieties have been prepared. Upon UV irradiation, the ONB protected amine group was released, which subsequently induced a crosslinking by a spontaneous reaction with pentafluorophenyl esters, resulting in stable, reactive patterned thin films. Remaining esters were converted with a fluorescent dye.

Introduction

Ortho-Nitrobenzyl (ONB) alcohol derivatives, known as *caged* groups, have attracted increasing interest in biochemistry and synthetic chemistry as photolabile protecting groups.¹ Recently, ONB gained attention in the field of polymer chemistry and materials science² in applications such as photocleavable hydrogels,³ polymer thin films patternings,⁴ self-assembled monolayers,⁵ photocleavable block copolymers⁶ and photocleavable bioconjugates.⁷ However, controlling the polymerization of ONB containing monomers is still difficult as nitro-aromatic compounds can act as inhibitors/retarders during the radical polymerization process. It was found that 2-nitrobenzyl methacrylate can be polymerized under controlled radical polymerization (CRP) with some degree of control, however, only with low monomer conversion. 2-Nitrobenzyl acrylate cannot be polymerized under CRP conditions.⁸ The development of well-defined ONB containing homo- and copolymers remains still a challenge, which has not been addressed yet satisfactorily.⁹

Post-polymerization modification of well-defined reactive polymers provides a suitable possibility for the introduction of chemical functionalities that would otherwise interfere with the polymerization process.¹⁰ In previous studies, we could present polymers featuring pentafluorophenyl (PFP) ester as very promising reactive polymeric precursor for the synthesis of well-defined multifunctional polymers.¹⁰ This encouraged us to develop well-defined ONB containing polymers utilizing polymeric active esters. Herein, we report on the synthesis of ONB containing homo- and copolymers by post-polymerization modification of poly(pentafluorophenyl acrylate) (PPFPA) with a mono ONB-protected diamine (PPFPA-ONB). Under UV irradiation, ONB protected amine group in PPFPA-ONB is released, which can subsequently induce a crosslinking via activated ester-amine chemistry resulting in a network formation. Consequently, amine reactive micropatterns are prepared by photolithography. The synthetic strategy shown in **Scheme 1**, combines the advantages of activated ester-amine chemistry with the photochemistry of *o*-nitrobenzyl (ONB) derivative. The key idea is the use of a mono ONB-protected diamine (*N,N'*-dimethyl-*N*-(2-nitrobenzyl)ethane-1,2-diamine **1**), which can be used as an irreversible photo-protected crosslinking agent. Hence compound **1** was used as photo-crosslinker because a) it is easily accessible in a one-step reaction, b) it can be incorporated by reaction of the free amine with polymers bearing activated ester groups, allowing a facile control of the ONB unit ratio and c) it enables a photo-deprotection by UV-light irradiation.^{1,2} The ONB protected amine would release the desired amine quantitatively along with *o*-nitrosobenzaldehyde upon irradiation.¹ Consequently, the spontaneous reaction of the photo-released amines with the activated ester side groups of the polymer would result in a network formation.



Scheme 1 Synthesis of mono ONB-protected diamine (1) and PPFPA-ONB.

Results and discussion

First, a post-polymerization modification of the activated ester polymer and ONB labile amine was performed. As can be seen from the proton NMR (Figure 1, left), intensifying signals of aromatic protons (around 8 to 6.8 *ppm*) are observed due to increasing the amount of ONB incorporated within the polymer. In Table 1, the targeted and measured ONB contents are compared, which are matching within experimental accuracy. The molecular weights were measured by GPC in THF and are listed in Table 1. The molecular weights (M_n) of PPFPA-ONB were slightly smaller than the initial PPFPA, due to the marginal chemical variation of the polymer side groups. The molecular weight distribution (PDI) of the obtained copolymers was slightly broader than the PDI of its parent polymer PPFPA, but still smaller than 1.5. It should be noted that the incorporated ONB amount in PPFPA-ONB can be up to 100mol%, according to ^{19}F NMR (Figure 1H, right).

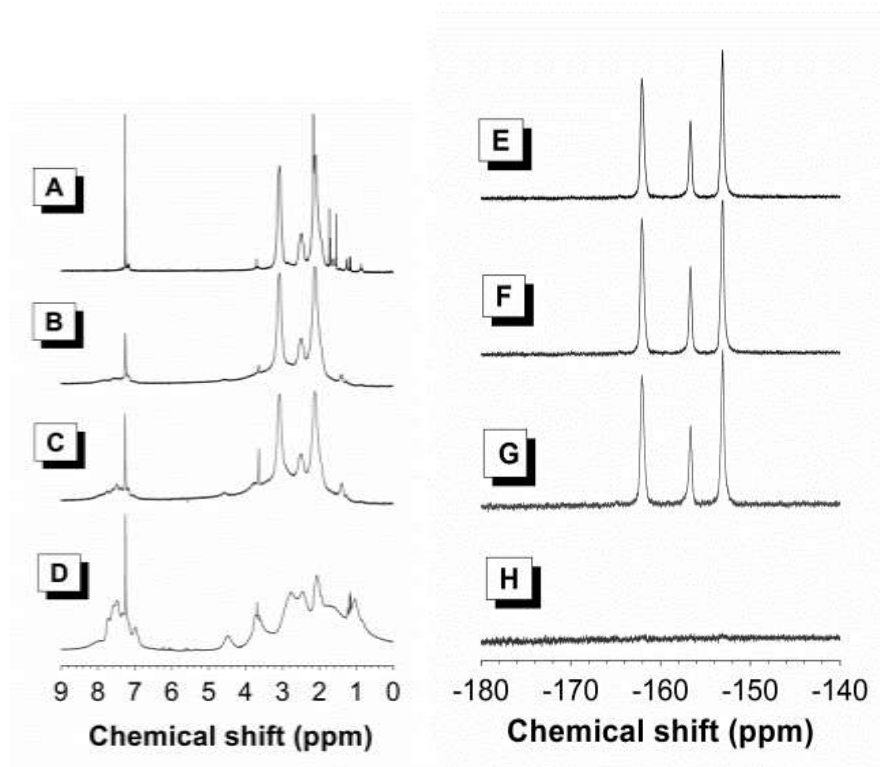


Figure 1 ^1H NMR (A-D) and ^{19}F NMR (E-H) for PPFPA-ONB in CDCl_3 . ONB ratio (mol%): 0 (A,E), 5 (B,F), 10 (C,G) and 100 (D,H).

Table 1 P(PFPA-ONB) copolymer.

Nr	ONB (mol%) calculated	ONB (mol%) measured ^a	M_n (g mol^{-1}) ^c	PDI ^c	Yield (%)	Pattern formation
1	0	0	12800	1.38	50	NA
2	1	0.8	12000	1.47	65	no
3	5	4.5	10800	1.45	60	no
4	10	9.5	10700	1.45	73	yes
5	100	100 ^b	10400	1.40	40	NA

^a according to ^1H NMR; ^b according to ^{19}F NMR and IR; ^c GPC in THF, PS standard. NA, not analysis.

Next, the photo-deprotection of poly(pentafluorophenyl acrylate) featuring ONB-amine moieties (PPFPA-ONB) with 10mol% ONB units was investigated in solution (Table 1, entry #4). For that reason, a polymer solution in THF (10 mg/mL) was prepared and irradiated in a quartz glass cuvette for 3 hour at 313 nm and UV/Vis spectra were recorded before and after irradiation. As shown in **Figure 2A**, a new peak appeared at around 350 nm after 45 min of irradiation with UV light, corresponding to the formation of the cleaved byproduct nitrosobenzaldehyde.⁶

Additionally, the polymer solution in THF became turbid after irradiation as a consequence of the photo-deprotection of the amines of the copolymer and their reaction with active ester groups (see Figure S2). After 1 hour of UV irradiation, the transmittance of the PPFPA-ONB solution decreased down to 30% of the initial value, indicating the formation of an insoluble network due to the cross-linking reaction (see Figure 2B).

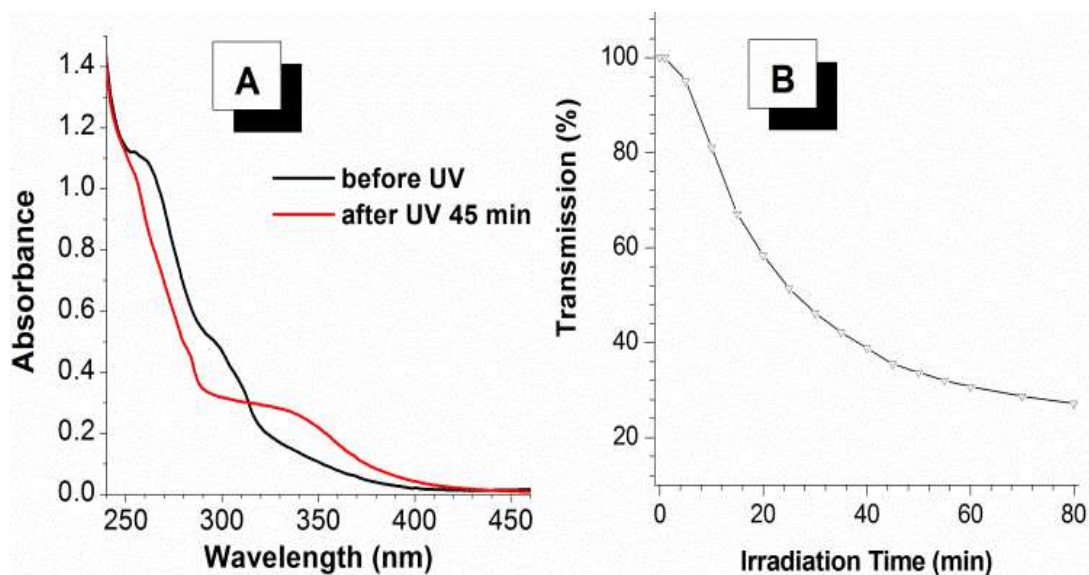


Figure 2 Irradiation ($\lambda = 313$ nm) time dependent UV spectra and turbidity curve of PPFPA-ONB in THF (1 mg/mL).

Motivated by these results, photo-induced crosslinking reactions were performed within thin polymer films to study the possibility of photopatterning. Chart 1 outlines the photopatterning of PPFPA-ONB on glass and the consecutive functionalization of the remaining activated ester groups with

an amine-functionalized fluorescent dye. After spin coating PPFPA-ONB onto a glass substrate (10 wt% in THF, 3000 rpm), reactive patterns could be obtained by irradiation of the thin films for 3 hours at 313 nm through optical masks followed by 3 washing steps in THF (process A in Chart 1). The stability of the patterns was strongly depended on the ONB content within PPFPA-ONB polymers. Stable patterns were only obtained from copolymers with an incorporated ONB moiety of at least 10 mol% (see Table 1). The non-irradiated and thus non-crosslinked areas of the polymer thin film could easily be removed by simply washing with solvent, making it a good negative photoresist As can be seen from Figure 3A and 3E, the obtained patterns were of micrometer scale and very stable on glass, even after a subsequent 12 h treatment in THF. The active ester groups of the polymer remained stable during and after UV irradiation. The FT-IR spectra showed the characteristic band of C=O bond in PFPA ester at 1780 cm^{-1} , and the band of aromatic C-F bond in pentafluorophenyl group in 1520 cm^{-1} (Figure S1A).

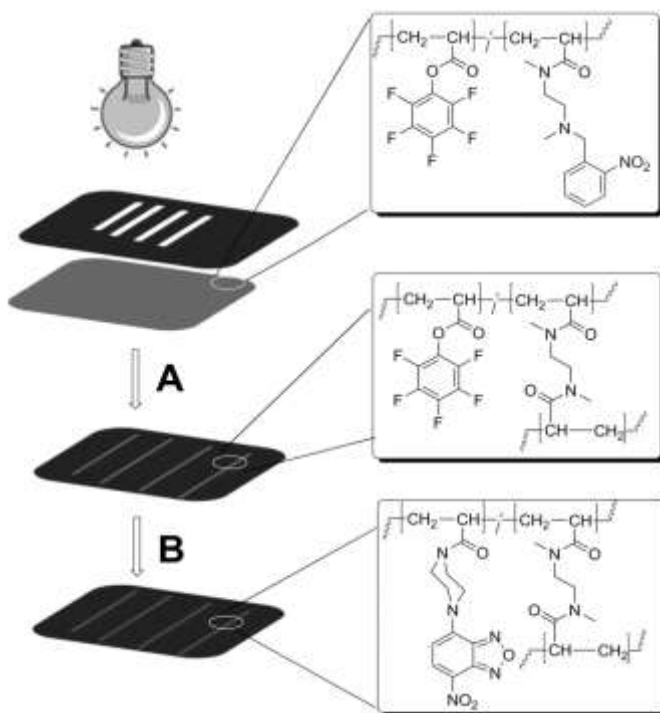


Chart 1 Photolithography of PPFPA-ONB. A): Irradiation of a spin-coated ONB-copolymer with activated ester units for 3 hours through optical masks. The non-crosslinked residues were washed with THF. B): functionalization of the active ester patterns with pip-NBD in solution for 12 hours with a following washing procedure.

The subsequent functionalization of the activated ester polymer patterns with a fluorescent dye (process B in **Chart 1**) was characterized by fluorescence microscopy. Dye functionalized patterns were obtained by immersing the polymer patterns in a solution of a dye labeled amine (piperazinyl-4-chloro-7-nitrobenzofuran (pip-NBD)) for 12 hours and thorough washing with THF. The fluorescent confocal microscope images provided a direct proof of the successful post-functionalization of the polymer patterns. The patterns in **Figure 3C** and **3G** showed a green fluorescence originated from the incorporated dye under UV light excitation ($\lambda_{\text{ex}} = 488 \text{ nm}$). **Figure 3B** and **3C** show smaller patterns after functionalization with the fluorescent dye. Small dislocations of the lines can be observed, which are likely due to the volume change accompanying the polymer modification. Further, the 2-dimensional profile of the polymer patterns has been recorded with a surface profilometer. The functional patterns showed a good homogeneity within nanometer scale in perpendicular direction (height) and micrometer scale along parallel direction (width) of the surface (**Figure 3D** and **3H**).

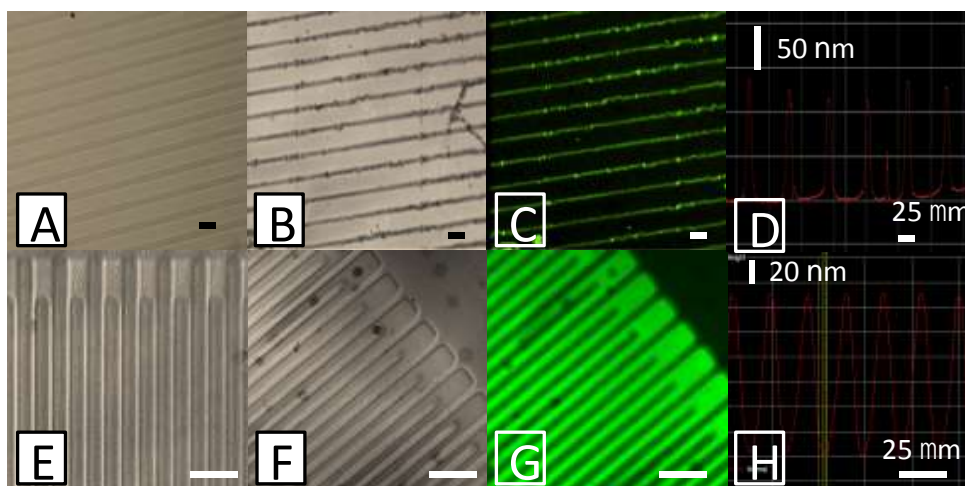


Figure 3 Microscopic images of crosslinked PFPA film patterns on glass before (A,E) and after (B,F) reaction with Pip-NBD; Fluorescence microscopic image (C,G) of crosslinked PFPA film patterns on glass after reaction with Pip-NBD ($\lambda_{\text{ex}}=488\text{nm}$); Stepper profile (D,H) of dye functionalized patterns (red line labelled parts in B and F). Scale bar: 25 μm .

Conclusion

In summary, we have developed a post-polymerization modification strategy to synthesize copolymers containing ONB protected amine moieties and activated esters. The ONB ratio could be fine-tuned based on a quantitative conversion of the activated ester units with a mono ONB-protected diamine. Upon UV irradiation, a sequence of events was triggered: deprotection and subsequent crosslinking, resulting in the production of reactive polymeric patterns with high-resolution through a photolithography process. After photolithography the majority of the polymeric activated ester groups on the patterns remained intact, which renders these patterns as useful templates for advanced functional patterns via a simple consecutive post-modification step with amines.

Acknowledgements

Financial support from the German Science Foundation (DFG) under grant TH 1104/4-1 and an International Collaboration in Chemistry award from the National Science Foundation (CHE 0924435) is gratefully acknowledged. This research was partly supported by the WCU (World Class University) program through the National Research Foundation of Korea funded by the Ministry of Education, Science and Technology (R31-10013). The authors thank Dr. S. Pang and Mr. D. Wang (MPIP Mainz) and Dr. F. Jochum (University of Mainz) for helpful discussions and support in lithography and fluorescent confocal microscope measurements.

Notes and references

Experimental part, FT-IR spectra and photo of PPFPA-ONB before and after crosslinking by irradiation, time dependent UV spectra of PPFPA-ONB.

- 1 G. Mayer, A. Heckel, *Angew. Chem. Int. Ed.* 2006, **45**, 4900.
- 2 H. Zhao, E. Sterner, E. B. Coughlin and P. Theato, *Macromolecules*, 2012, **45**, 1723.
- 3 A. M. Kloxin, A. M. Kasko, C. N. Salina and K. S. Anseth, *Science*, 2009, **324**, 59-63.

- 4 (a) J. Doh and D. J. Irvine, *J. Am. Chem. Soc.*, 2004, **126**, 970. (b) P. G. Taylor, J. K. Lee, A. A. Zakhidov, M. Chatzichristidi, H. H. Fong, J. A. DeFranco, G. G. Malliaras and C. K. Ober, *Advanced Materials* 2009, **21**, 2314.
- 5 B. Zhao, J. S. Moore and D. J. Beebe, *Science*, 2001, **291**, 1023.
- 6 (a) M. Kang and B. Moon, *Macromolecules*, 2009, **42**, 455. (b) J. M. Schumers, J. F. Gohy and C. A. Fustin, *Polym. Chem.*, 2010, **1**, 161. (c) H. Zhao, W. Gu, E. Sterner, T. P. Russell, E. B. Coughlin and P. Theato, *Macromolecules*, 2011, **44**, 6433. (d) E. Cabane, V. Malinova and W. Meier, *Macromolecular Chemistry and Physics*, 2010, **211**, 1847. (e) D. Han, X. Tong and Y. Zhao, *Macromolecules*, 2011, **44**, 437.
- 7 (a) W. E. Georgianna, H. Lusic, A. L. McIver and A. Deiter *Bioconjugate Chemistry*, 2010, **21**, 1404. (b) A. Shigenaga, J. Yamamoto, Y. Sumikawa, T. Furuta and A. Otaka, *Tetrahedron letter*, 2010, **51**, 2868.
- 8 J. M. Schumers, C. A. Fustin, A. Can, R. Hoogenboom, U. S. Schubert, J. F. Gohy, *J. Polym. Sci. Part A. Polym. Chem.*, 2009, **47**, 6504.
- 9 Examples for well-defined polymerization of ONB containing monomers are very limited. Thomas and coworkers reported they could make well-defined ONB containing polymers by Ring-opening metathesis polymerization. See: P. Gumbley, D. Koylu, and S. W. Thomas, III. *Macromolecules* 2011, **44**, 7956–7961.
- 10 (a) P. Theato, *J. Polym. Sci. Part A. Polym. Chem.*, 2008, **46**, 6677. (b) P. Theato and H. A. Klok (Ed.) “*Functional Polymer by Post-polymerization on Modification: Concepts, Guideline and Application*”, 2012, **Wiley-VCH, Weinheim**.

Supporting Information

Copolymers Featuring Pentafluorophenyl Ester and Photolabile Amine Units: Synthesis and Application as Reactive Photopatterns

Experimental section

Materials. All chemicals and solvents were commercially available and used as received unless otherwise stated. Tetrahydrofuran (THF) was dried over sodium and freshly distilled before use. Triethylamine (Et₃N) was dried over calcium chloride and distilled previously. Poly(pentafluorophenyl acrylate) (PPFPA) was synthesized following a procedure described earlier¹ Piperazinyl-4-chloro-7-nitrobenzofuran (pip-NBD) was synthesized as reported.²

Instrumentation. ¹H- NMR spectra were recorded on a Bruker 300 MHz FT-NMR spectrometer in deuterated solvents. The chemical shifts (δ) were given in ppm relative to trimethylsilane (TMS). Gel permeation chromatography (GPC) was used to determine the molecular weight and the corresponding molecular weight distributions, (M_w/M_n), of the polymer samples with respect to polystyrene standards. GPC measurements were performed in THF. The flow rate was 1mL*min⁻¹ at 25°C. IR spectra were recorded using a Bruker Vector 22 FT-IR spectrometer with an ATR unit. Fluorescence measurements were performed by using an inverted laser scanning microscope (Leica TCS SL) with an immersion

objective (20). An argon laser ($\lambda_{\text{ex}}=488$ nm) was used for the excitation of pip-NBD. An Oriel LSH302 500W UV-lamp equipped with a 313 nm filter was used for UV-irradiation.

Photo-patterning of PPFPA-ONB and post-modification. A PPFPA-ONB solution (10 wt %) was spin-coated onto clean glass slides (15 s, 3000 rpm). An optical mask was tightly set up on the surface of the film and the samples were then exposed to UV light (313 nm, 500 W) irradiation for 3 h. After irradiation, the samples were immersed in dry THF for 1 hour to remove any non-crosslinked polymer. For a functionalization of the patterns, the samples were then immersed in a pip-NBD solution in THF at room temperature for 12h. To remove any excess of pip-NBD, the substrate was washed thoroughly with THF.

Synthesis of *N,N'*-dimethyl-*N*-(2-nitrobenzyl)ethane-1,2-diamine (1). A mixture of *N,N'*-dimethylethane-1,2-diamine (8.8g, 100 mmol, 5 equiv.) and K_2CO_3 (2.35g, 60 mmol, 3 equiv.) was stirred in acetone (15 mL) for 15 min at 50 °C. Then *1*-(bromomethyl)-2-nitrobenzene (4.3g, 20 mmol, 1 equiv.) was added dropwise. The mixture was stirred for 12 hours at 55 °C. Acetone was removed under reduced pressure, the residue was dissolved in CH_2Cl_2 and washed with water. The organic phases were combined, dried over MgSO_4 , filtered and the solvent was removed *in vacuo*. A slightly brown liquid product (2.2 g, yield: 50%) was obtained by column chromatography (MeOH/ NH_3 H_2O =100:1, volume ratio). ^1H NMR (δ , ppm, DMSO): 7.83 (d, 1H, ONB), 7.65 (m, 2H, ONB), 7.52 (t, 1H, ONB), 3.69 (s, 2H, ONB- (CH_2) $\text{N}(\text{CH}_3)$), 2.49 (t, 2H, $-\text{N}(\text{CH}_3)\text{CH}_2\text{CH}_2\text{N}(\text{CH}_3)(\text{H})$), 2.37 (t, 2H, $-\text{N}(\text{CH}_3)\text{CH}_2\text{CH}_2\text{N}(\text{CH}_3)(\text{H})$), 2.18 ($-\text{N}(\text{CH}_3)\text{CH}_2\text{CH}_2\text{N}(\text{CH}_3)(\text{H})$), 2.02 ($-\text{N}(\text{CH}_3)\text{CH}_2\text{CH}_2\text{N}(\text{CH}_3)(\text{H})$). ESI MS (m/z): calcd. for $\text{C}_{11}\text{H}_{17}\text{N}_3\text{O}_2$: 213.13; found: 214.13 [$\text{M} + \text{H}$] $^+$.

Synthesis of PPFPA-ONB (example, ONB content: 10 mol%). 600 mg (2.6 mmol) of PPFPA, 0.02 mL (0.26 mmol) of Et_3N and 56 mg (0.26 mmol) of compound **1** (correspond to 10% in respective to the pentafluorophenyl moieties) were dissolved in freshly distilled THF (5 mL). The mixture was stirred overnight at room temperature. The resulting polymer was isolated by precipitation into *n*-hexane and was then dried in vacuum. Yield: 410 mg of PPFPA-ONB. FT-IR: (cm^{-1}) 1750 (C=O) and 1520 (C-

F). ^1H NMR (δ , ppm, CDCl_3): 7.8-7.2 (broad, proton in *o*-nitrobenzene), 3.2-1.2 (m, proton in backbone and linker of ONB).

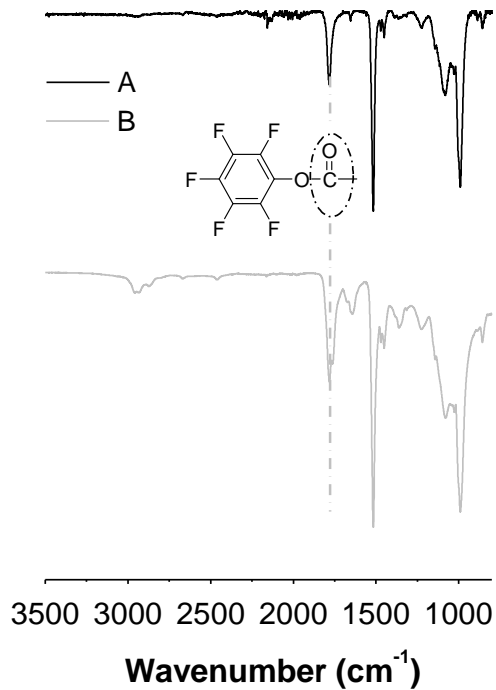


Figure S1. FT-IR for PPFPA (A) and PPFPA-ONB (ONB ratio, 10%) (B) after photo-crosslinking.

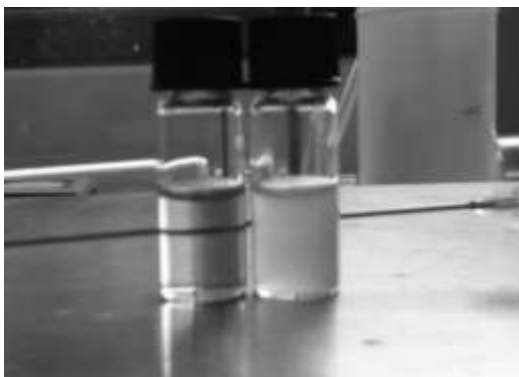


Figure S2. Photos for PPFPA (A) and PPFPA-ONB (ONB ratio, 10%) (B) after photo-crosslinking.

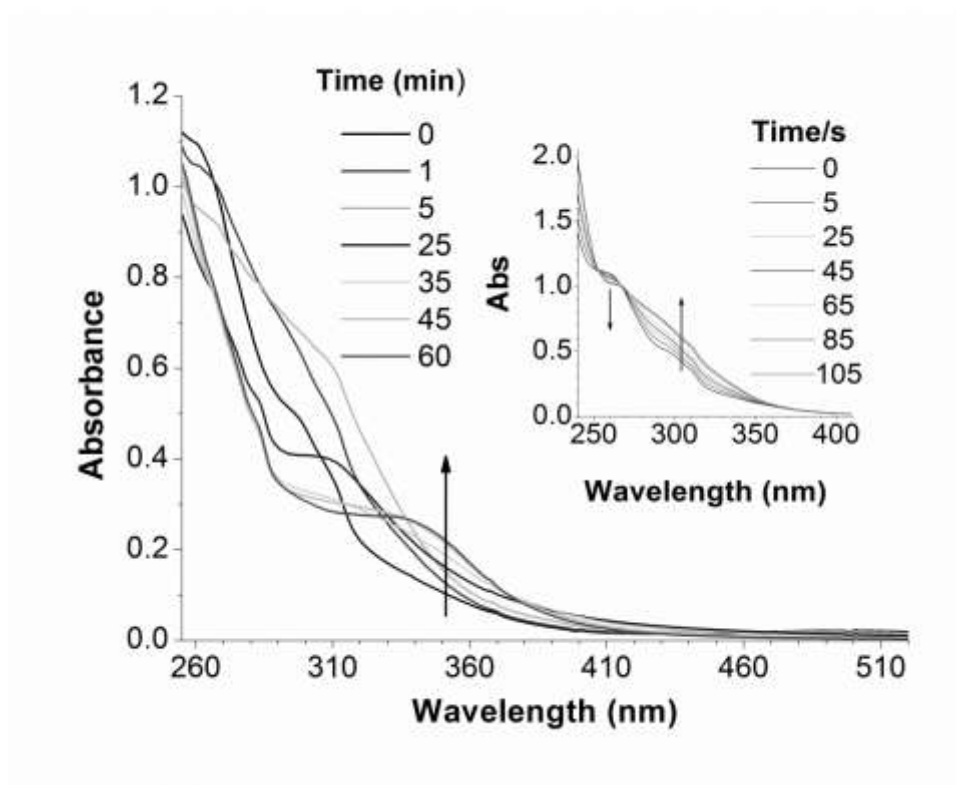


Figure S3. Irradiation (wavelength = 313 nm) time dependent UV spectra of PPFPA-ONB in THF. Concentration = 1 mg/mL.

1. F. D. Jochum and P. Theato, *Polymer*, 2009, **50**, 3079.
2. R. Nudelman, O. Ardon, Y. Hadar, Y. Chen, J. Libman and A. Shanzer, *J. Med. Chem.*, 1998, **41**, 1671.

9 Lists of Publications

1. **Zhao, H.**; Theato, P.*

“Copolymers Featuring Pentafluorophenyl Ester and Photolabile Amine Units: Synthesis and Application as Reactive Photopatterns”

Polymer Chemistry **2013**, 4, 891-894.

2. **Zhao, H.**; Gu, W.; Sterner, E.; Russell, T. P; Coughlin, E. B.; Theato, P.* “Highly-ordered Nanoporous Thin Films from Photocleavable Block Copolymers”

Macromolecules **2011**, 44, 6433.

My contribution in paper #1 and #2 was the synthesis (100%), the characterization (paper #1: 100%, paper #2: 80%) and analysis (paper #1: 80%, paper #2: 60%) of the described polymers. In both papers, I designed all experiments (100%) and personally contacted experts to support me in conducting the required analysis (paper #1: confocal laser scanning microscope, paper #2: AFM and TEM). For both papers, I independently wrote the drafts of the manuscript and finalized them together with my supervisor.

I, Prof. Dr. Patrick Theato, herewith confirm that the above given contributions of Mr. Hui Zhao to the individual papers are correct.

10 Acknowledgement

The research presented in this thesis would not have been possible without the support and aid of different people and institutions. First of all, I would like to thank my advisor Prof. Dr. Patrick Theato for the nice research topic, the valuable discussions, his suggestions and support during the last three years. I gratefully thank my co-advisor Professor Dr. E. Bryan Coughlin in UMass Amherst for accepting me into his work group for twice visiting. I appreciate Prof. Theato's ideas towards my PhD work and the financial support. I thank Professor Dr. Thomas P. Russell in UMass Amherst and his student Weiyin Gu for the help on the preparations of highly ordered thin films. I thank Elizabeth Sterner for her kind help on discussion about our collaboration and revising my manuscripts.

I thank former members in Mainz. They are Dr. Katja Nilles, Dr. Kerstin Wiss, Dr. Florian Jochum, Dr. Niko Haberkorn. Especially, I thank Florian for his kind help at the beginning of my PhD.

I thank current members in Hamburg. They are Christina Khenkhar, Alexander Florian, Wilaiporn Graisuwan, Lirong He, Iilona Inselmann, Hanju Jo, Dr. Ryohei Kakuchi, Adrian Ketelsen, Fenja Moldenhauer, Anja Pauly, Emma Pelegri-O'Day, Philipp Schattling, Denis Seuyep, Inna Slepchuk, Michael Thielke, and Natalie Wagner.

I thank visiting students for helping me on assistant on my lab work. They are Hyunji Lee from Korea and Mayuka Yamada from Japan.

I thank Xiaojun Wu from Luinstra group. Especially, I thank him for treating me with his big pan chicken so many times, really delicious.

I thank Ning Zhu from Moritz group. I thank him for sharing his experience on job hunting.

I thank my friend Tony for chatting so much. It not only helps me practice oral English but also is a good way to release my stress.

I thank my parents and brother in China. Thank you for continuous support on my study. Because of you, I have a big motivation to work hard and try my best to have a bright future. I know that finally you will be proud of me.

In a twinkling of an eye, the end of my PhD course is coming. Looking back to my PhD life, it just looks like a movie. I appreciate all my friends and colleagues again. Because of you, this movie becomes lovely and unforgettable.

Finally, I thank all the people who once helped or inspired me on work or life but their names are not listed in the acknowledgement.

Hui ZHAO

Hamburg, April 2013

Chemicals

Acrylsäurechlorid

Summenformel	C ₃ H ₃ ClO
CAS Nummer	814-68-6
Molmasse	90.5 g/mol
Dichte	1.12 g/cm ³
Siedepunkt	75°C
Gefahrensymbol	GHS02, GHS06, GHS05, GHS09
H-Sätze	225-290-330-302+312-400
P-Sätze	210-280-273-301+330+331-302+352-304+340-305+351+338-309+310

2,2'-Azo-bis-[2-(2-Imidazolin-2-yl)-Propan]-Dihydrochlorid

VA-044

Summenformel	C ₁₂ H ₂₂ N ₆ · 2HCl
CAS Nummer	27776-21-2
Hersteller	Wako Pure Chemical Industries, Ltd.
Molmasse	323.33 g/mol
Dichte	g/cm ³
Schmelzpunkt	188 – 193°C
Gefahrensymbol	-
H-Sätze	-
P-Sätze	-

Azo-bis-(Isobutyronitril)

AIBN

Summenformel	C ₈ H ₁₂ N ₄
CAS Nummer	78-67-1
Molmasse	164.21 g/mol
Dichte	1.11 g/cm ³
Schmelzpunkt	105°C
Gefahrensymbol	GHS02, GHS07
H-Sätze	242-332-302-412

P-Sätze 273

Diethylether

Summenformel	C ₄ H ₁₀ O
CAS Nummer	60-29-7
Molmasse	74.12 g/mol
Dichte	0.71 g/cm ³
Siedepunkt	35°C
Gefahrensymbol	GHS02, GHS07
H-Sätze	224-302-336

P-Sätze 210-240-403+235

4,5-Dimethoxy-2-nitrobenzyl chloroformate

Summenformel C₁₀H₁₀ClNO₆
CAS Nummer 42855-00-5
Molmasse 275,64/mol
Dichte -
Siedepunkt -
Gefahrensymbol GHS02
H-Sätze 314
P-Sätze 280

Ethanol

Summenformel C₂H₆O
CAS Nummer 64-17-5
Molmasse 46.07g/mol
Dichte 0.79 g/cm³
Siedepunkt 78°C
Gefahrensymbol GHS02
H-Sätze 225
P-Sätze 210

n-Hexan

Summenformel C₆H₁₄
CAS Nummer 110-54-3
Molmasse 86.18 g/mol
Dichte 0.66 g/cm³
Siedepunkt 69°C
Gefahrensymbol GHS02, GHS08, GHS07, GHS09
H-Sätze 225-361f-304-373-315-336-411
P-Sätze 210-240-273-301+310-331-302+352-403+235

Magnesiumsulfat

Summenformel MgSO₄
CAS Nummer 7487-88-9
Molmasse 120.37 g/mol
Dichte 2.66 g/cm³
Gefahrensymbol -
H-Sätze -
P-Sätze -

Methanol

Summenformel CH₄O
CAS Nummer 67-56-1

Molmasse 32.04 g/mol
Dichte 0.79 g/cm³
Siedepunkt 65°C
Gefahrensymbol GHS02, GHS06, GHS08
H-Sätze 225-331-311-301-370
P-Sätze 210-233-280-302+352

N-Methyl-N,N-Dioctyloctan-1-Ammoniumchlorid

Aliquat 336

Summenformel C₂₅H₅₄ClN
CAS Nummer 63393-96-4
Molmasse 404.16 g/mol
Dichte 0.884 g/cm³
Siedepunkt 225°C
Gefahrensymbol GHS05, GHS06, GHS09
H-Sätze 301-315-318-410
P-Sätze 273-280-301+310-305+351+338-501

Natrium

Summenformel Na
CAS Nummer 7440-23-5
Molmasse 23 g/mol
Dichte 0.97 g/cm³
Gefahrensymbol GHS02, GHS05
H-Sätze 260-314
P-Sätze 280-301+330+331-305+351+338-309-310-370+378-422

2-Nitro-benzylbromid

Summenformel C₇H₆BrNO₂
CAS Nummer 3958-60-9
Molmasse 216.03 g/mol
Dichte -
Gefahrensymbol -
H-Sätze 314
P-Sätze 280

Pentafluorphenol

PFP

Summenformel C₆F₅OH
CAS Nummer 771-61-9
Molmasse 184.06 g/mol
Dichte 1.757 g/cm³
Gefahrensymbol GHS07
H-Sätze 315-319-335

P-Sätze 261-305+351+338

Pentafluorphenylacrylat

PFPA

Summenformel $C_9H_3F_5O_2$
CAS Nummer 71195-85-2
Molmasse 238.11 g/mol
Dichte 1.446 g/cm^3
Gefahrensymbol GHS07
H-Sätze 315-319-335
P-Sätze 261-305+351+338

Salzsäure (37%)

Summenformel HCl
CAS Nummer 7647-01-0
Molmasse 36.46g/mol
Dichte 1.19 g/cm^3
Siedepunkt 50°C
Gefahrensymbol GHS05, GHS07
H-Sätze 314-335
P-Sätze 260-301+330+331-303+361+353-305+351+338-405-501

Styrol

Summenformel C_8H_8
CAS Nummer 100-42-5
Molmasse 104.15 g/mol
Dichte 0.91 g/cm^3
Siedepunkt 145°C
Gefahrensymbol GHS02, GHS07, GHS08
H-Sätze 226-332-319-315-304-335-372
P-Sätze 260-280-305+351+338-403+233

Triethylamin

TEA

Summenformel $C_6H_{15}N$
CAS Nummer 121-44-8
Molmasse 101.19 g/mol
Dichte 0.73 g/cm^3
Siedepunkt 89°C
Gefahrensymbol GHS02, GHS05, GHS07
H-Sätze 225-332-312-302-314
P-Sätze 210-280-303+361+353-305+351+338-310-312

Toluol

Summenformel C_7H_8
CAS Nummer 108-88-3
Molmasse 92.14 g/mol
Dichte 0.87 g/cm^3
Siedepunkt 111°C
Gefahrensymbol GHS02, GHS08, GHS07
H-Sätze 225-361d-304-373-315-336
P-Sätze 210-301+310-331-302+352

Lebenslauf

Angaben zur Person

Nachname, Vorname	Zhao, Hui (Master)
Adresse	Falkenried 34a, Hamburg
Telefon	+49 176 9572 4723
Email	huizhao.com@gmail.com
Geburtsdatum/-ort	27.12.1982 in Shandong, China

Angaben zur Ausbildung

09.1999 – 06. 2002	Cangshan Number 1. High School, Shandong, China
09.2002 – 07.2006	Studium der Bauingenieurwissenschaft an der Shandong Polytechnic University, Jinan, China
09.2007 – 03.2010	(master degree) Studium an Chemie an der Zhejiang University, Hangzhou, China
05.2010 – 08.2011	Studium der Chemie an der Universität Mainz
09.2010 – 02.2011	Studium der Chemie (as visiting student) an der University of Massachusetts Amherst USA
10.2012 – 12.2012	
08.2011 – 04.2013	Promotion der Chemie an der Universität Hamburg

Erklärung über frühere Promotionsversuche

Ich versichere, dass von mir, HUI ZHAO, keine früheren Promotionsversuche mit dieser oder einer anderen Dissertation erfolgt sind. Es wurde nur dieser Antrag auf Eröffnung eines Promotionsverfahrens eingereicht.

HUI ZHAO

Hamburg, 05. 04. 2013

Eidesstattlicher Erklärung

Hiermit versichere ich, dass ich die vorliegende Arbeit eigenständig erstellt und alle benutzten Quellen ordnungsgemäß zitiert habe. Diese Arbeit ist zuvor in gleicher oder ähnlicher Form keine Prüfungsbehörde vorgelegt worden.

HUI ZHAO

Hamburg, 05. 04. 2013